Electronic and spin structure of quantum materials probed by angle-resolved photoemission

Dmitry Usachov

SPbU, MIPT, MISIS usachov.d@gmail.com

Contents

Aim of this lecture:

To demonstrate the capabilities of photoemission techniques by several examples including 4f-compounds and 2D materials

Contents:

1. ***Review of photoemission research methods***
2. ***Electronic and spin structure at the surfaces of 4f compounds***
3. ***Magnetic proximity effects in the interfaces of graphene and MoS_2 with cobalt***

Part 1

Review of photoemission research methods

History of photoemission

The photoelectric effect was first observed in **1887** by **Heinrich Hertz**

H. R. Hertz, Annalen der Physik **267**, 983 (1887).

And first explained by **Albert Einstein** in **1906**

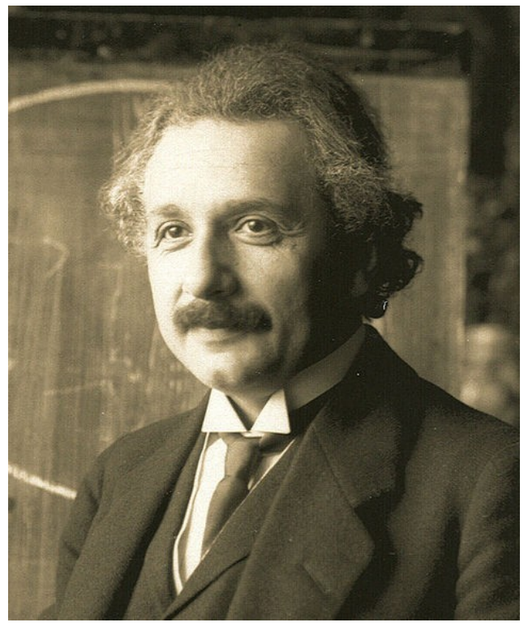

A. Einstein, Annalen der Physik **325**, 199 (1906).

Kai Siegbahn in **1981**

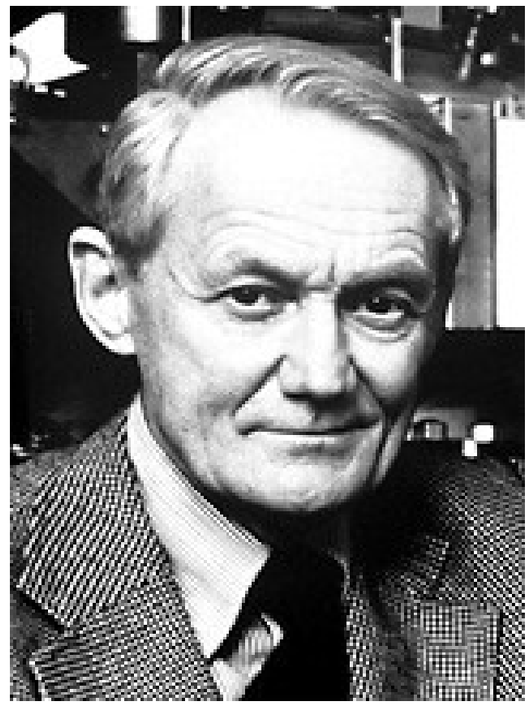

C. Nordling, E. Sokolowski, and K. Siegbahn,
Precision Method for Obtaining Absolute Values of Atomic Binding Energies
Phys. Rev. **105**, 1676 (1957).

"…We have recently developed a precision method of investigating atomic binding energies, which we believe will find application in a variety of problems in atomic and solid state physics…"

K. Siegbahn obtained the Nobel Prize for developing the method of Electron Spectroscopy for Chemical Analysis (ESCA), now usually described as **X-ray photoelectron spectroscopy** (XPS).

Photoelectron spectroscopy

(a) **Experiment**

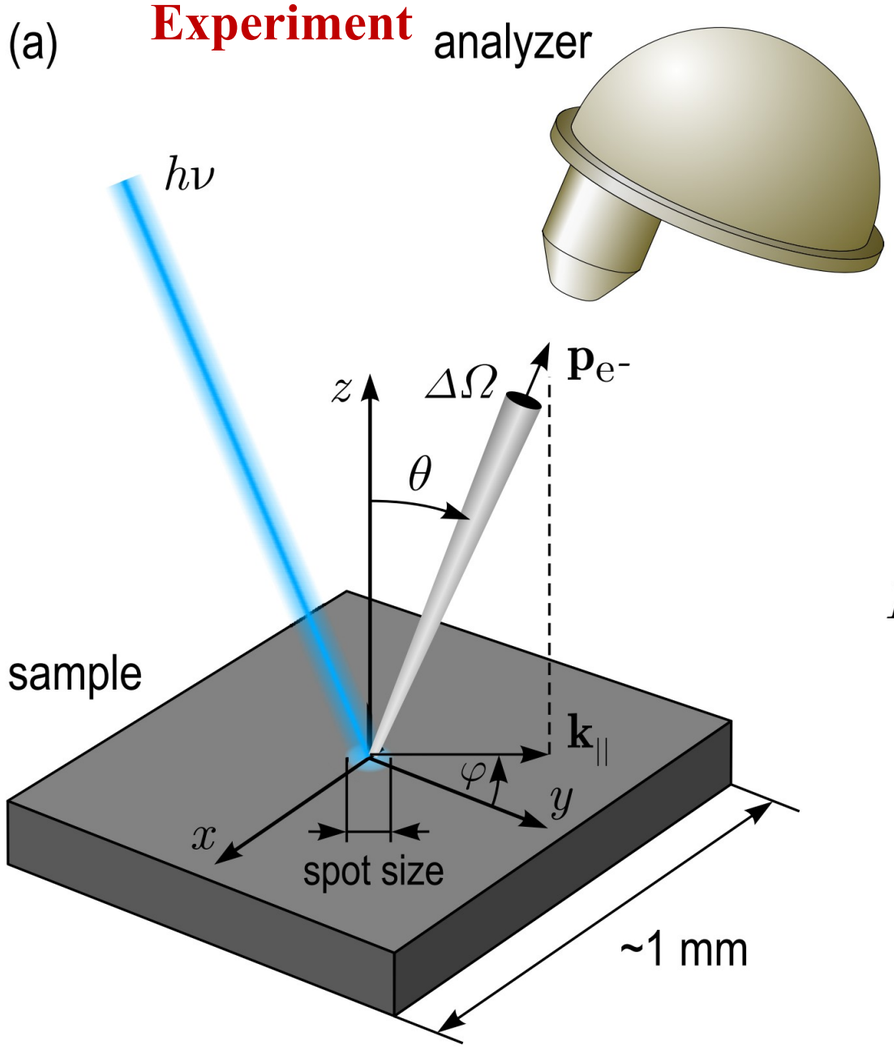

(b) **Energy diagram**

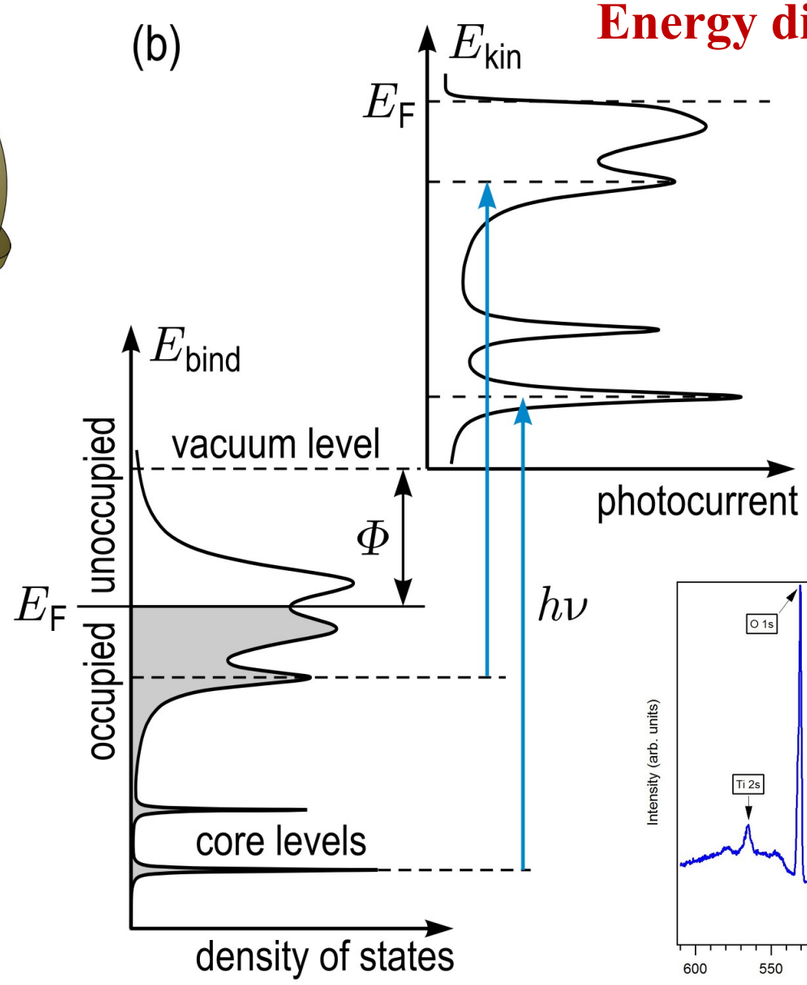

(c) **XPS (ESCA)**

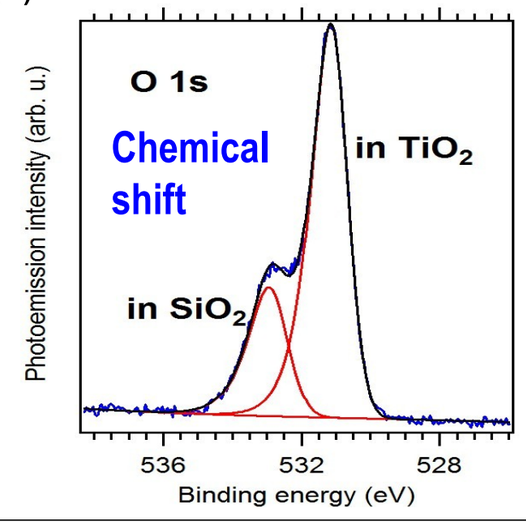

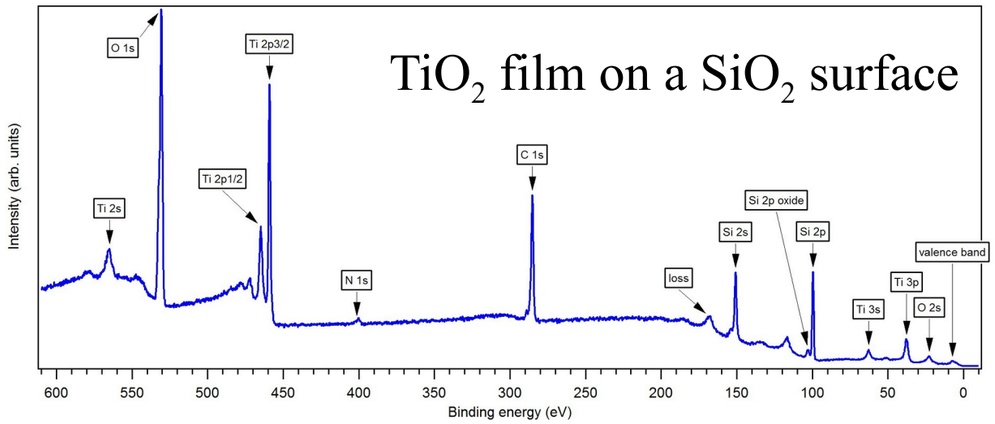

$$E_{Kin}(k_f) = h\nu - E_{Bind}(k_i) - \Phi$$

a) A **photon** beam **excites electrons** in the sample. The **number of photoelectrons is measured** as a function of their energy.

b) Exemplary electron transitions in a photoelectric process (shown by blue arrows). E_{Bind} and E_{Kin} stand for the binding energy of electrons in the solid and the kinetic energy of photoelectrons, Φ denotes the work function of the sample, E_F is the Fermi energy.

c) XPS (X-ray photoemission spectroscopy) or ESCA (Electron Spectroscopy for Chemical Analysis) – gives chemical composition.

Angle-resolved photoelectron spectroscopy

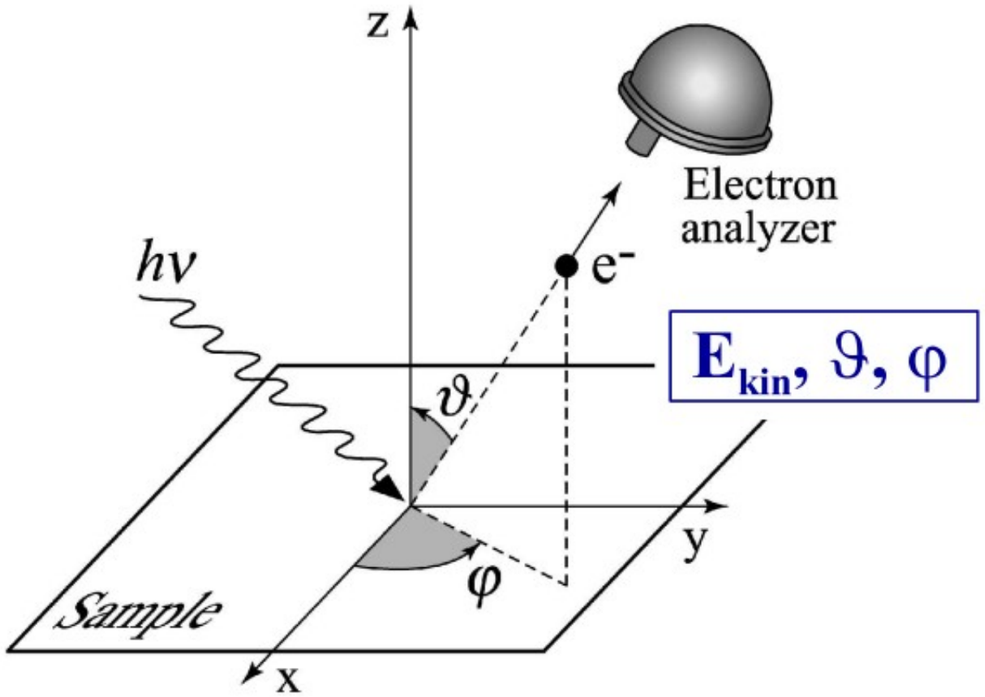

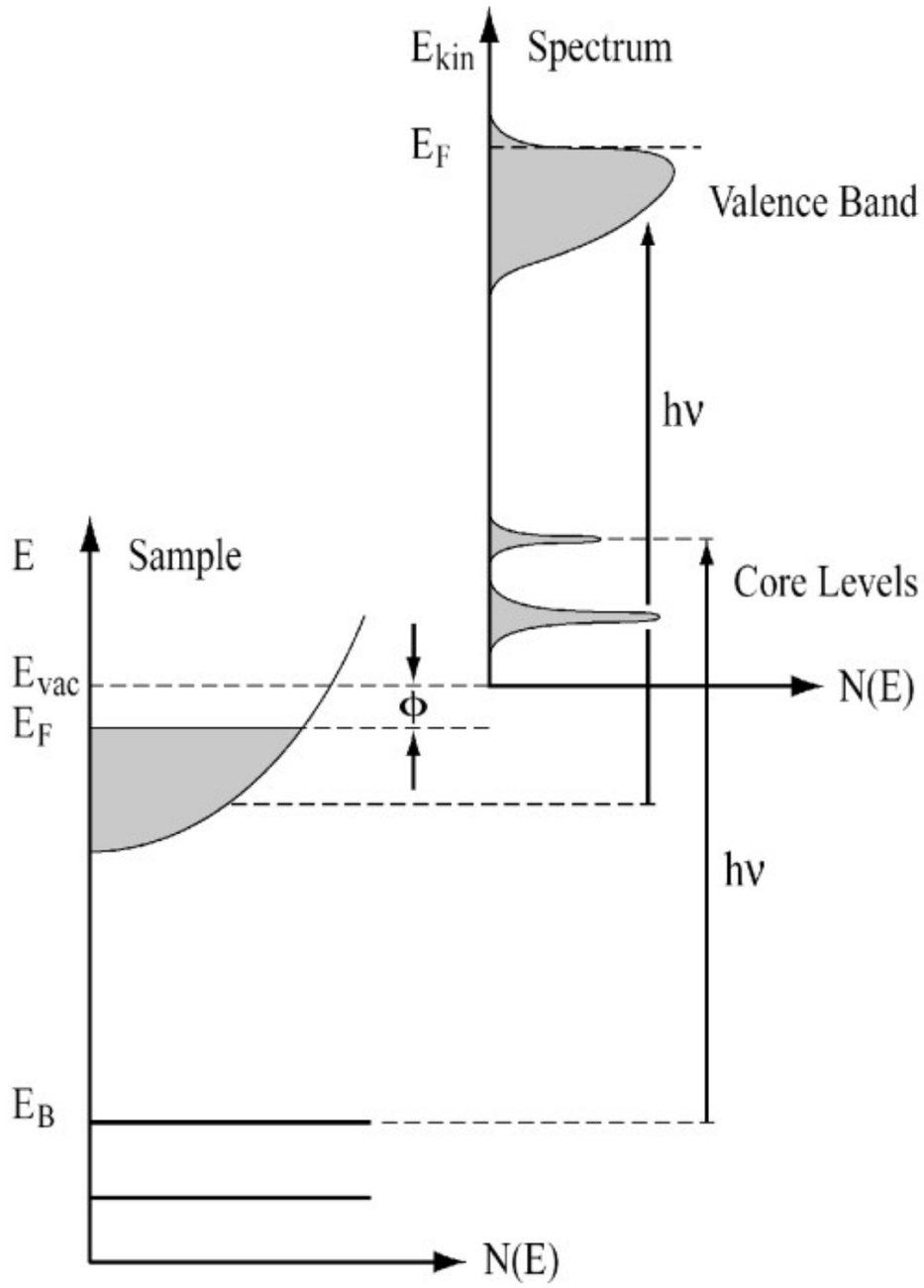

Energy Conservation

$$E_{kin} = h\nu - \phi - |E_B|$$

Momentum Conservation

$$\mathbf{p}_{\parallel} = \hbar \mathbf{k}_{\parallel} = \sqrt{2m E_{kin}} \cdot \sin\vartheta$$

Taking spectra at different emission angles, we find the relation between the energy and momentum: $E(k_{||})$

Angle-resolved photoelectron spectroscopy (ARPES)

(a)

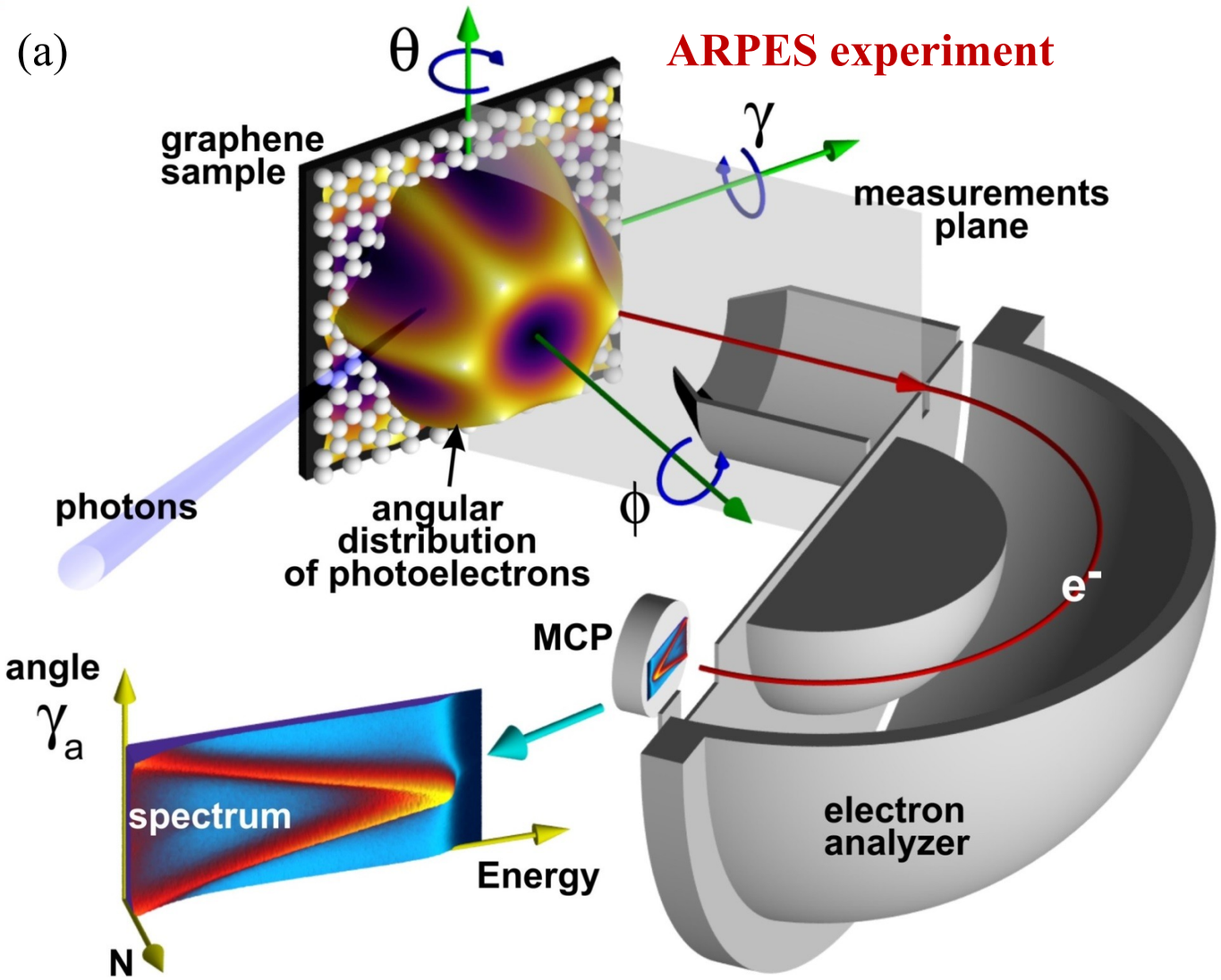

(b)

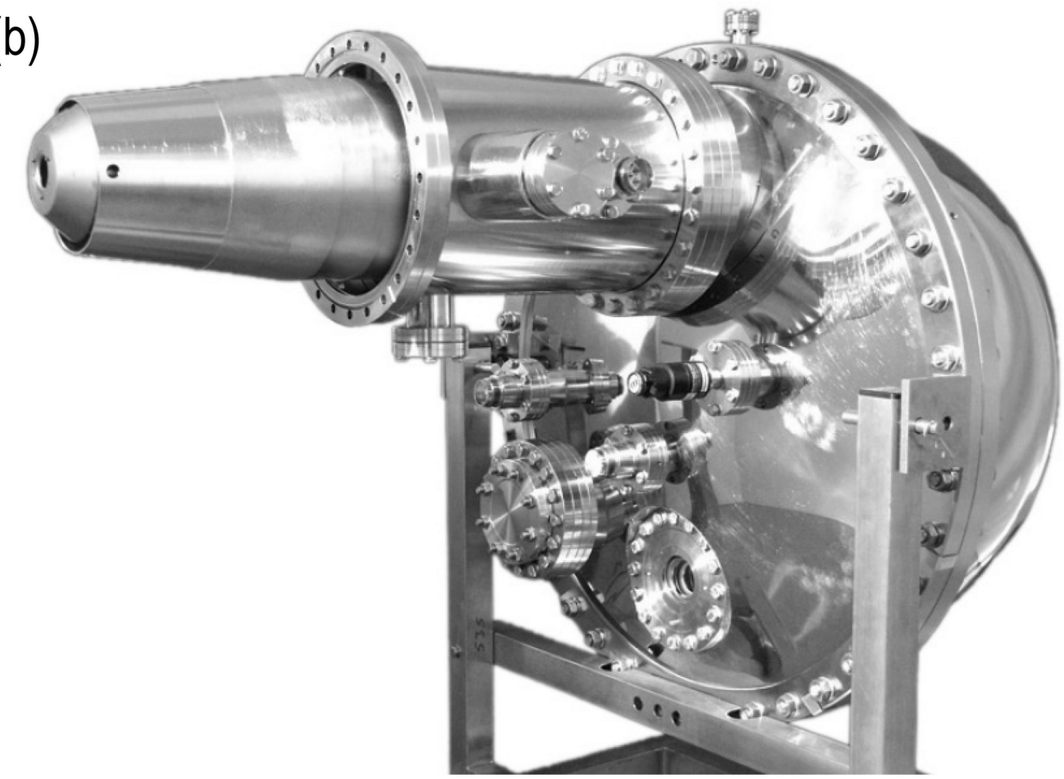

i) It measures the **intensity** of **photo**emitted **electrons** as a **function** of both their **kinetic energy** and **momentum**.

ii) In the **angle-resolved** mode, the photo**electrons** are **focused** by electron **lens** in such a way that **they reach** the **detector** at different **positions depending** on **their initial momentum**.

ARPES experiment

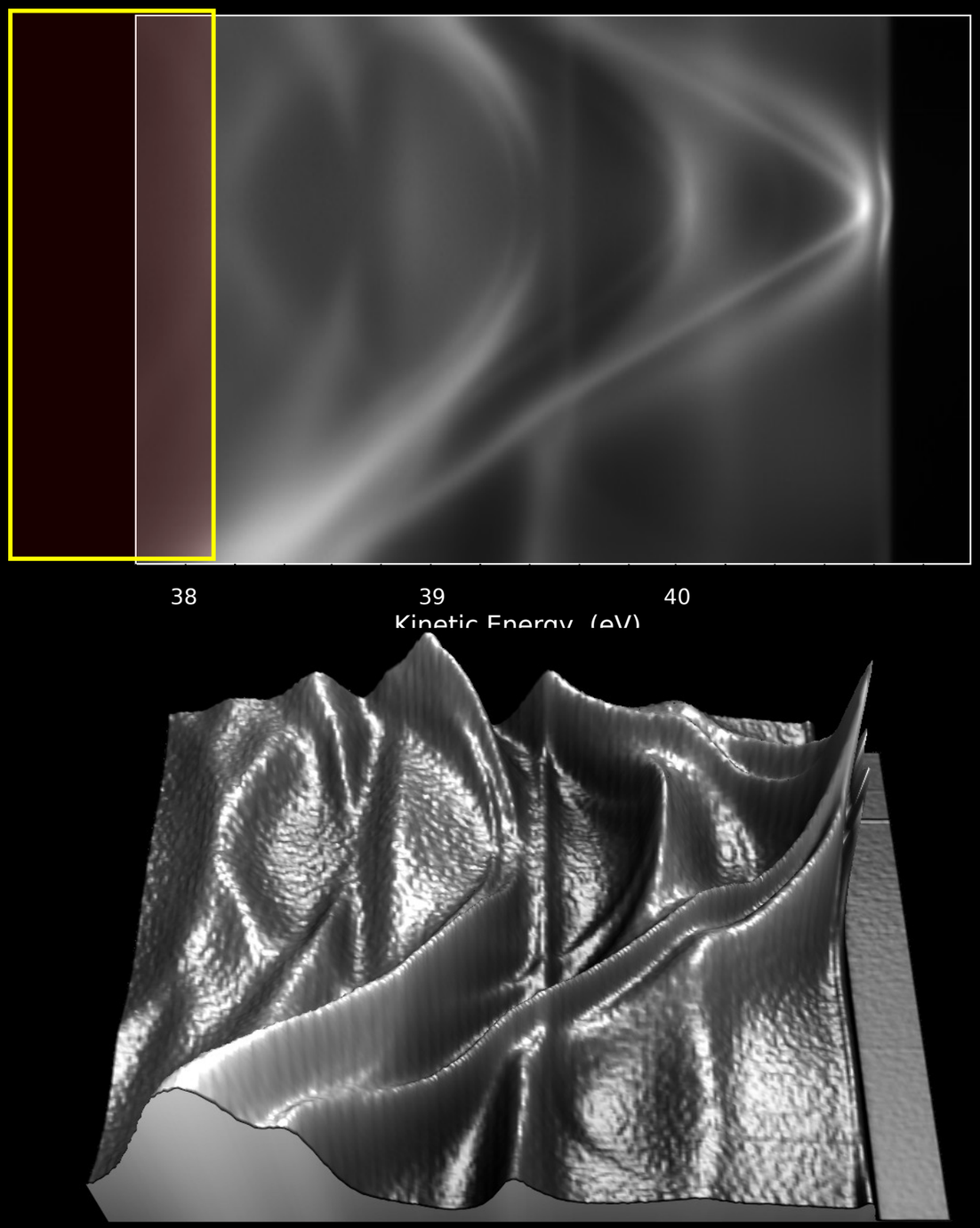

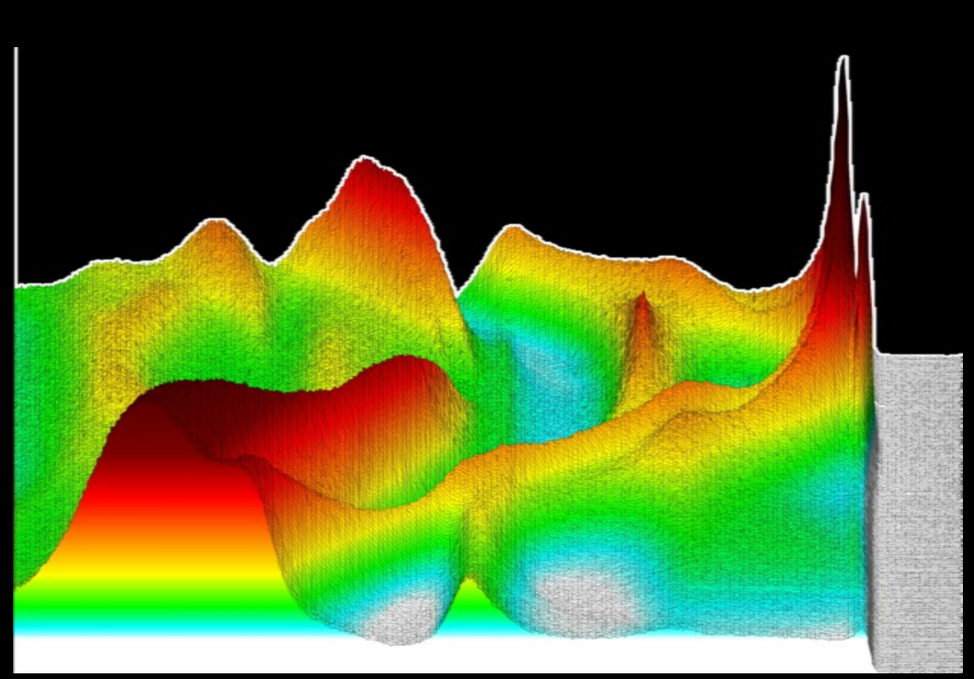

Interpretation of ARPES data

Non-interacting electrons - Band structure $E_0(\mathbf{k})$

Interacting electrons (correlated systems) – Spectral function $A(\vec{k},\varepsilon) = -\frac{1}{\pi} Im\, G(\vec{k},\varepsilon)$

Green's function

Electronic correlations lead to a "**dressing**" of the single particle, i.e. when the particle moves in the solid it is always screened by many-particle interactions. This system of particle and interaction may be seen as a new **quasiparticle**. The respective many-electron calculations result in **quasiparticle spectral functions** A(k,E) rather than conventional band structures E(k).

$$A(\mathbf{k},E) = \frac{1}{\pi}\frac{\Sigma''(\mathbf{k},E)}{[E - E_0(\mathbf{k}) - \Sigma'(\mathbf{k},E)]^2 + [\Sigma''(\mathbf{k},E)]^2}$$

Σ - self-energy

ARPES of Ni(110):

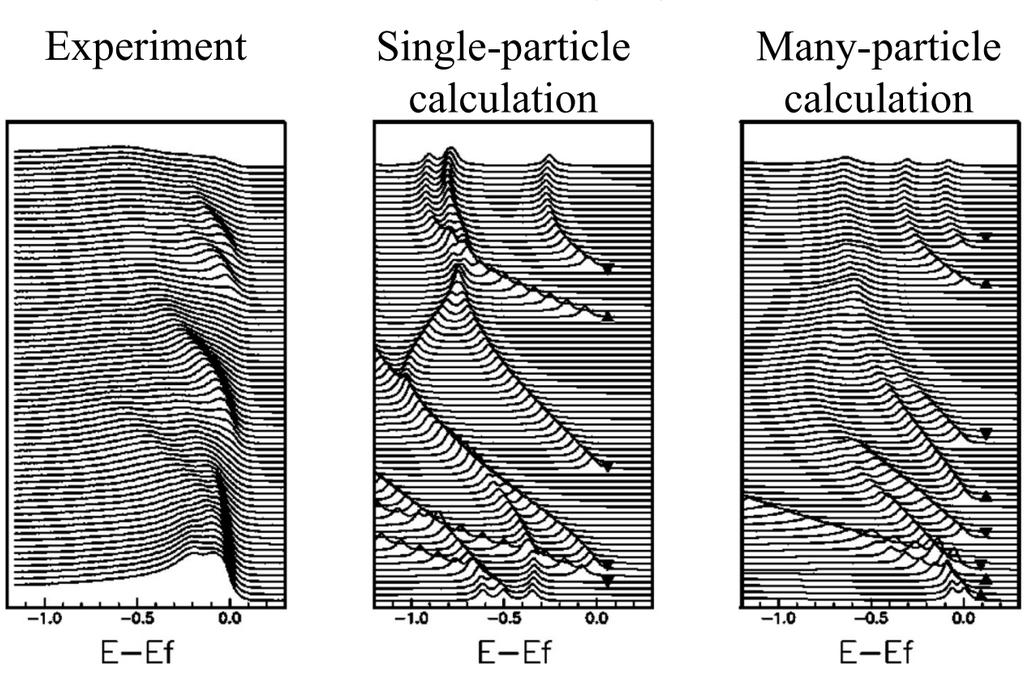

F. Manghi, et al. PRB 59, R10409 (1999).

Electron-boson coupling (phonons, magnons, etc.)

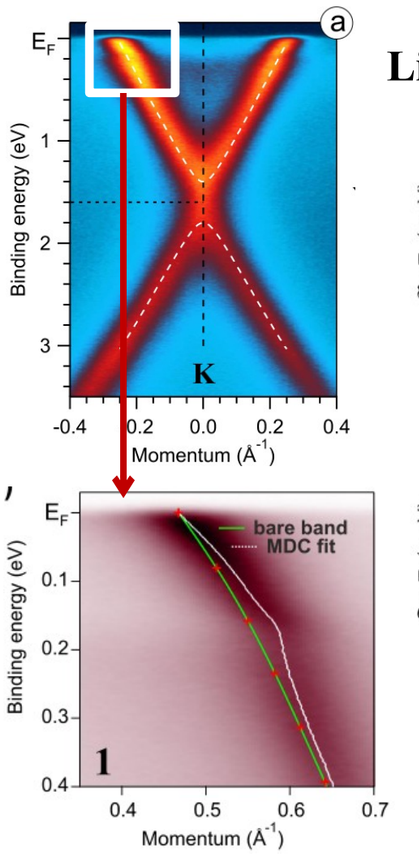

D. Usachov et al. PRB 97, 085132 (2018)

Li/Graphene

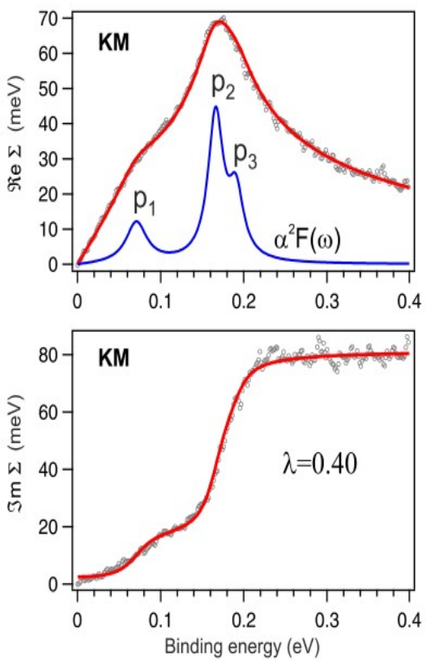

T. Kiss et al. PRL 94, 057001 (2005)

Superconducting gap

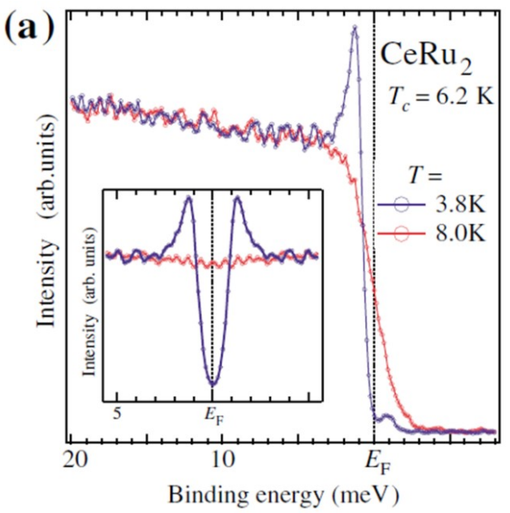

Spin-resolved ARPES

Spin-ARPES with a VLEED detector

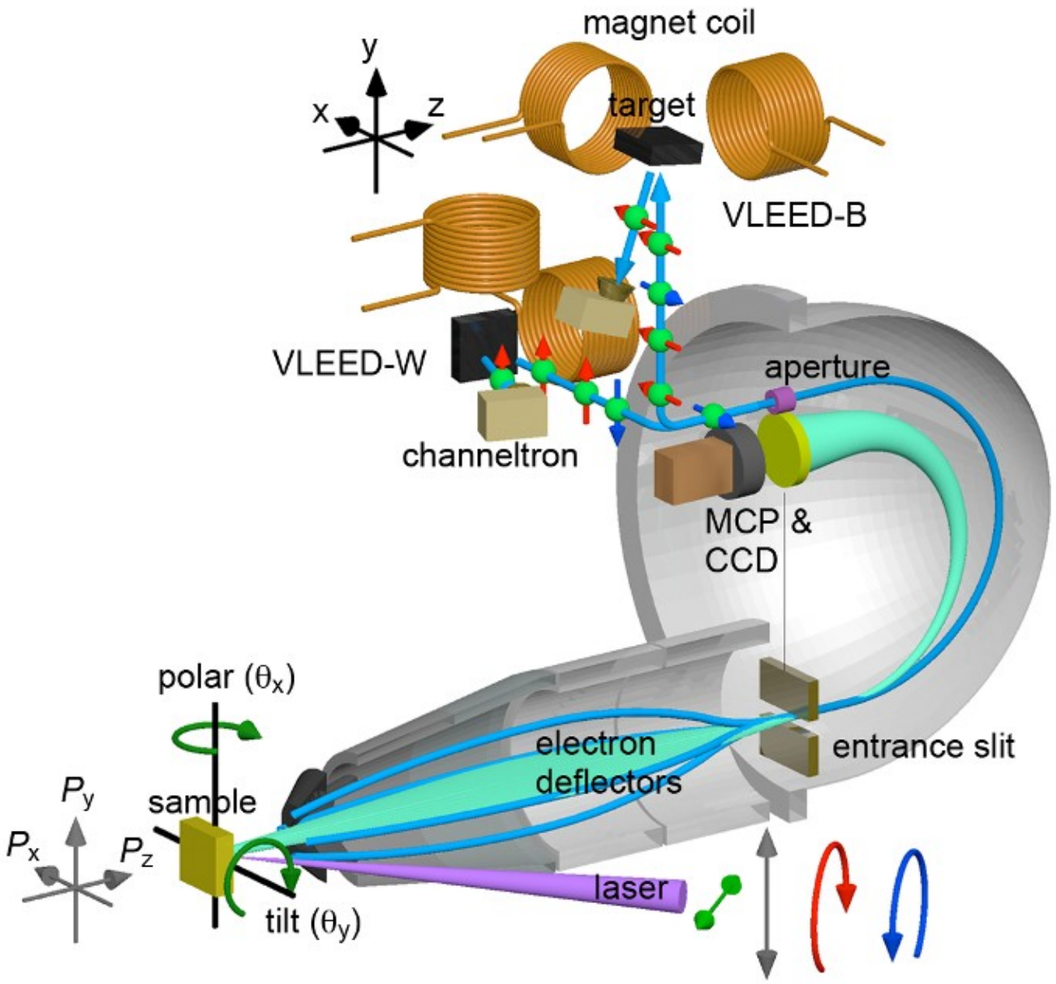

Based on spin-dependent reflection of electrons from the Fe target.

To measure different spin projections the target is magnetized in different directions.

Au(111) Rashba-split surface states

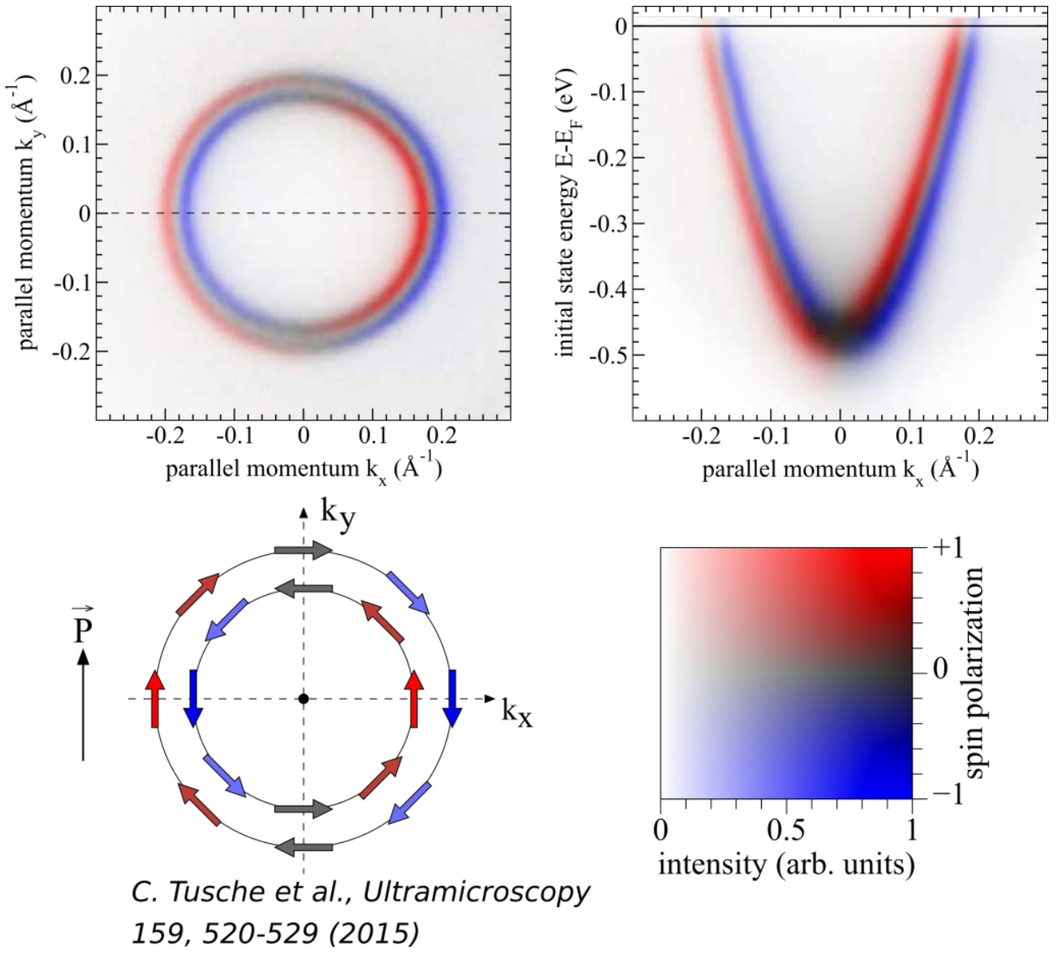

C. Tusche et al., Ultramicroscopy 159, 520-529 (2015)

Spin-ARPES may give three projections of spin in addition to the band structure

C. Jozwiak et al. Nature Commun. 7, 13143 (2016)

Time-resolved ARPES

Time-resolved ARPES

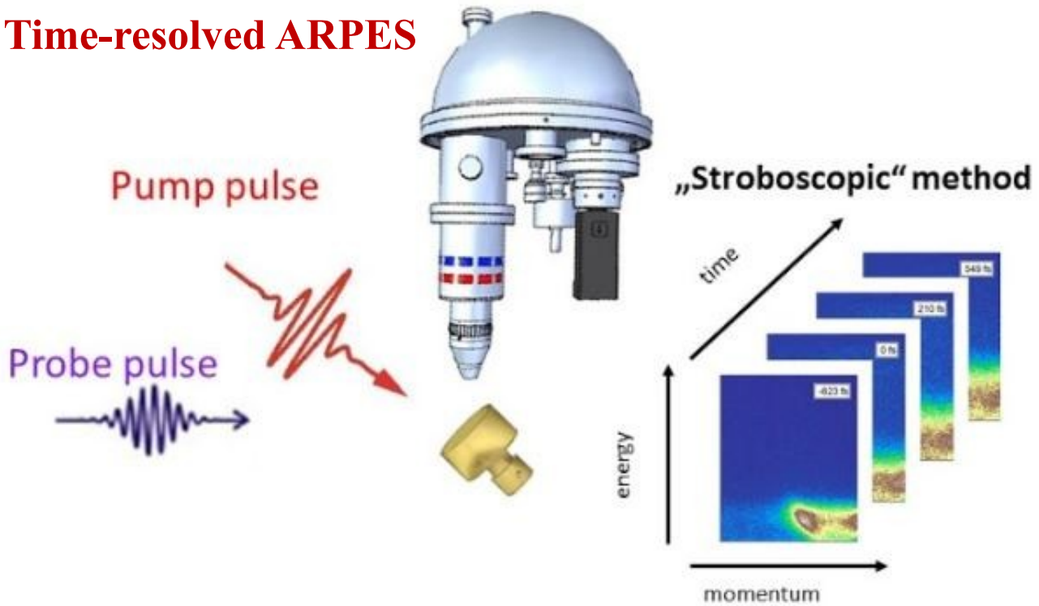

Time-resolved spin-ARPES (pump-probe experiment)

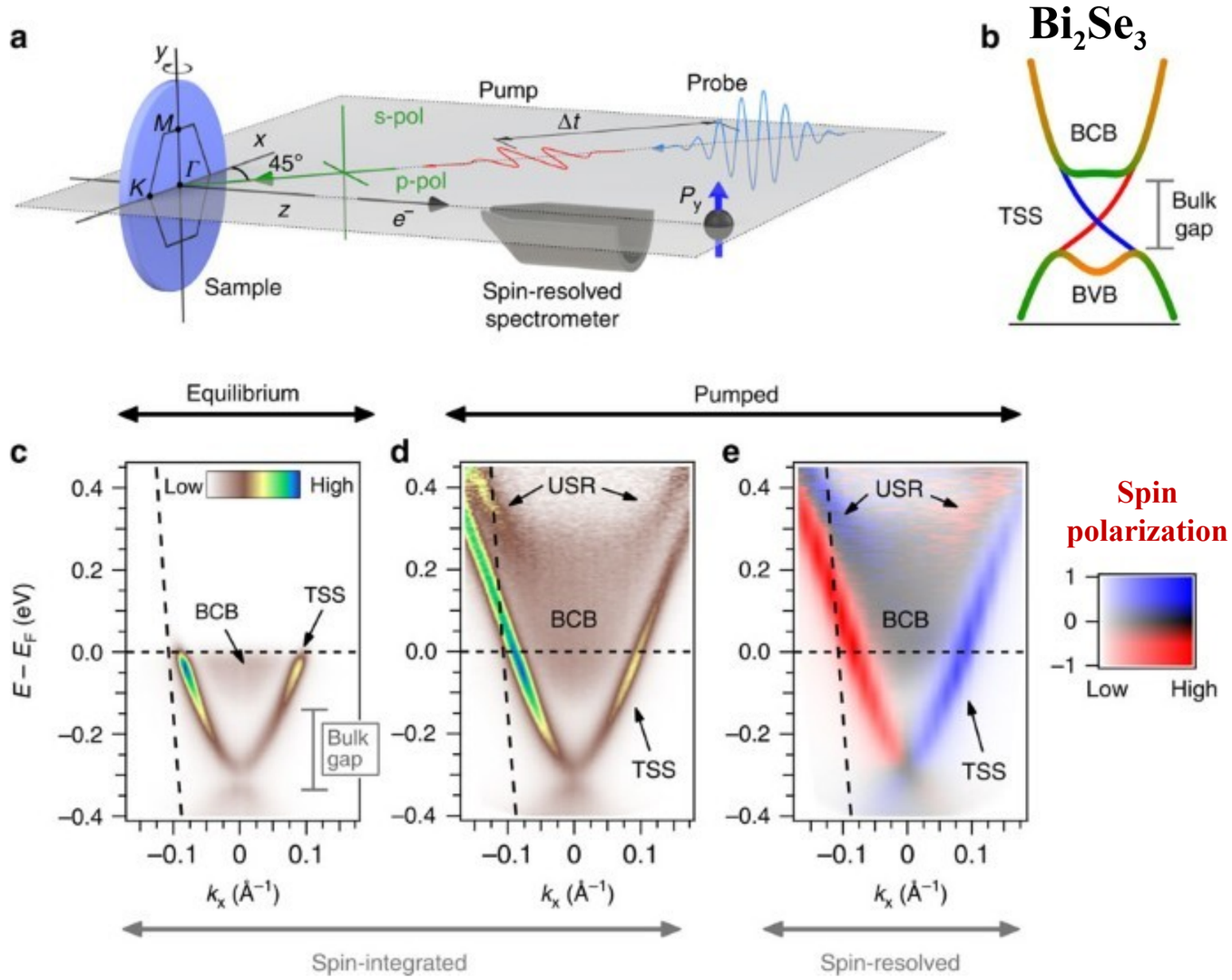

Pumping the system with laser pulses opens access to the unoccupied electronic states (possibly with spin resolution)

S. Zhu et al. Sci. Rep. 5, 13213 (2015)

C. Jozwiak et al. Nature Commun. 7, 13143 (2016)

Spatially-resolved photoemission

Spin-resolved momentum microscope

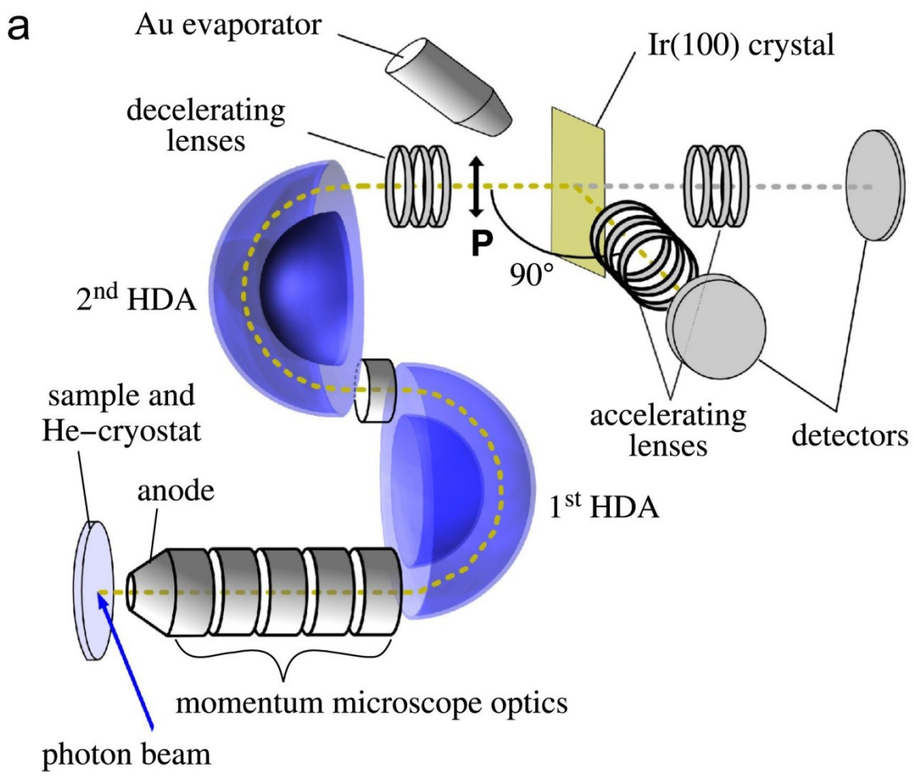

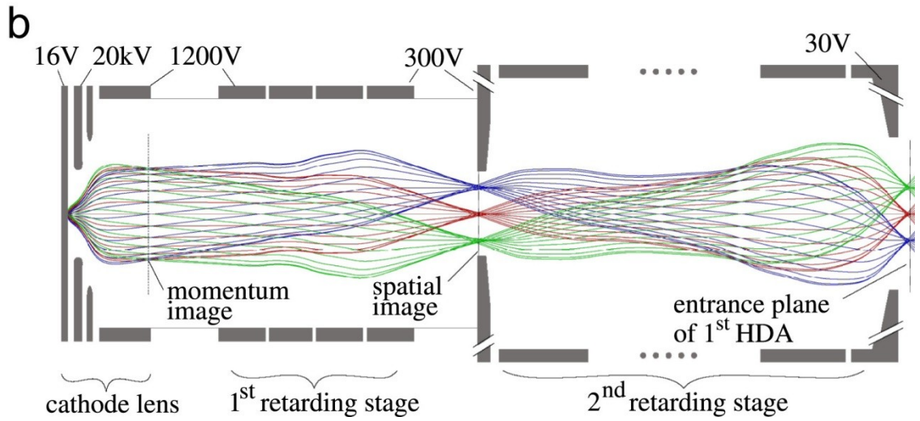

Can work in both angle-resolved and spatially-resolved modes

Magnetic domains of magnetite (Fe_3O_4)

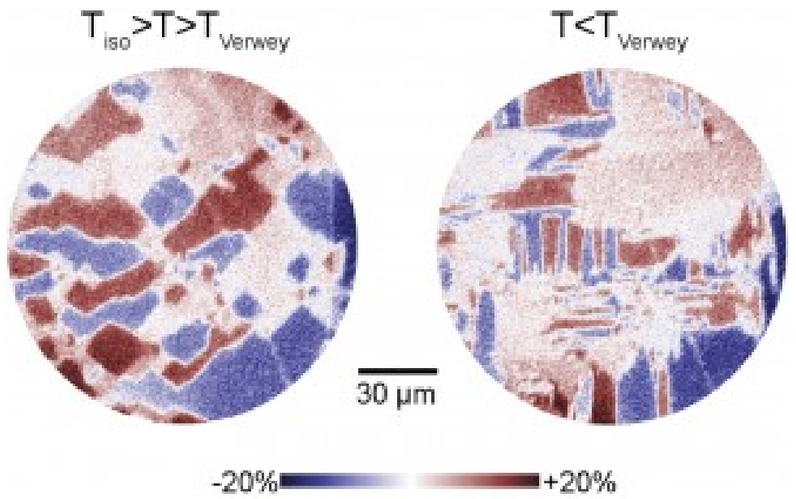

de la Figuera, J. & Tusche, C. Appl. Surf. Sci. 391, 66-69 (2017).

Nano-ARPES

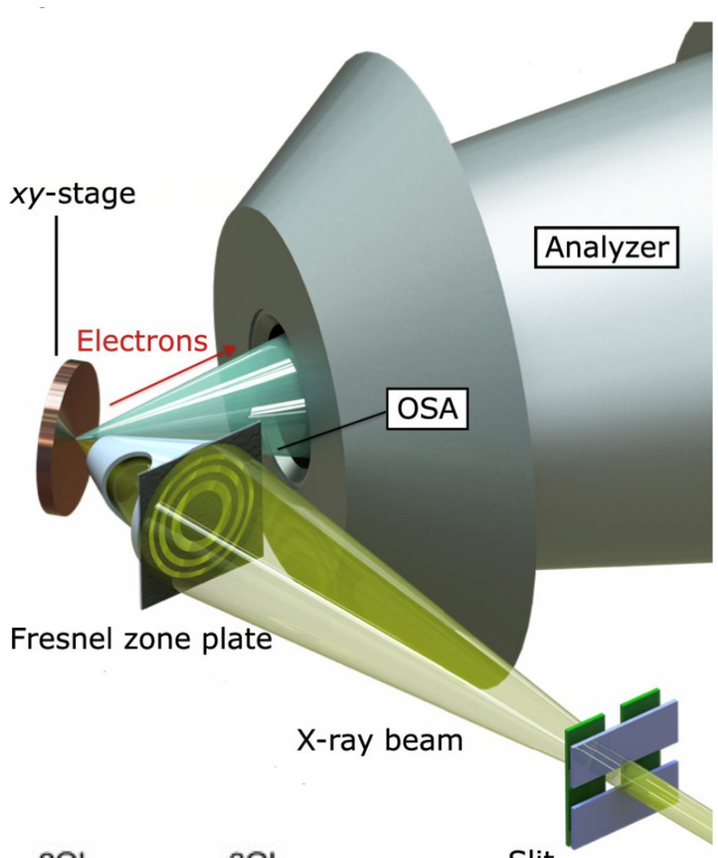

Cleaved surface of $Pb_5Bi_{24}Se_{41}$

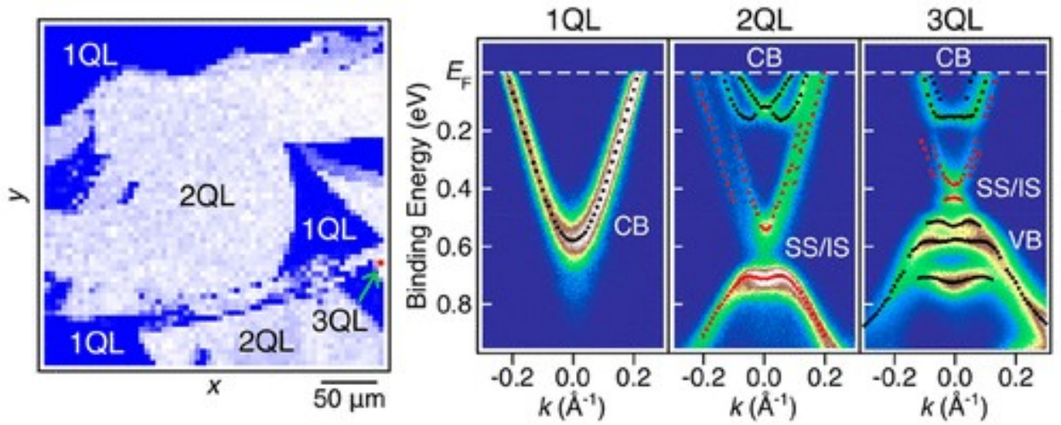

Alternate stacking of the topologically trivial insulator PbSe bilayer and four quintuple layers (QLs) of the topological insulator Bi_2Se_3

Ultramicroscopy 159, 520 (2015)

Nano Lett. 19, 6, 3737 (2019)

Photoelectron diffraction (PED)

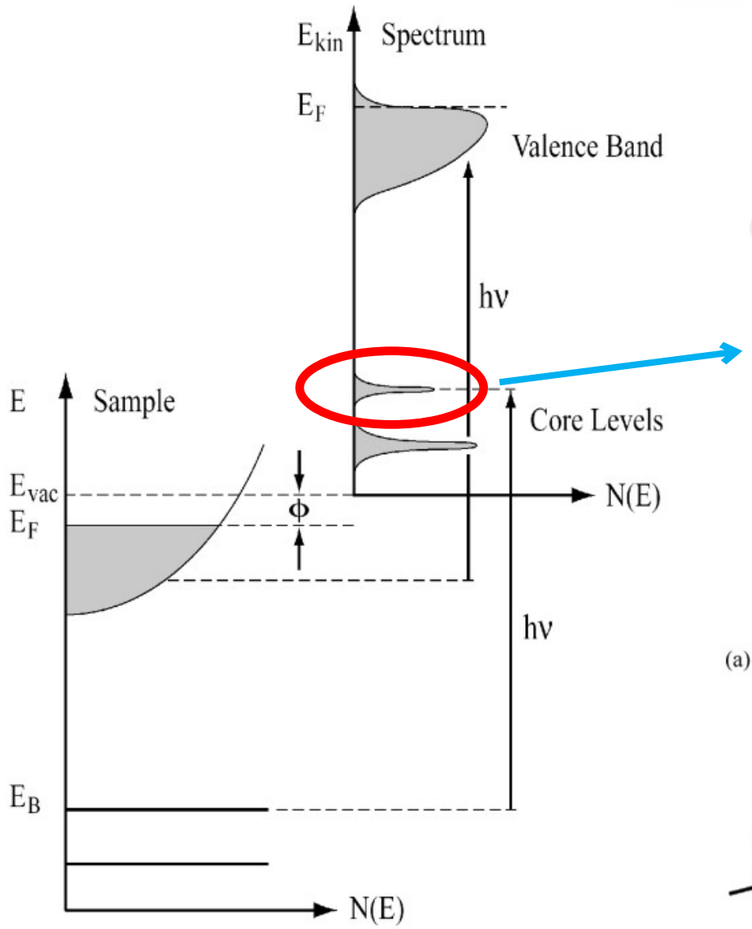

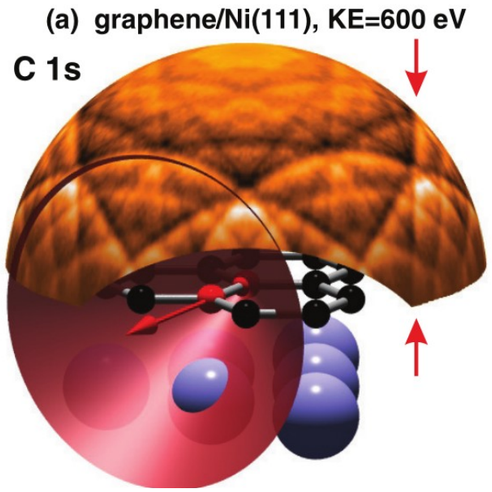

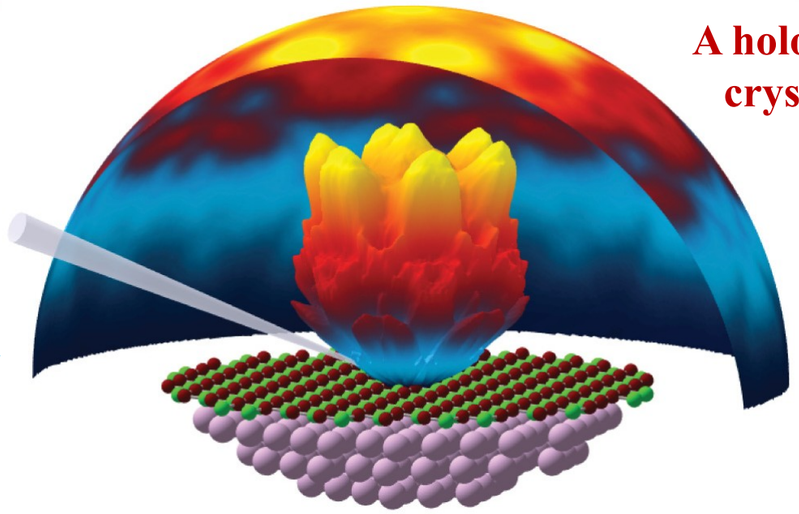

A hologram of the crystal surface

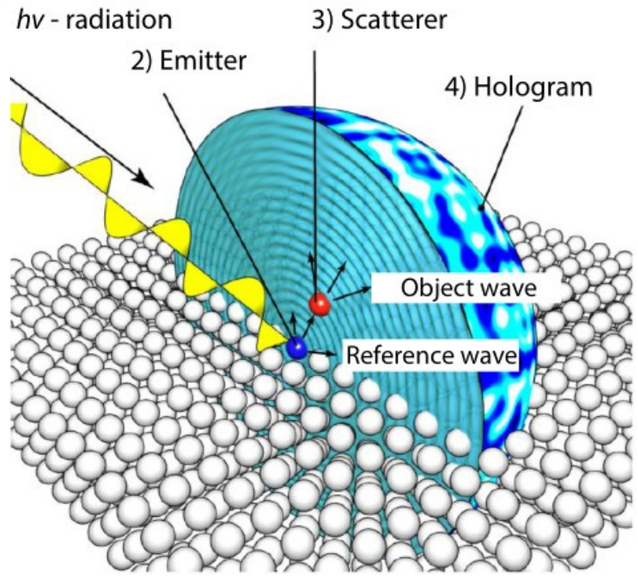

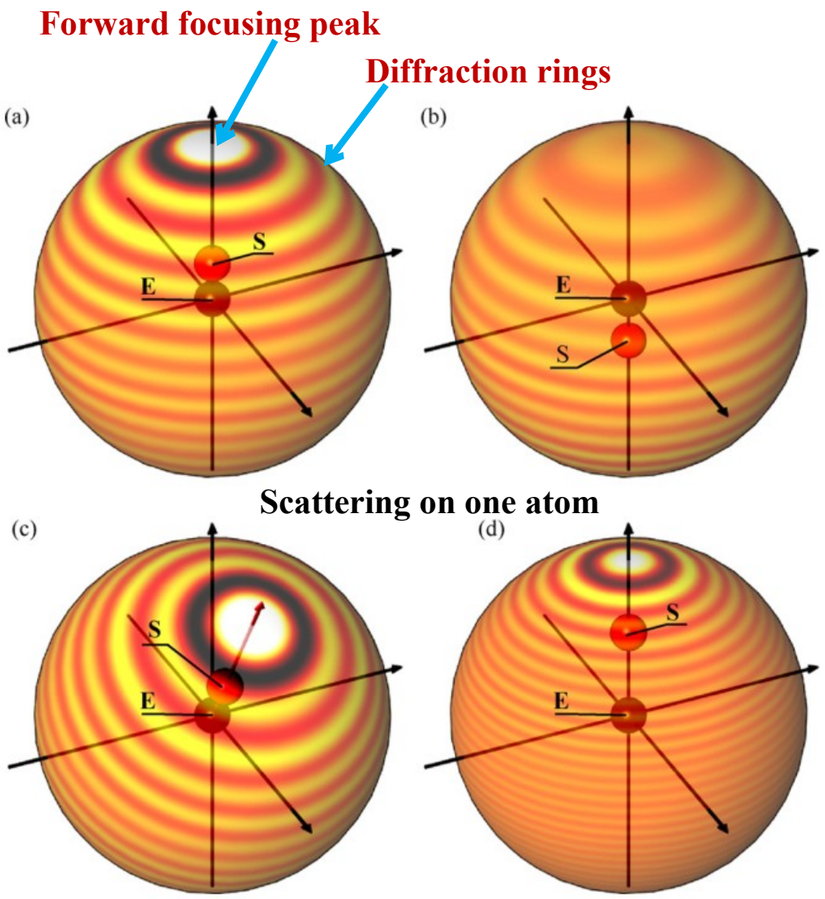

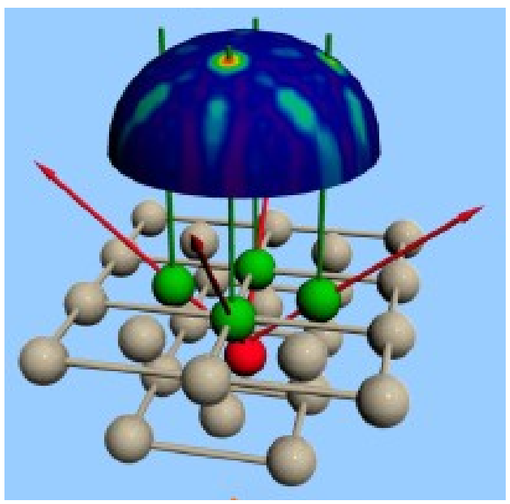

- **Atomic structure with chemical selectivity.**
- **Quantitative measurements of atomic positions. (Forward focusing peaks show us atomic rows, while diffraction rings are related to interatomic distances.)**
- **Structure of impurities (periodicity is not required).**
- **Distribution of elements between different lattice sites.**
- **Easily combined with ARPES.**

Laboratory spin-ARPES with He-lamp photon source

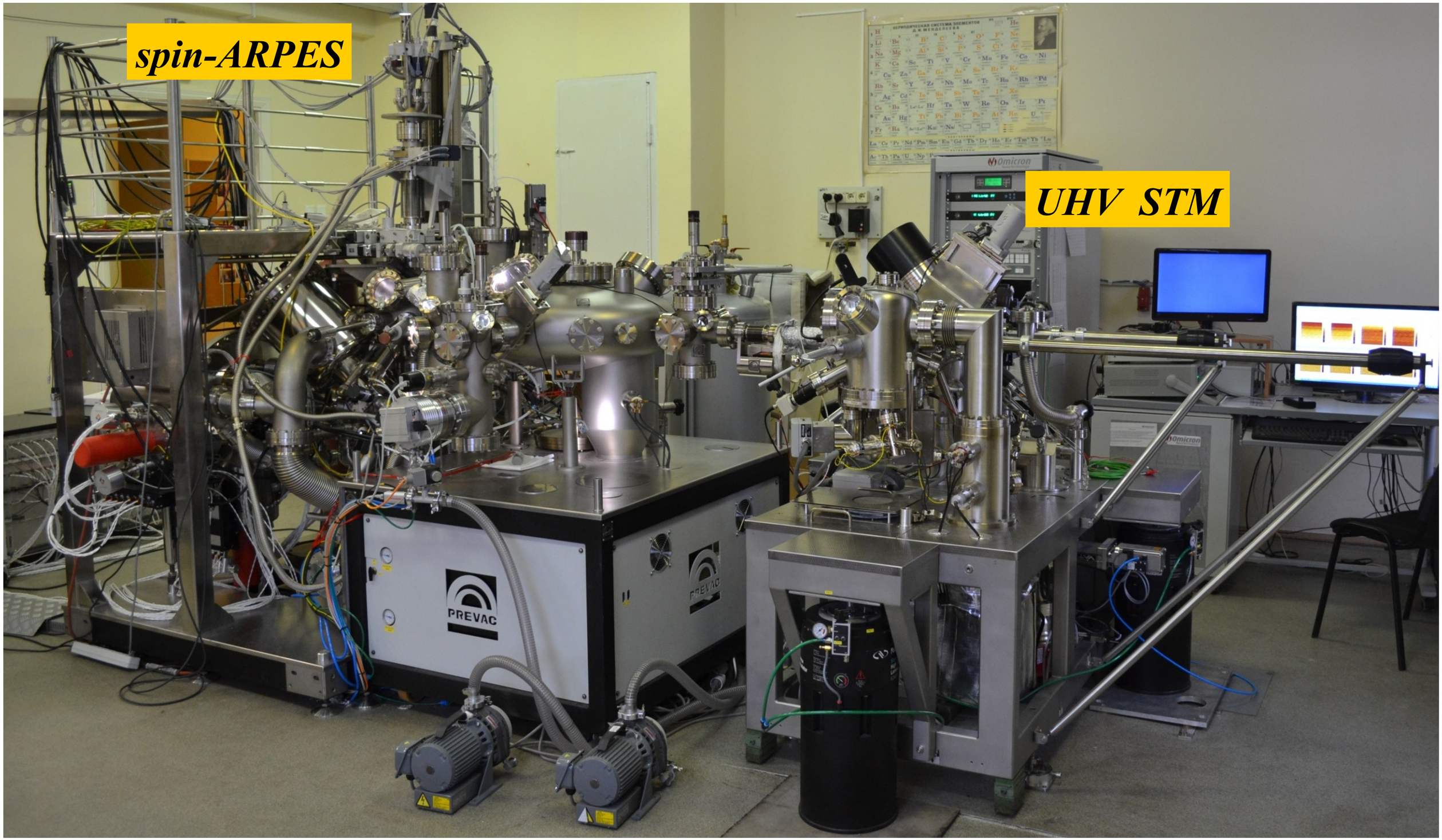

Synchrotron – advanced source of photons

ARPES station

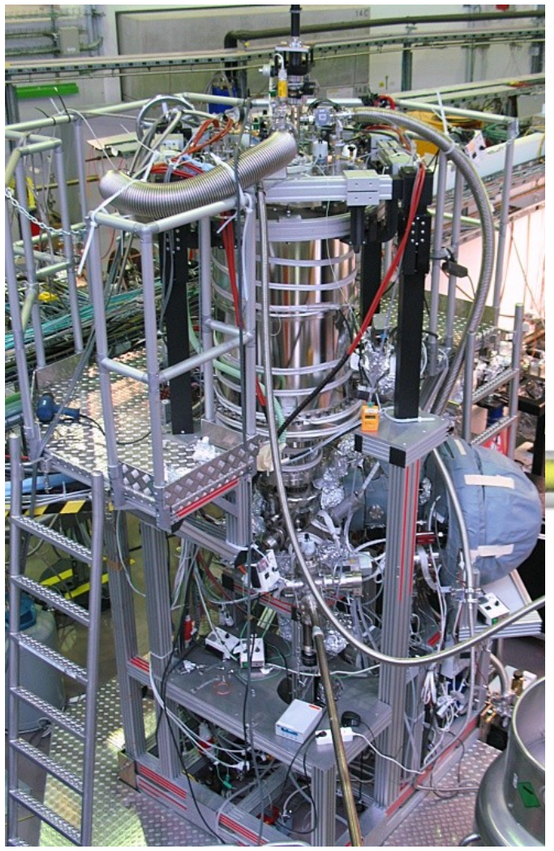

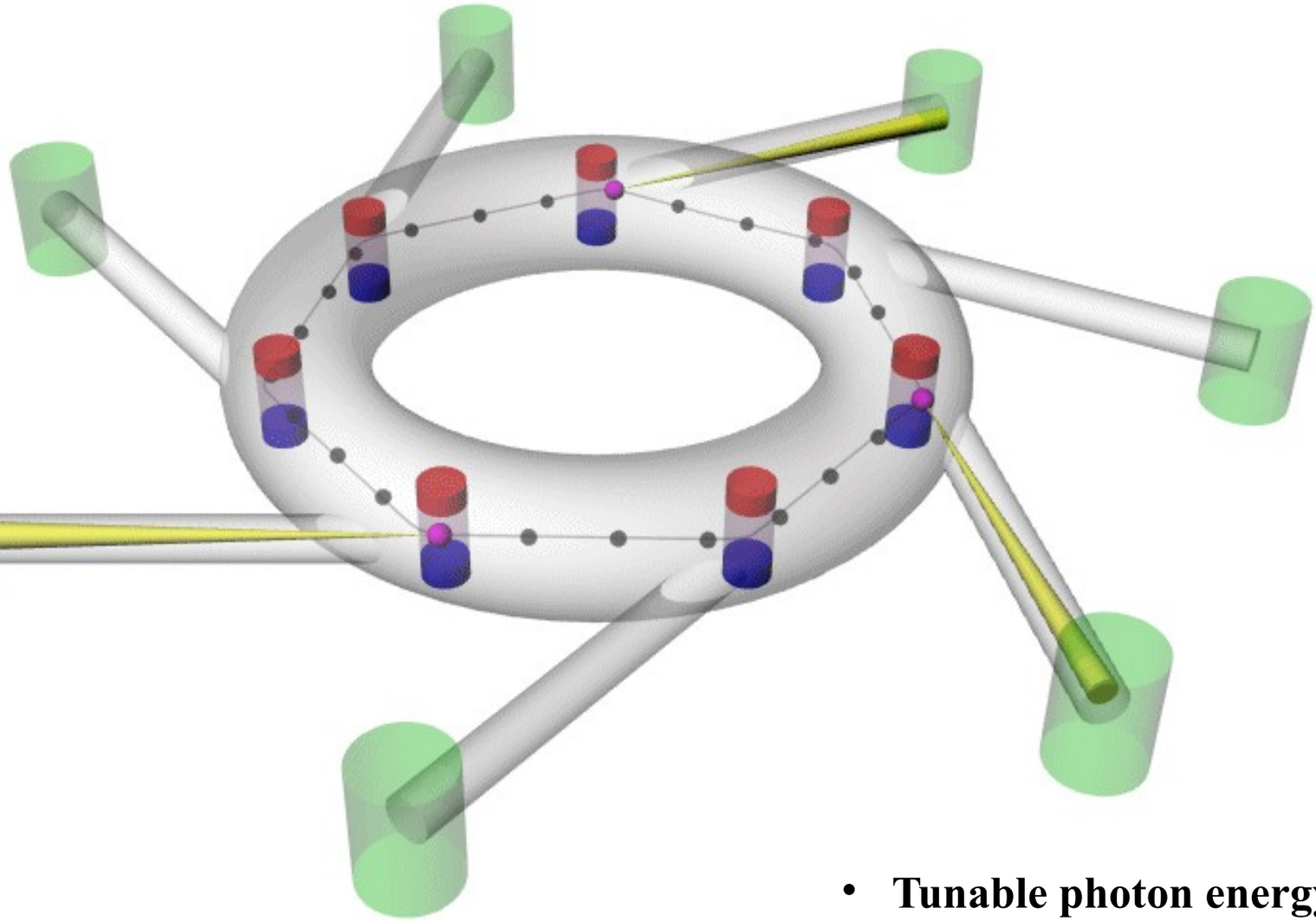

- **Tunable photon energy**
- **High photon flux**
- **Controllable polarization**
- **Well-defined time structure**
- **High coherence**

BESSY synchrotron (Berlin)

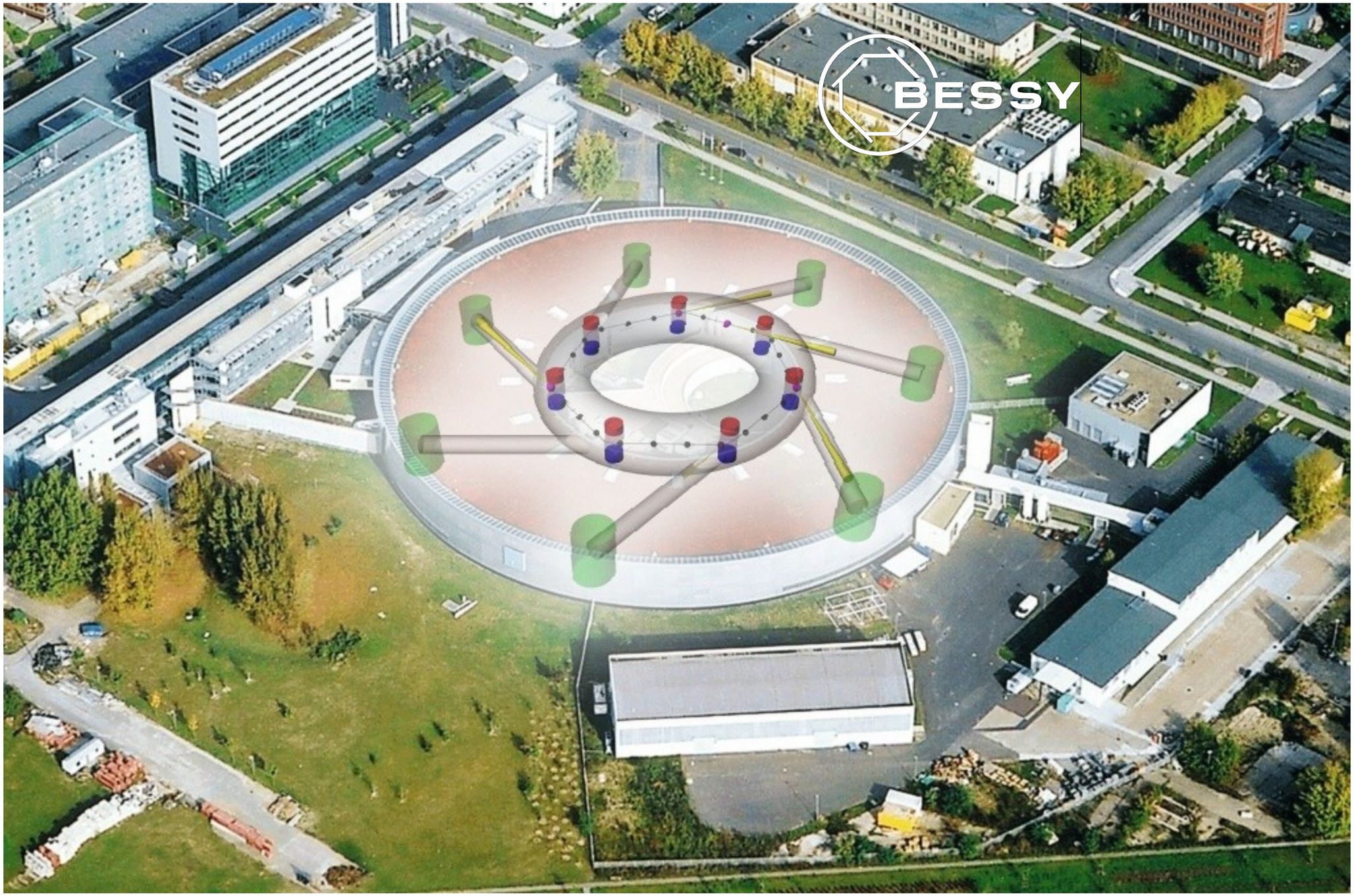

Synchrotron radiation sources worldwide

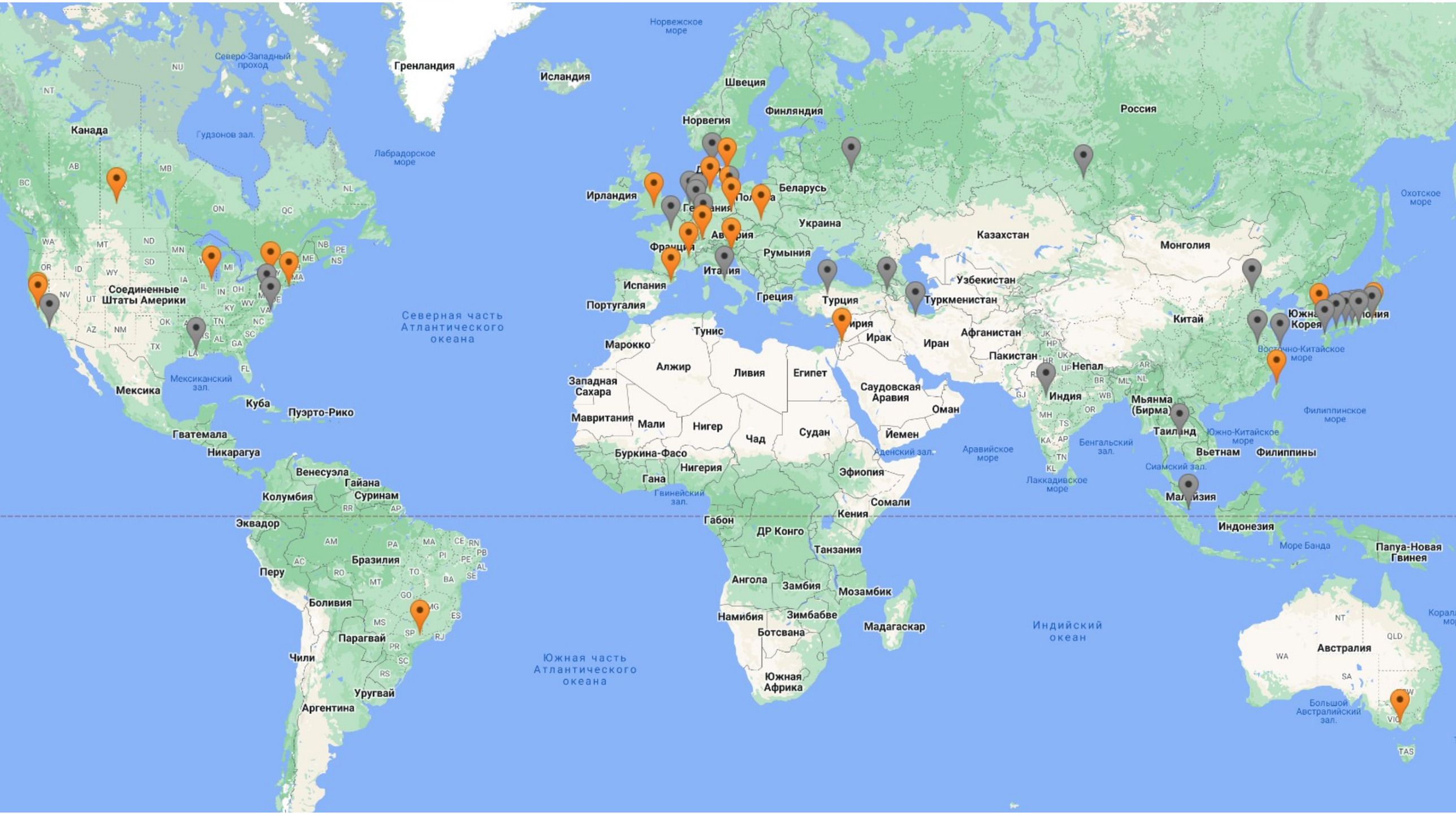

https://lightsources.org/lightsources-of-the-world/

Part 2

Electronic and spin structure at the surfaces of 4f compounds

Rare-earth elements (lanthanides)

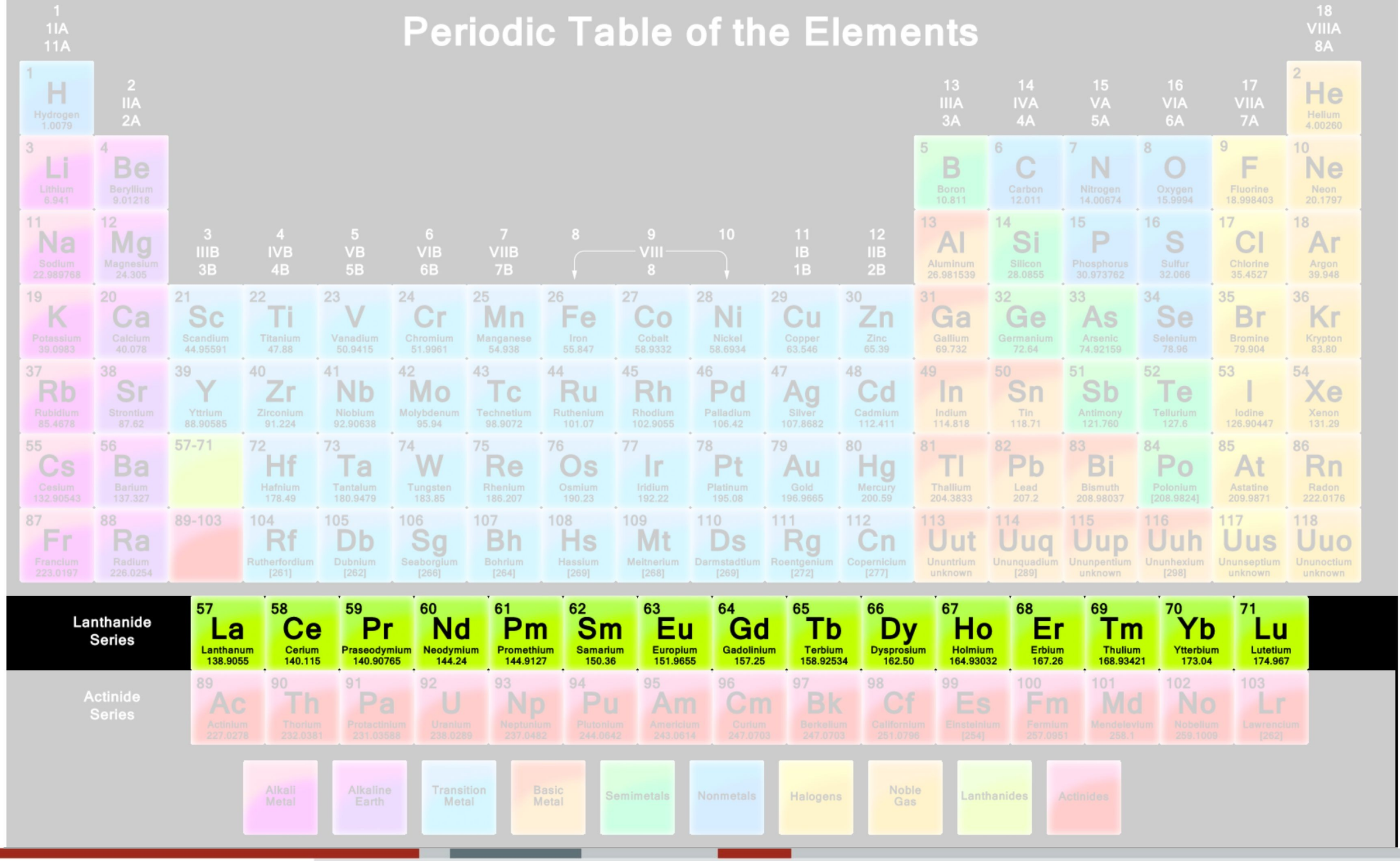

Rare-earth elements (lanthanides)

Free atom: [Xe] $4f^n$ $(5d6s)^m$ configuration

Ion in a solid: [Xe] $4f^n$ configuration

Lanthanide Series	57 La Lanthanum 138.9055	58 Ce Cerium 140.115	59 Pr Praseodymium 140.90765	60 Nd Neodymium 144.24	61 Pm Promethium 144.9127	62 Sm Samarium 150.36	63 Eu Europium 151.9655	64 Gd Gadolinium 157.25	65 Tb Terbium 158.92534	66 Dy Dysprosium 162.50	67 Ho Holmium 164.93032	68 Er Erbium 167.26	69 Tm Thulium 168.93421	70 Yb Ytterbium 173.04	71 Lu Lutetium 174.967

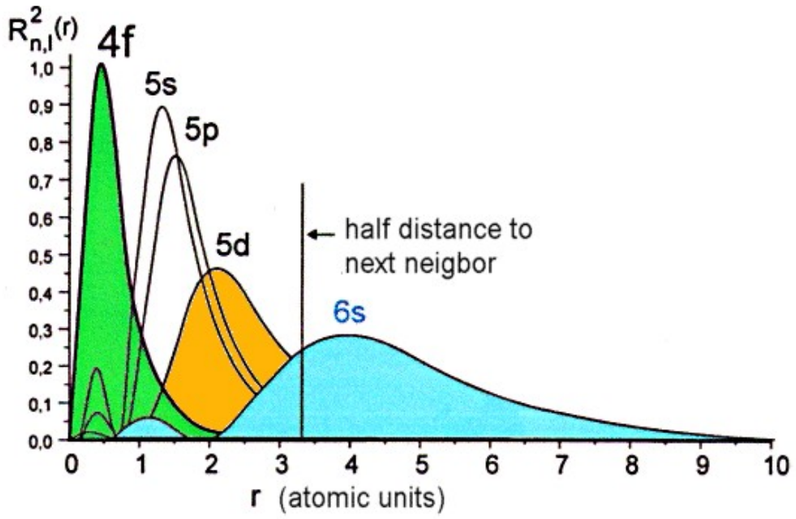

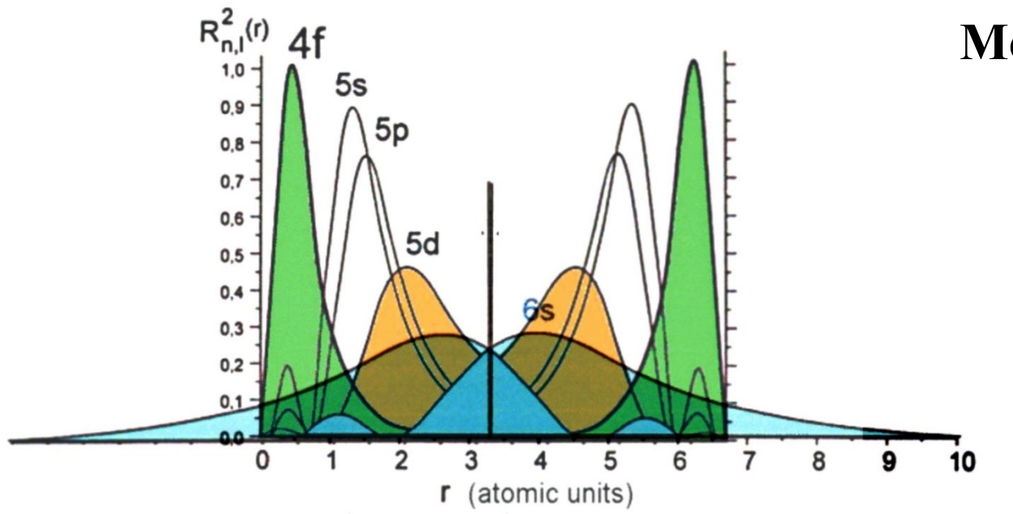

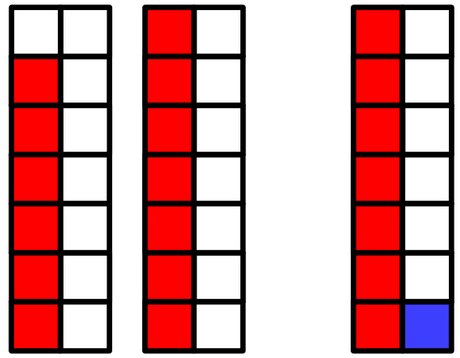

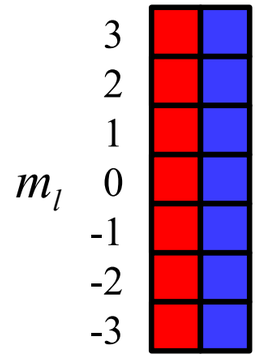

	Eu^{3+}	Eu^{2+}	Tb^{3+}	m_s	-½ ½
	$4f^6$	$4f^7$	$4f^8$		$4f^{14}$
Moment:	0	7	9 μ_B		

Band width is proportional to overlap of orbitals:

→ width of **4*f*-bands** ~ **10th of meV;**
→ **highly localized;**
→ **atomic-like magnetic moments.**

4f-states: localized or itinerant?

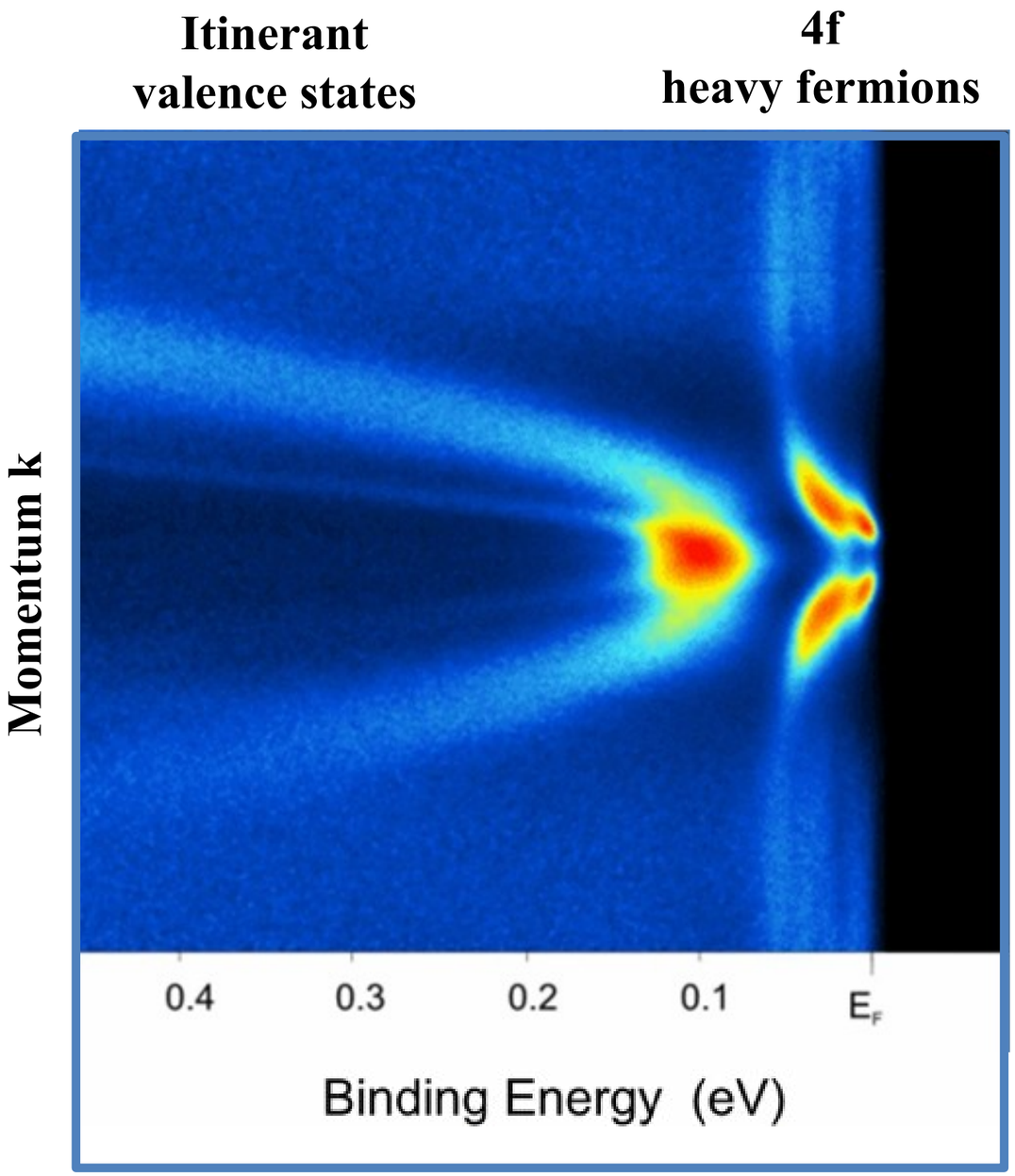

$YbRh_2Si_2$ – heavy fermion system (effective mass can be ~1000 m_e)

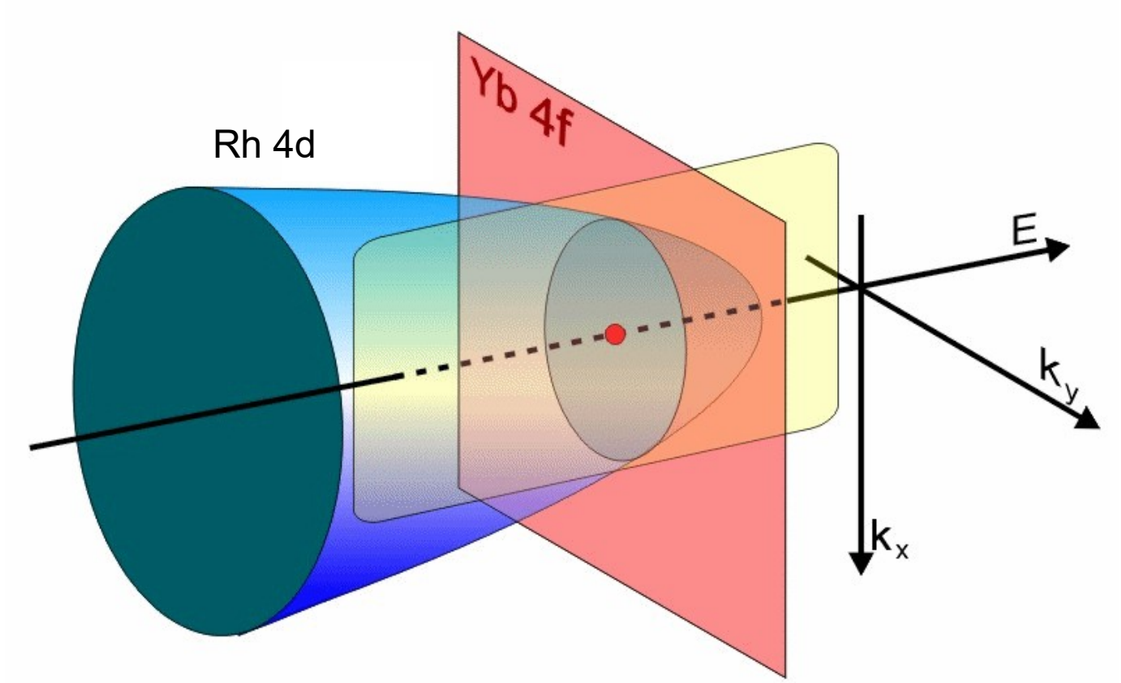

Band width is proportional to overlap of orbitals:

→ width of **4*f*-bands** ~ **10th of meV;**
→ **highly localized;**
→ **atomic-like magnetic moments.**

D. V. Vyalikh et al., PRL (2010)

Motivation

ARPES is the most direct probe of the electronic structure, but it is surface-sensitive. So it is important to understand how to distinguish the bulk an surface electronic and magnetic properties

Objects:

[RE] $[T]_2$ Si_2 layered compounds where

RE = Rare Earth metal – provides magnetic moment,

T = Transition metal [Rh, Ir, Pd, Co, Ni etc.].

Easily cleaved in situ.

Possess well-defined crystal terminations.

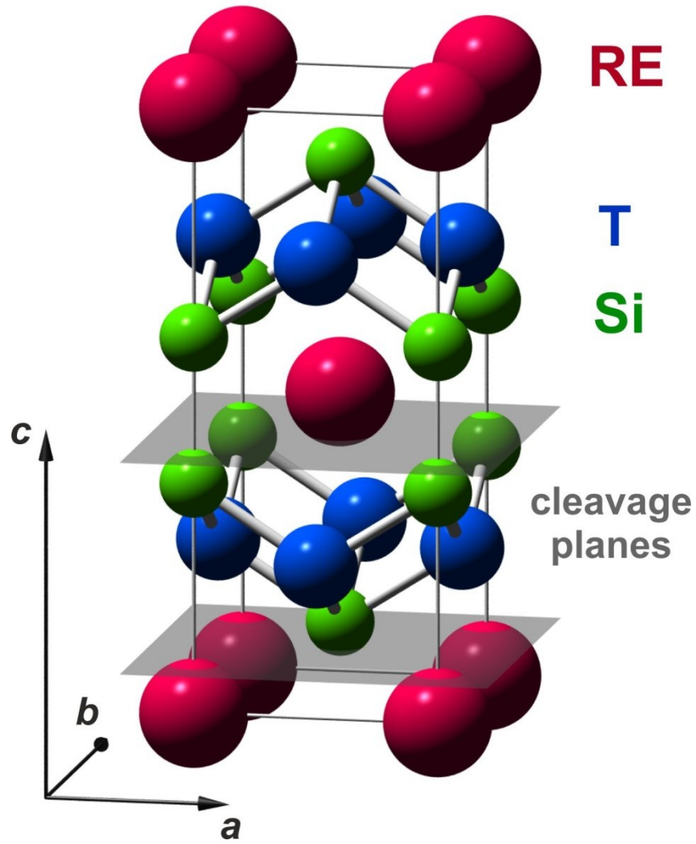

$TbRh_2Si_2$:

Bulk: *antiferromagnetic (AFM) below 94 K,*

Tb^{3+}: L=S=3, J=6 – split in CEF

Surface: *also Tb^{3+}*

$EuIr_2Si_2$:

Bulk: *Eu valency – noninteger, about 2.8 at low T*

Eu^{3+}: L=S=3, J=0 – no CEF splitting

No magnetic moment

Surface: *Eu^{2+}, L=0, J=S=7/2 – no CEF splitting*

Strong magnetic moment

Sample cleavage

$TbRh_2Si_2$: 4f XPS and ARPES

ARPES at low T (linear polarization)

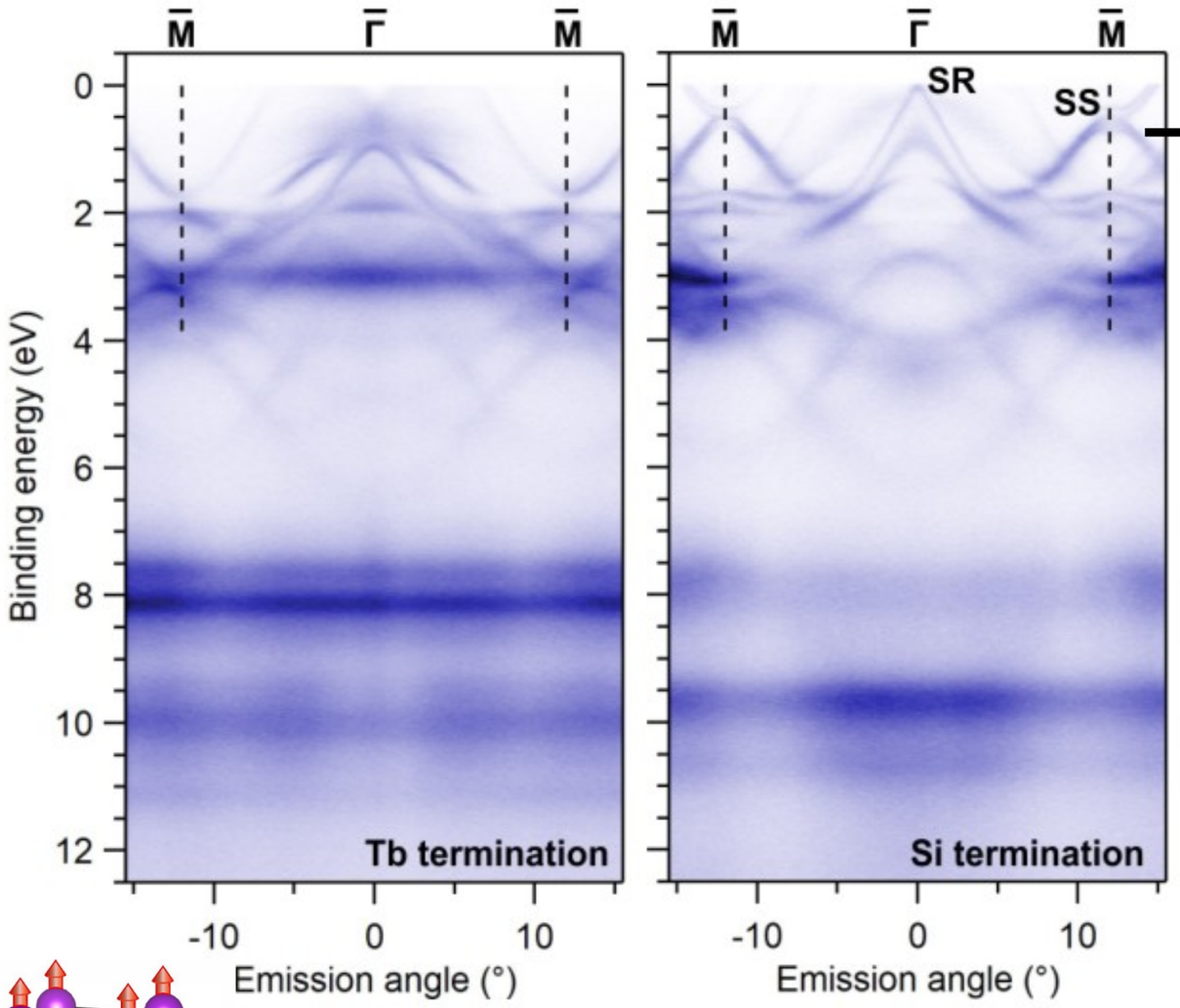

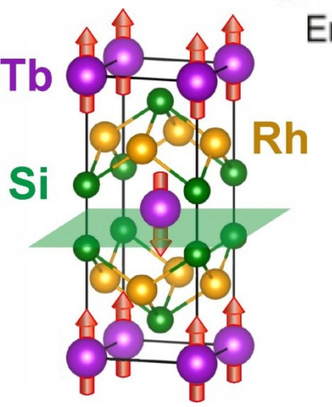

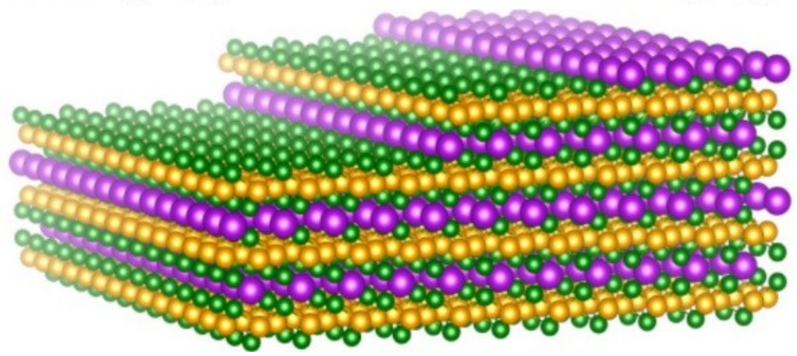

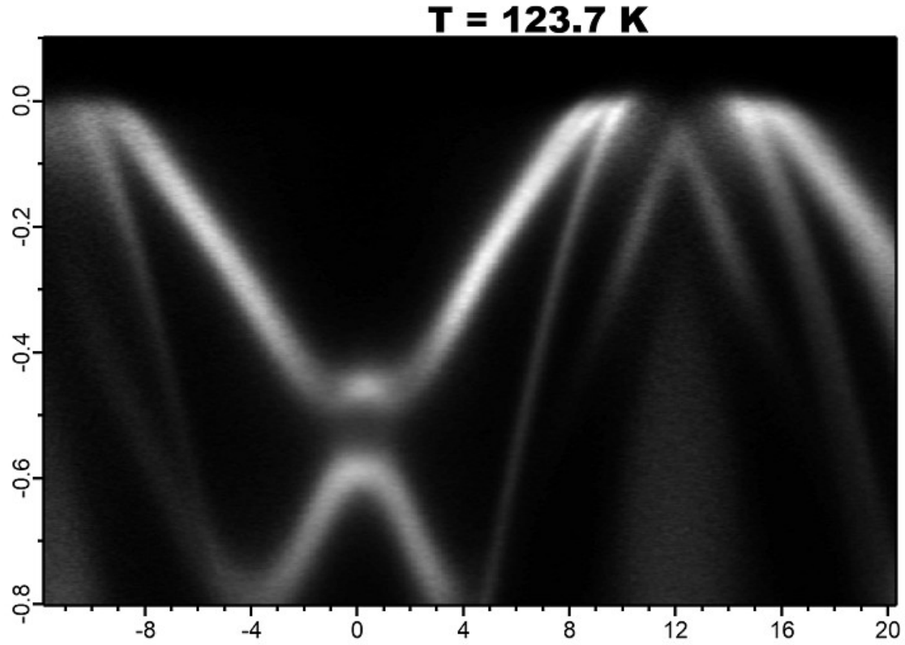

Surface states on Si termination show magnetic ordering, but there are no well-defined surface states on Tb surface

DFT predicts spin structure with triple winding of spin

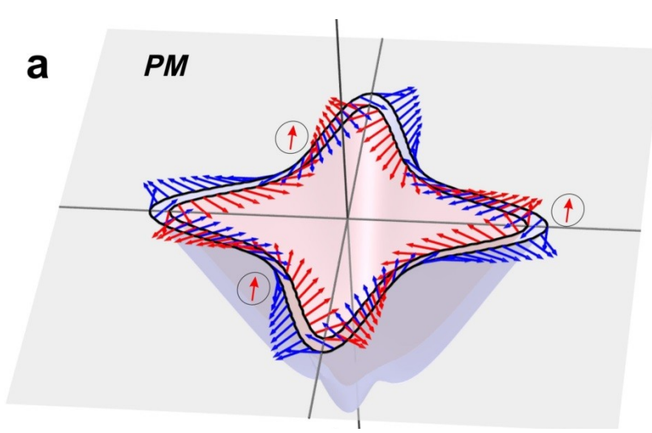

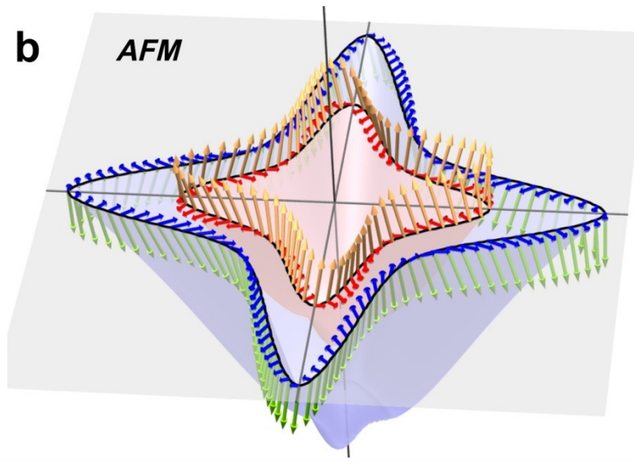

D. Usachov et al., PRL 124, 237202 (2020)

$TbRh_2Si_2$: spin-ARPES study of surface states

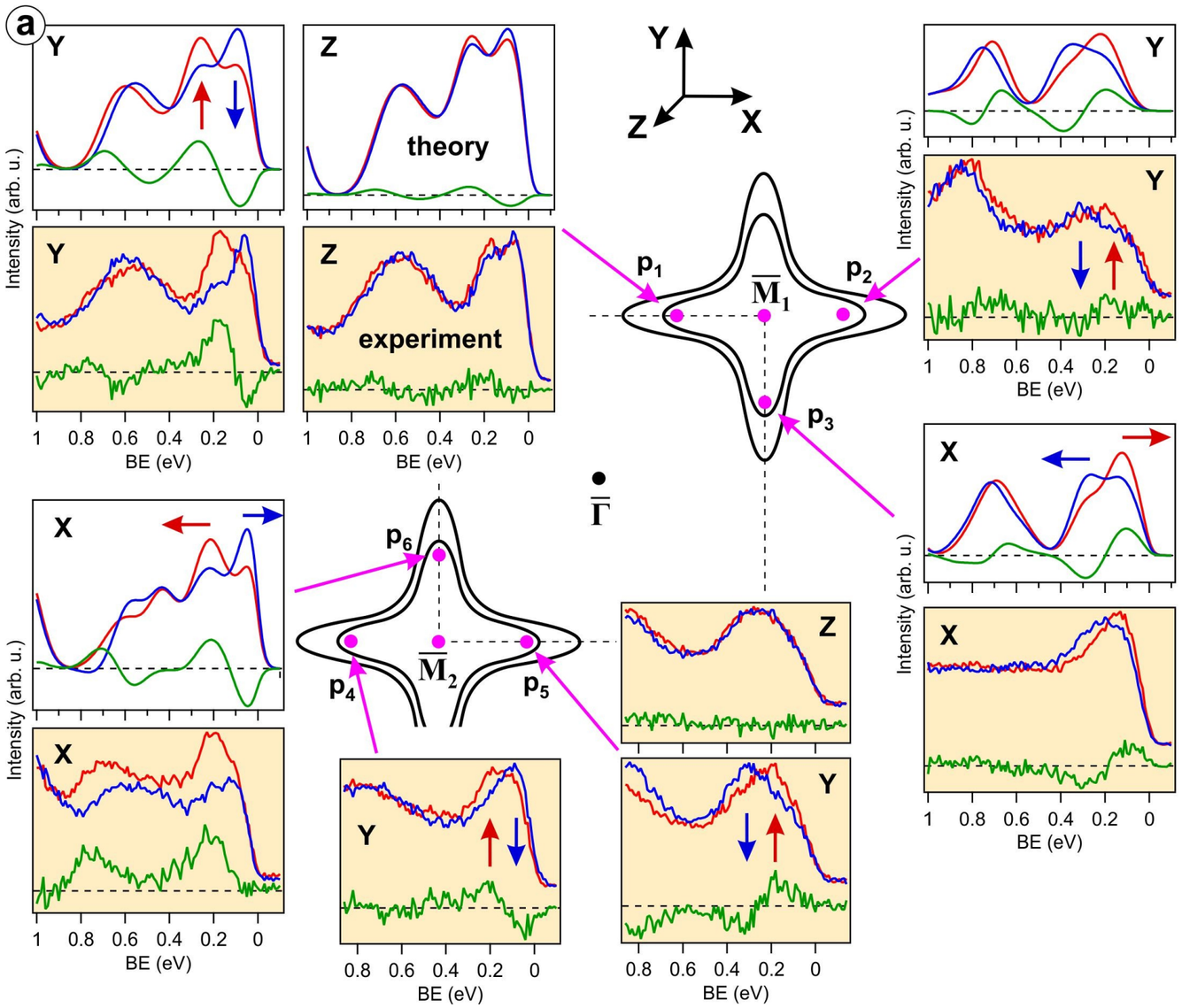

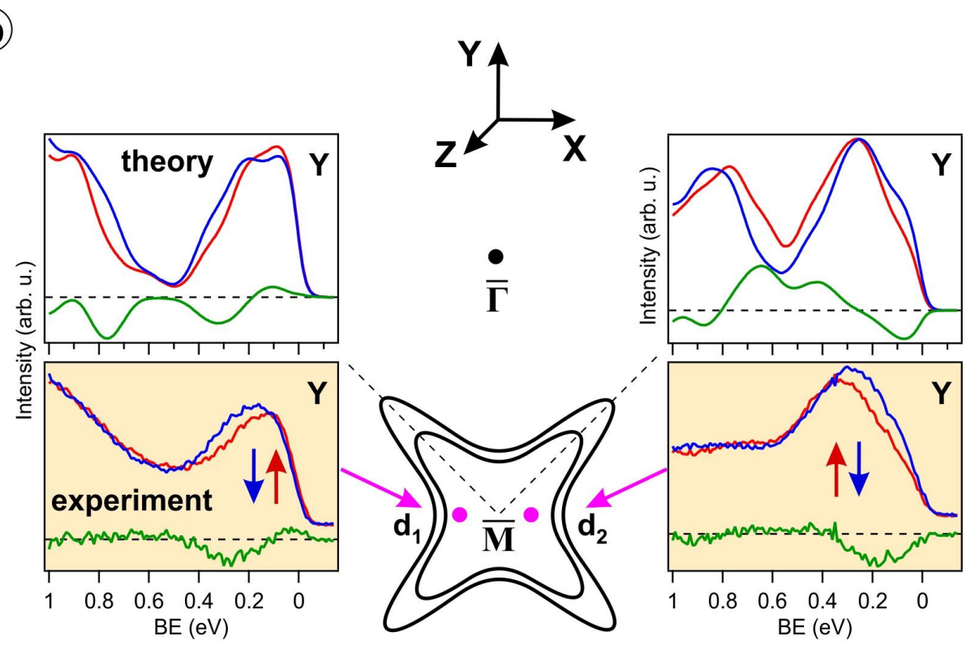

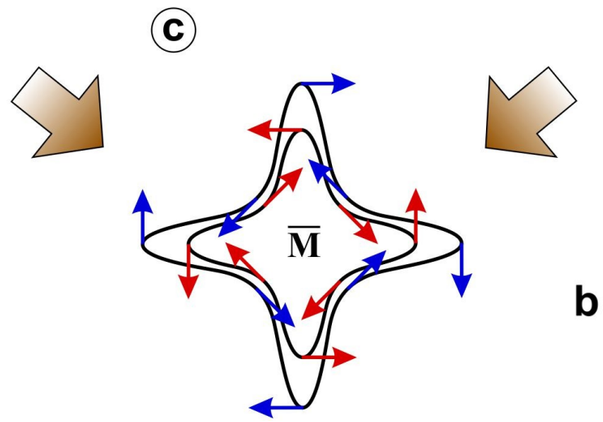

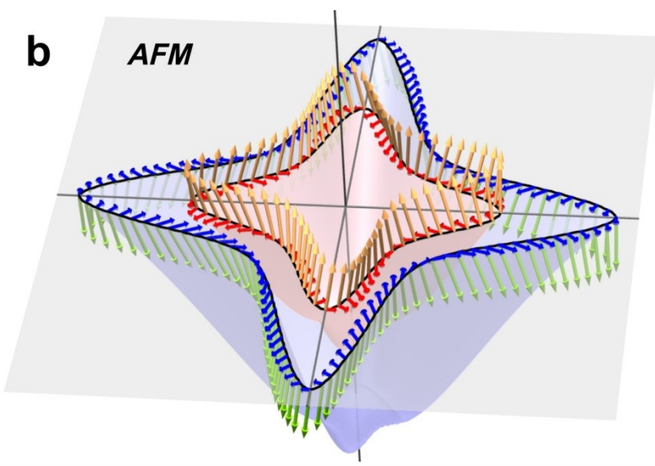

Spin-ARPES measurements confirm the predicted spin structure

D. Usachov et al., PRL 124, 237202 (2020)

Origin of spin structure: k·p model

Classical Rashba effect (linear in k)

$$H_{\mathrm{R}}^{(1)} = i\alpha(k_-\sigma_+ - k_+\sigma_-) = \alpha\boldsymbol{\sigma}\cdot\boldsymbol{\mathcal{B}}_{\mathrm{R}}^{(1)}$$

$$\boldsymbol{\mathcal{B}}_{\mathrm{R}}^{(1)} = k(\sin\varphi_{\mathbf{k}}, -\cos\varphi_{\mathbf{k}}, 0)$$

$$k_\pm = k_x \pm ik_y,\ \sigma_\pm = (\sigma_x \pm i\sigma_y)/2$$

$$\boldsymbol{\sigma} = (\sigma_x, \sigma_y, \sigma_z)$$ **- Pauli matrices**

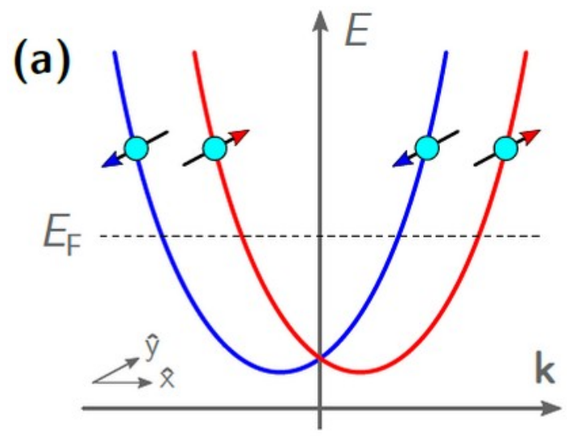

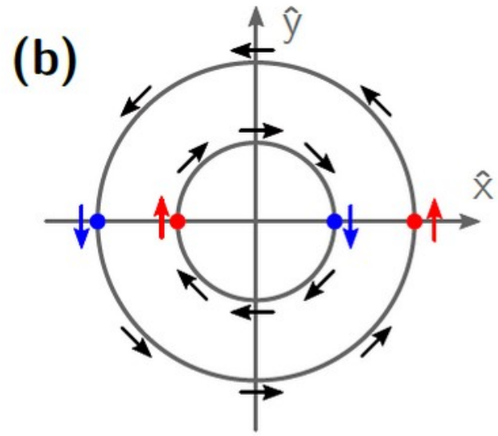

Cubic Rashba effect

$$H_{\mathrm{R}}^{(3)} = i\gamma(k_-^3\sigma_+ - k_+^3\sigma_-) = \gamma\boldsymbol{\sigma}\cdot\boldsymbol{\mathcal{B}}_{\mathrm{R}}^{(3)}$$

$$\boldsymbol{\mathcal{B}}_{\mathrm{R}}^{(3)} = k^3(\sin 3\varphi_{\mathbf{k}}, -\cos 3\varphi_{\mathbf{k}}, 0)$$

Cubic Rashba effect in our samples

$$H^{(3)} = i\gamma(k_-^3\sigma_- - k_+^3\sigma_+) = \gamma\boldsymbol{\sigma}\cdot\boldsymbol{\mathcal{B}}^{(3)}$$

$$\boldsymbol{\mathcal{B}}^{(3)} = k^3(\sin 3\varphi_{\mathbf{k}}, \cos 3\varphi_{\mathbf{k}}, 0)$$

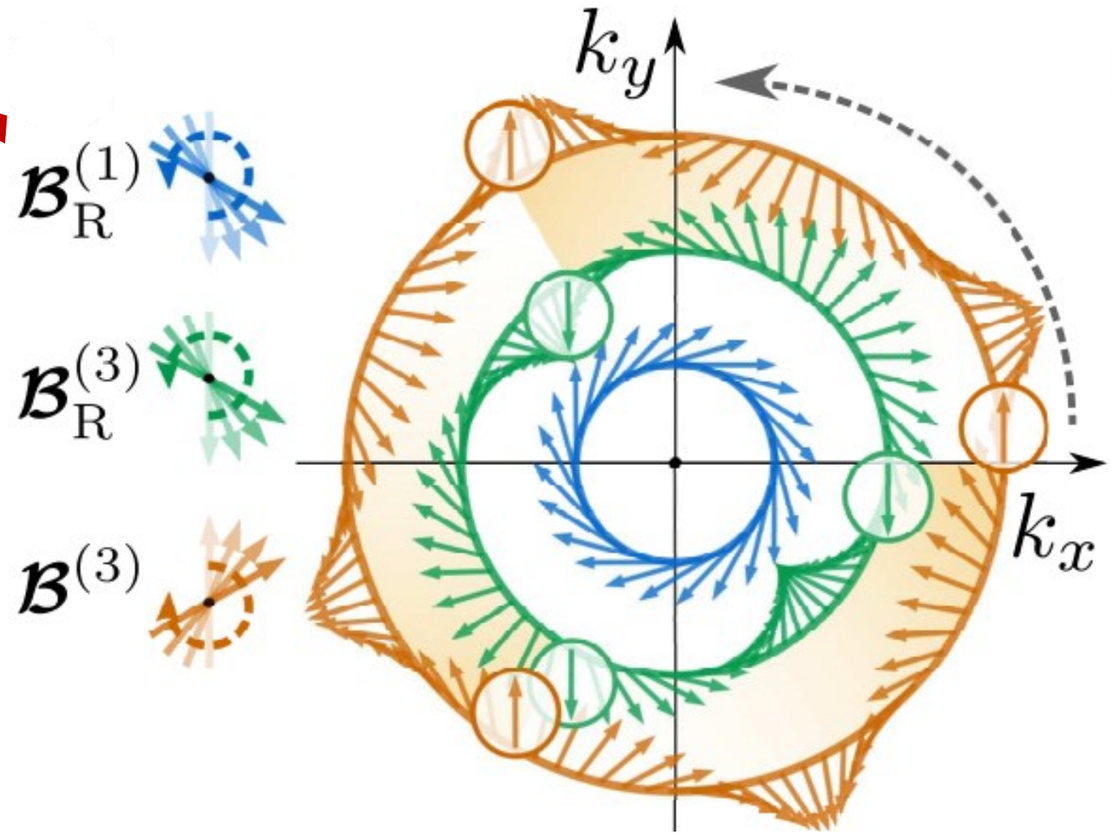

I. A. Nechaev, PRB 2018

D. Usachov et al., PRL 2020

$TbRh_2Si_2$: 4f XPS/ARPES

ARPES at low T (linear polarization)

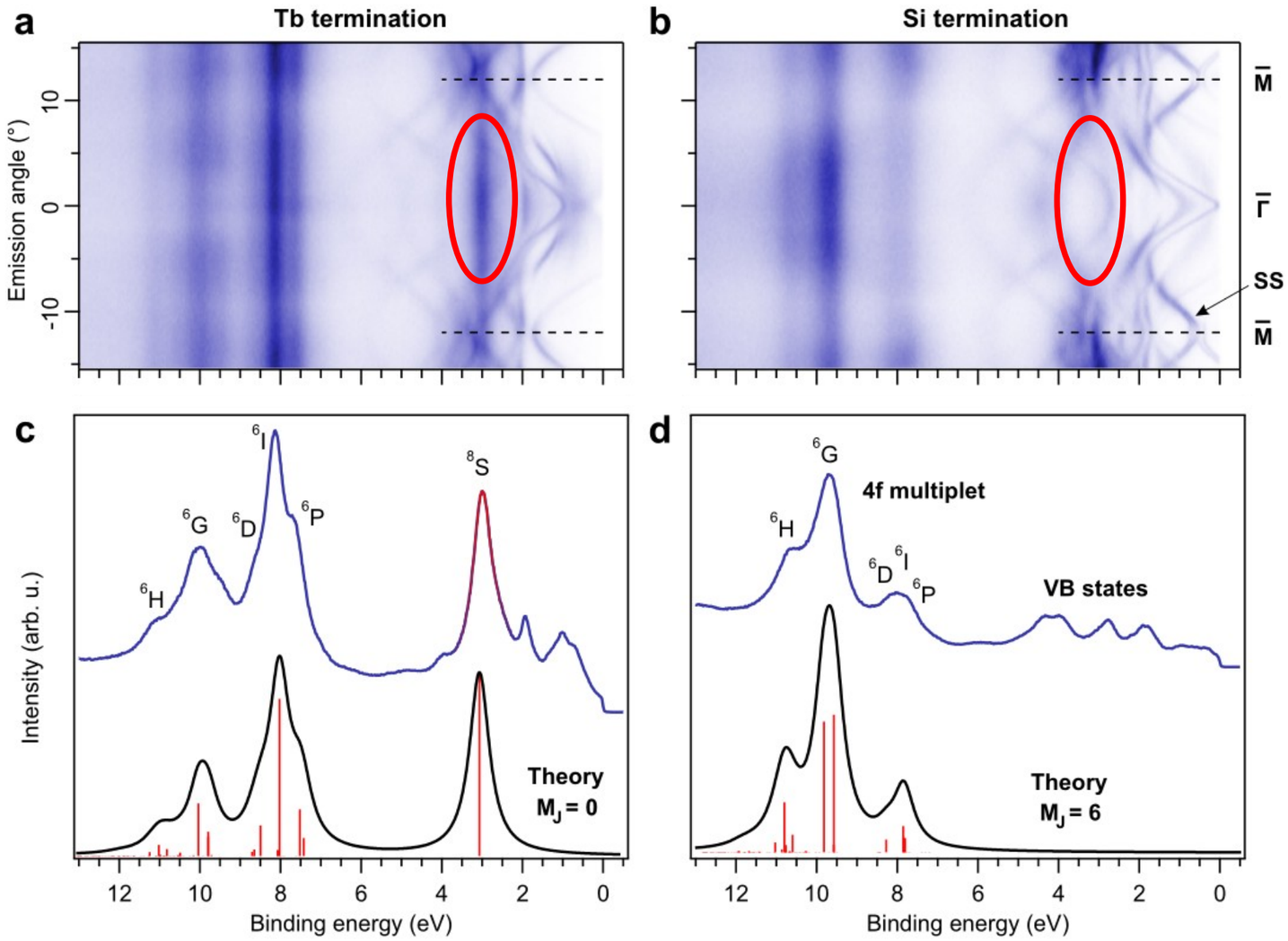

The moments are in-plane

The moments are oriented out-of-plane (as in the bulk)

Calculated normal-emission standard-geometry spectra for different M_J

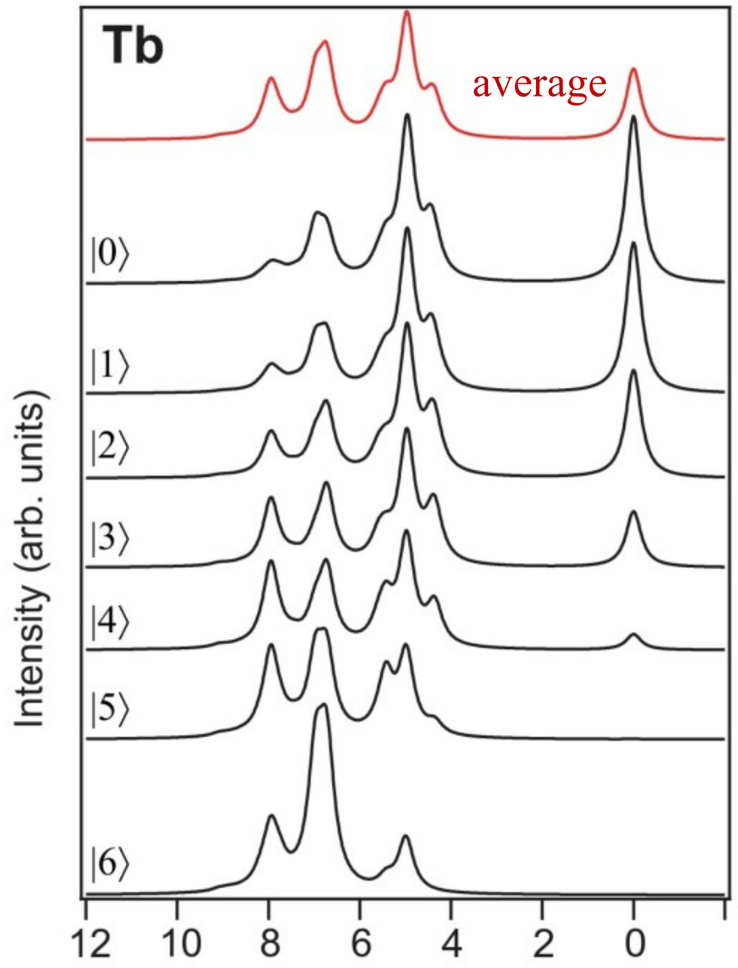

D. Usachov et al., J Phys. Chem. Lett. 2022

Estimating orientation of 4f moments

4f spectra allow to estimate qualitatively the orientation of the 4f-moments

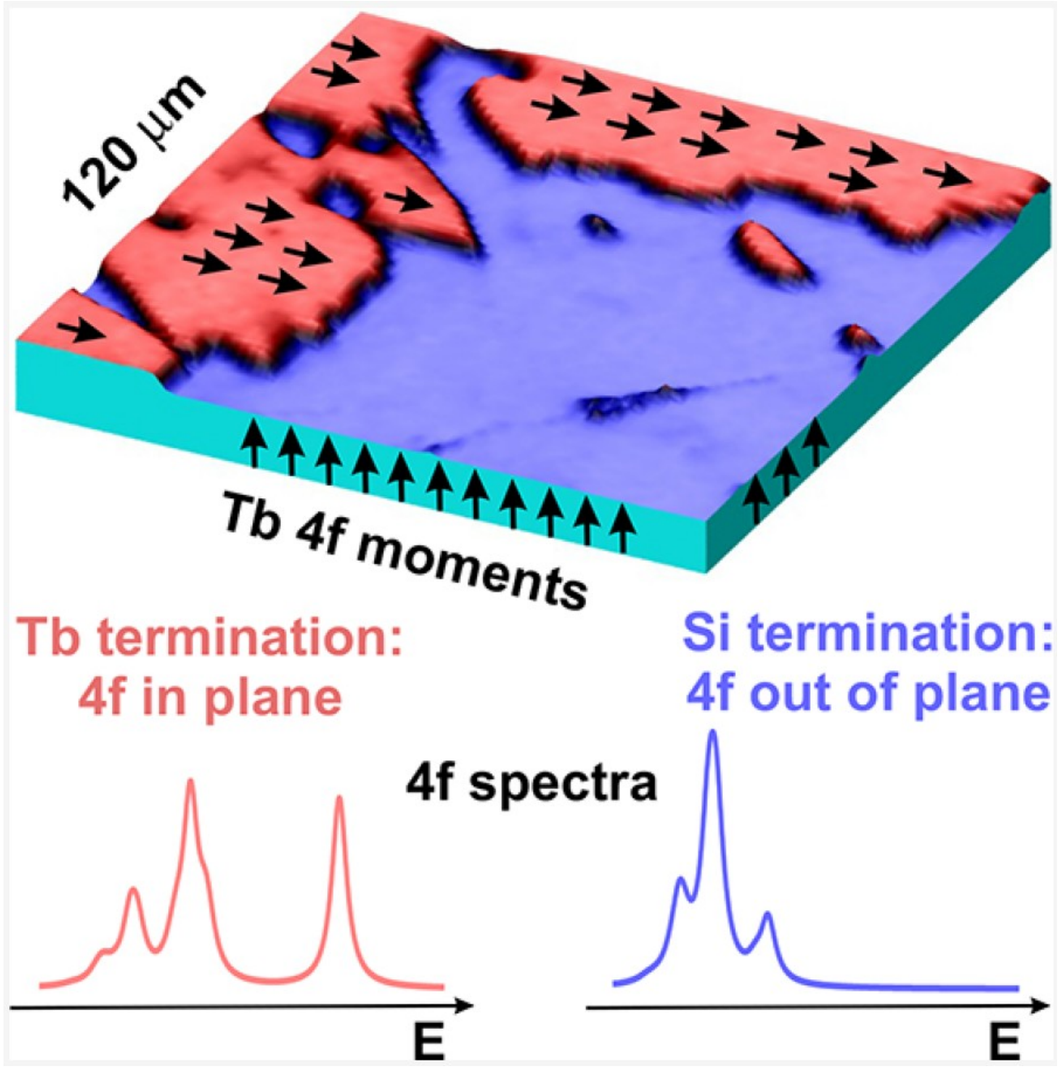

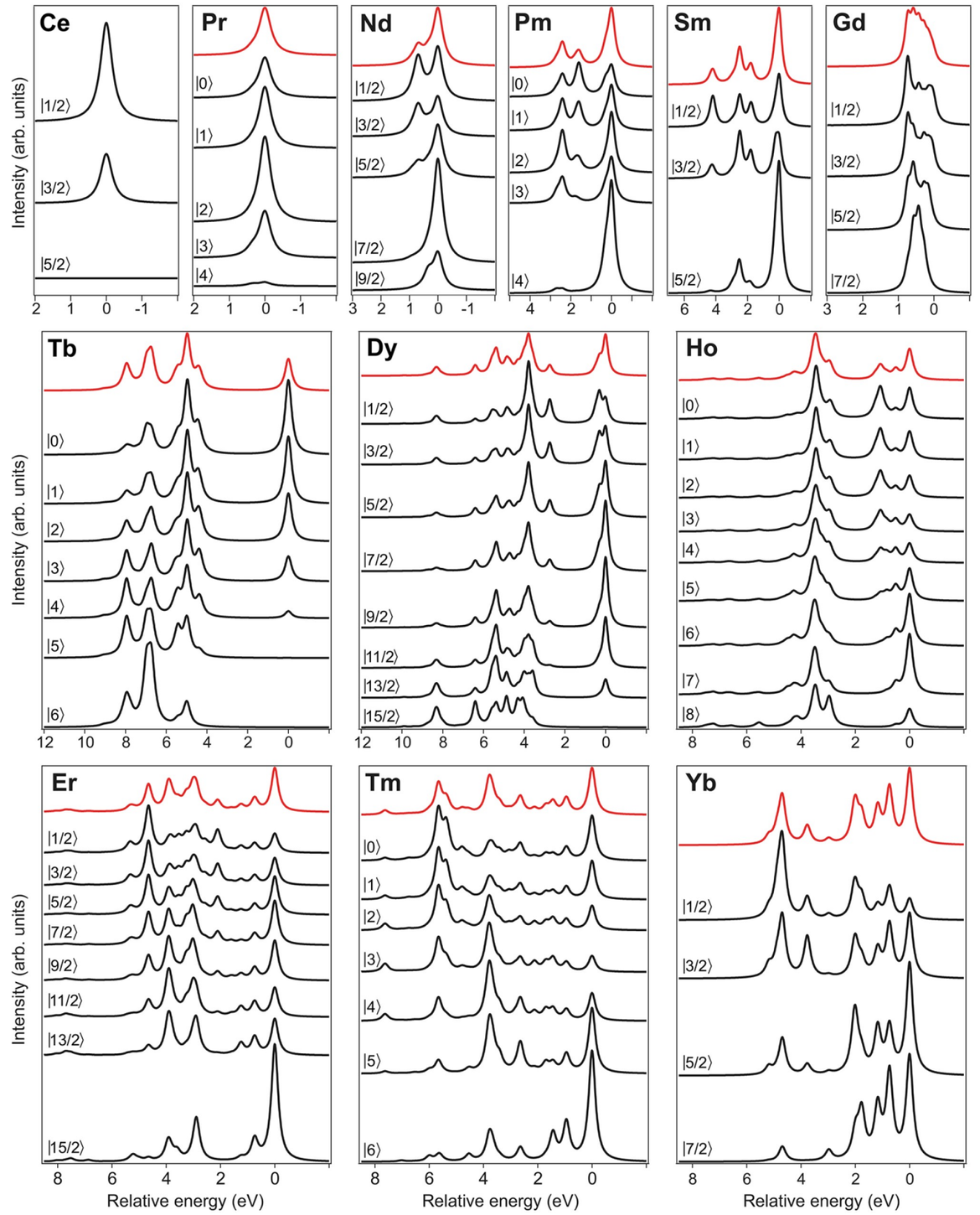

D. Usachov et al., J Phys. Chem. Lett. 2022

$TbRh_2Si_2$: what orients the moments?

Crystal electric field (CEF) orients the Tb moments

4f shell density:

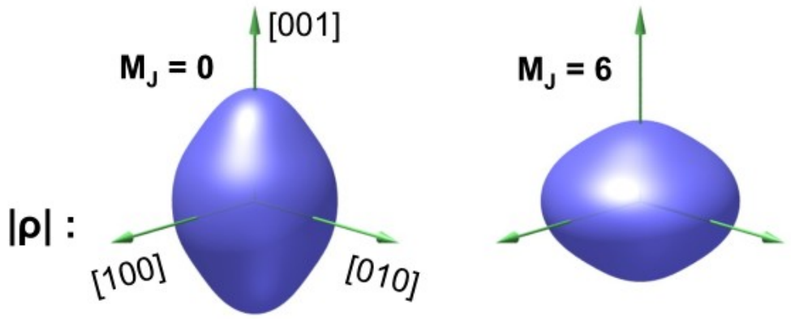

CEF:

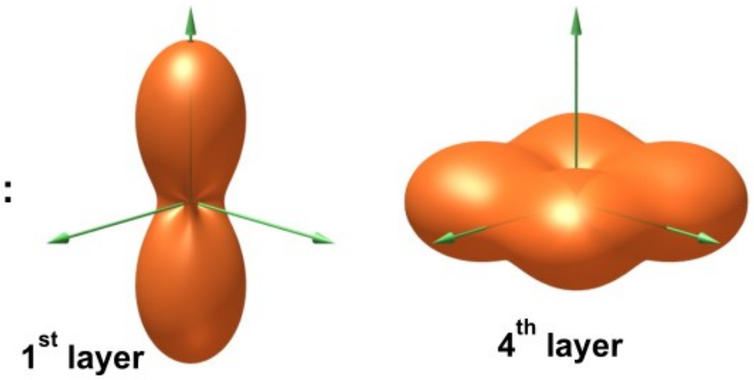

CEF at the surface is very different from CEF in the bulk

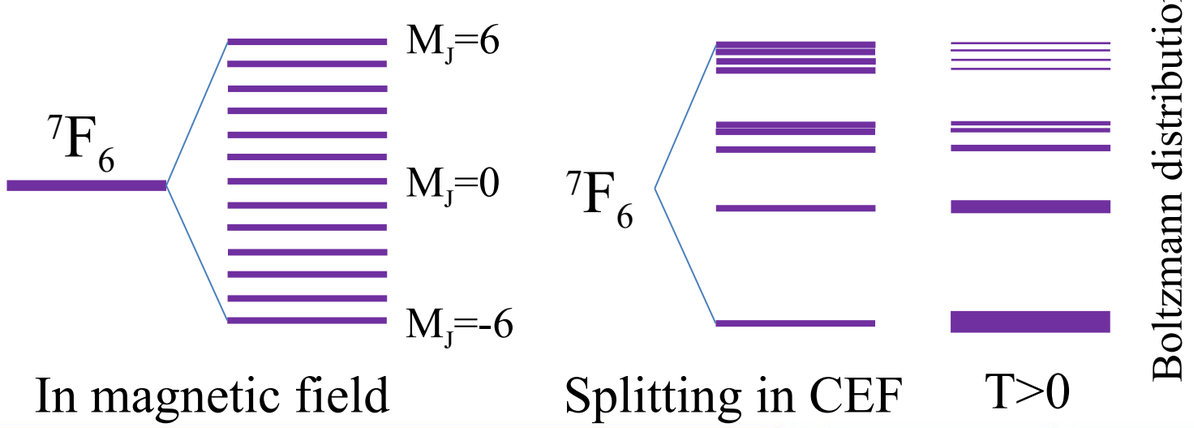

T-dependence of 4f spectra (Si termination)

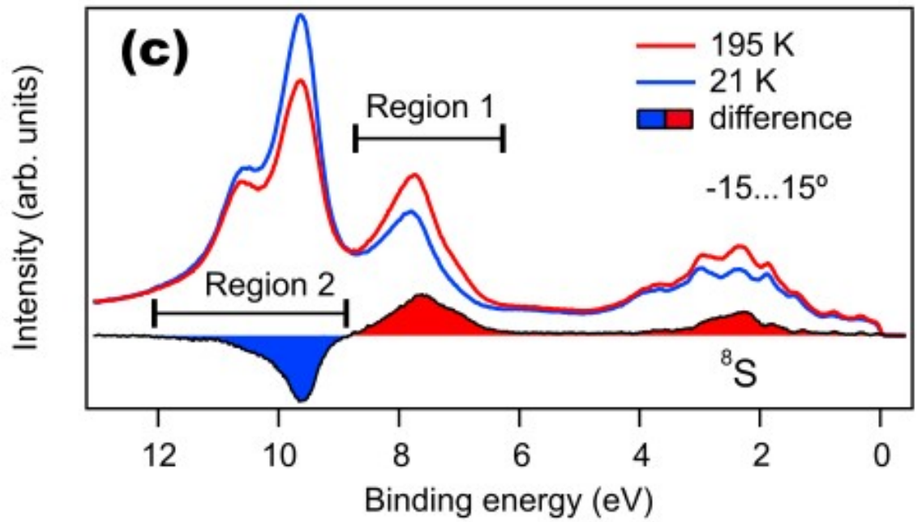

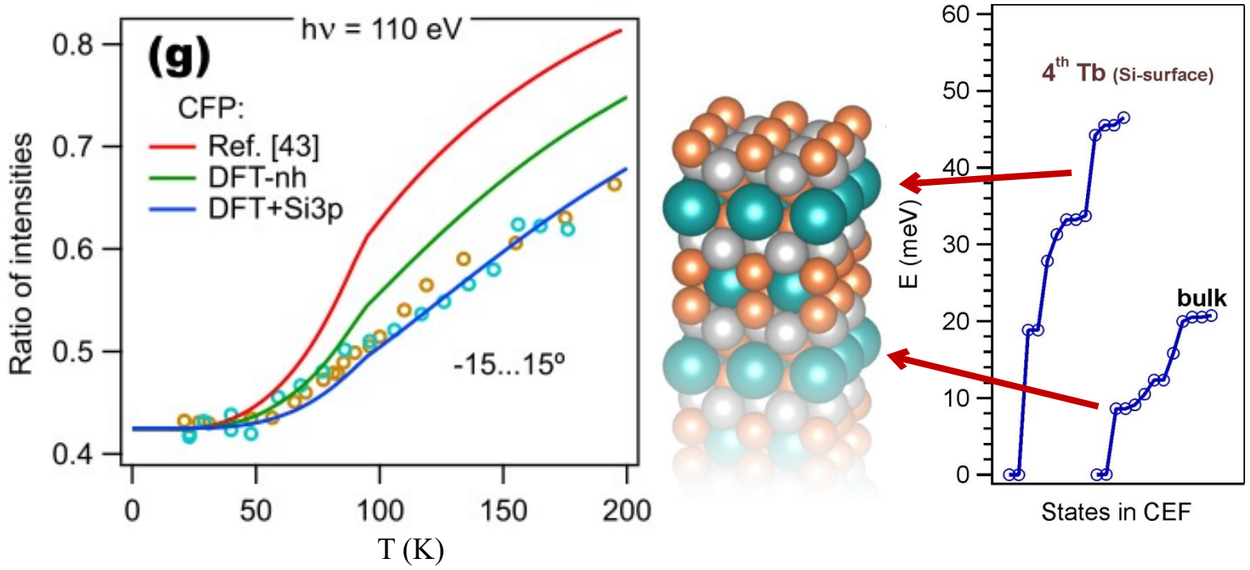

T-dependence of 4f spectra allows to estimate the CEF splitting

A. Tarasov, D. Usachov et al., PRB 2022

Temperature-dependent canting of moments in $HoRh_2Si_2$

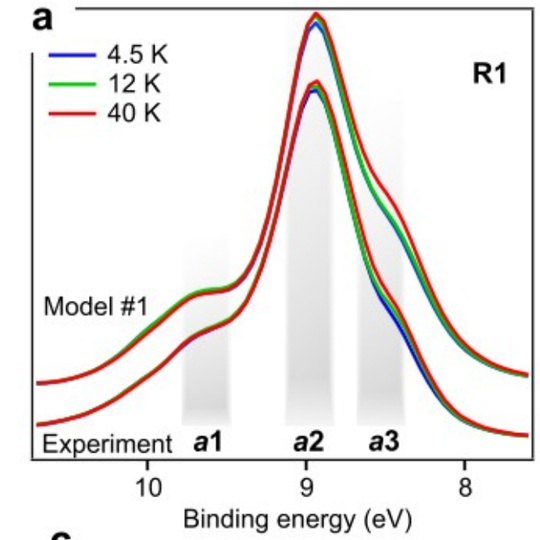

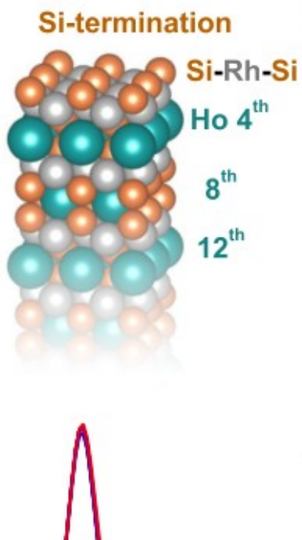

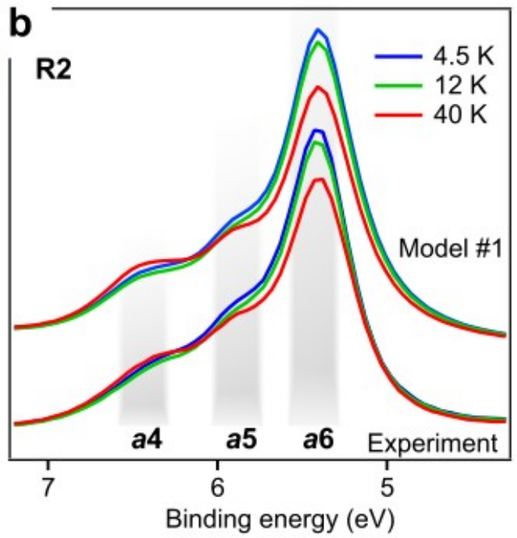

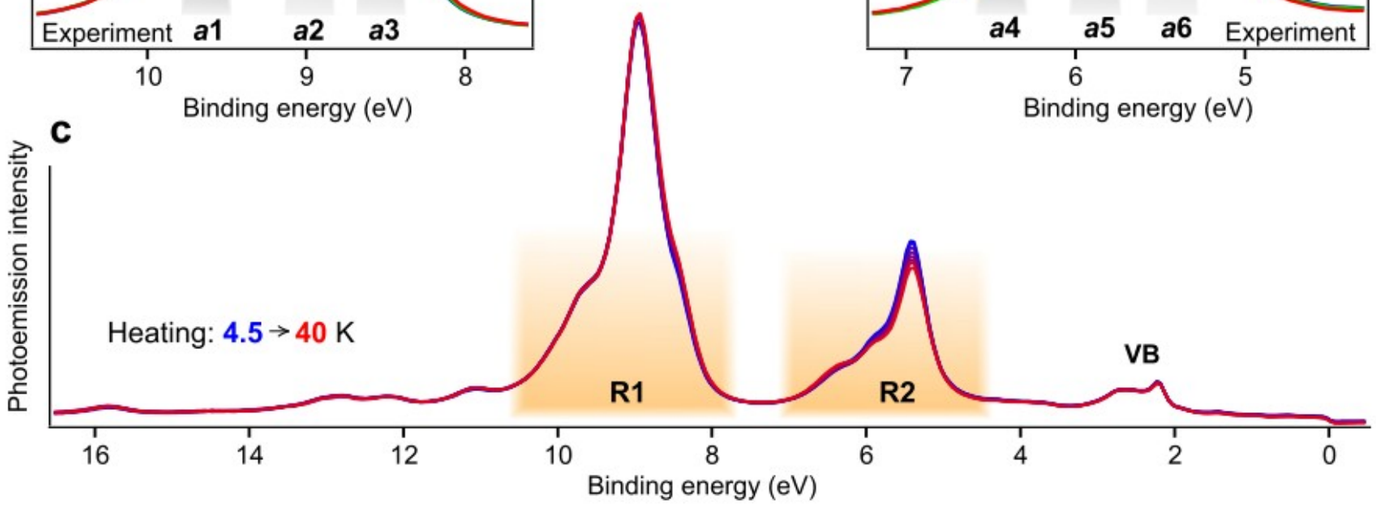

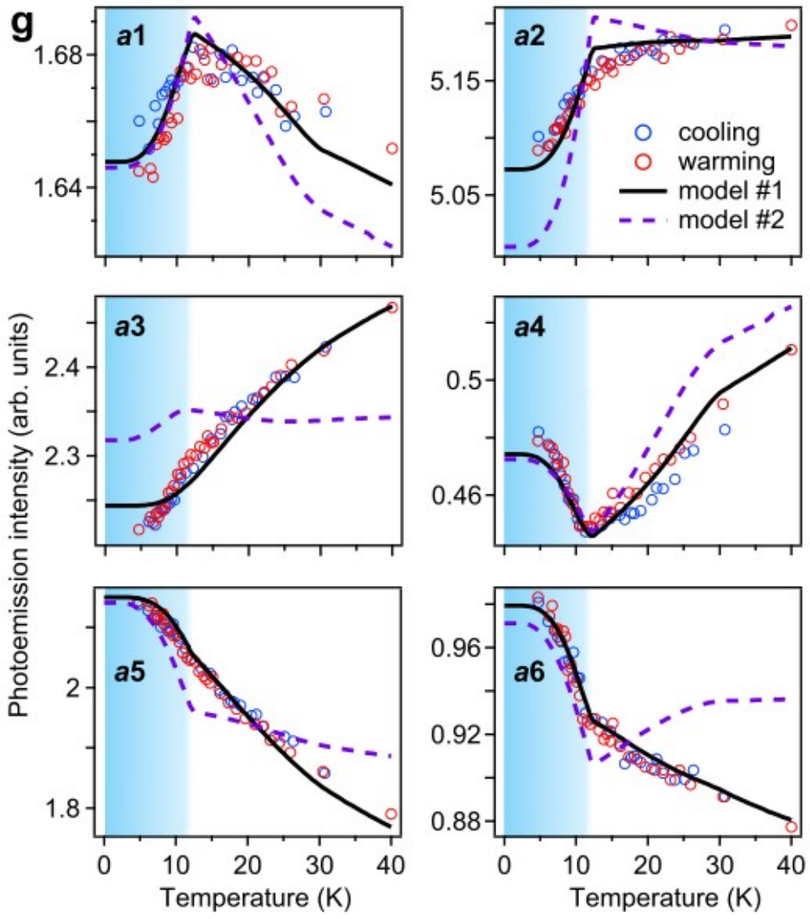

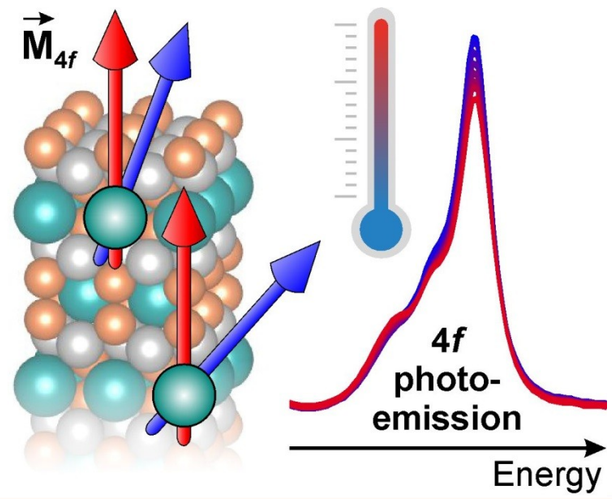

- **T-dependent 4f photoemission spectra demonstrate canting of moments**
- **Canting at the surface starts at the same temperature at in the bulk**
- **Canting angle near the surface is smaller than in the bulk**

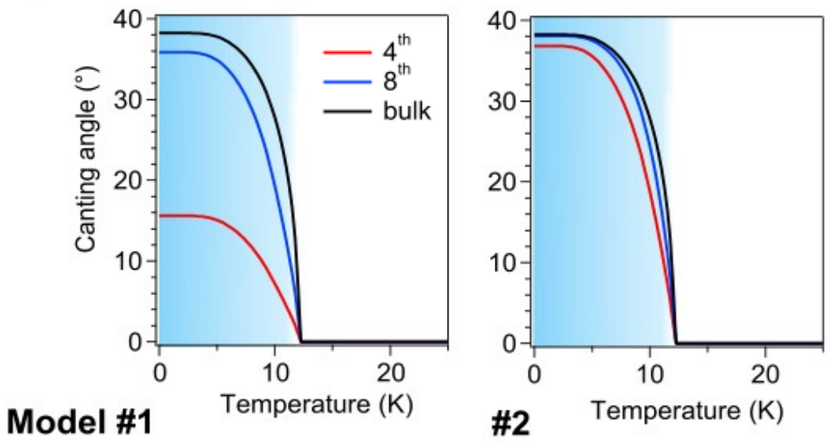

D. Usachov et al., JPCL 14, 5537 (2023)

Example of $EuIr_2Si_2$

(nonmagnetic in the bulk)

$EuIr_2Si_2$: What can we learn from the surface states?

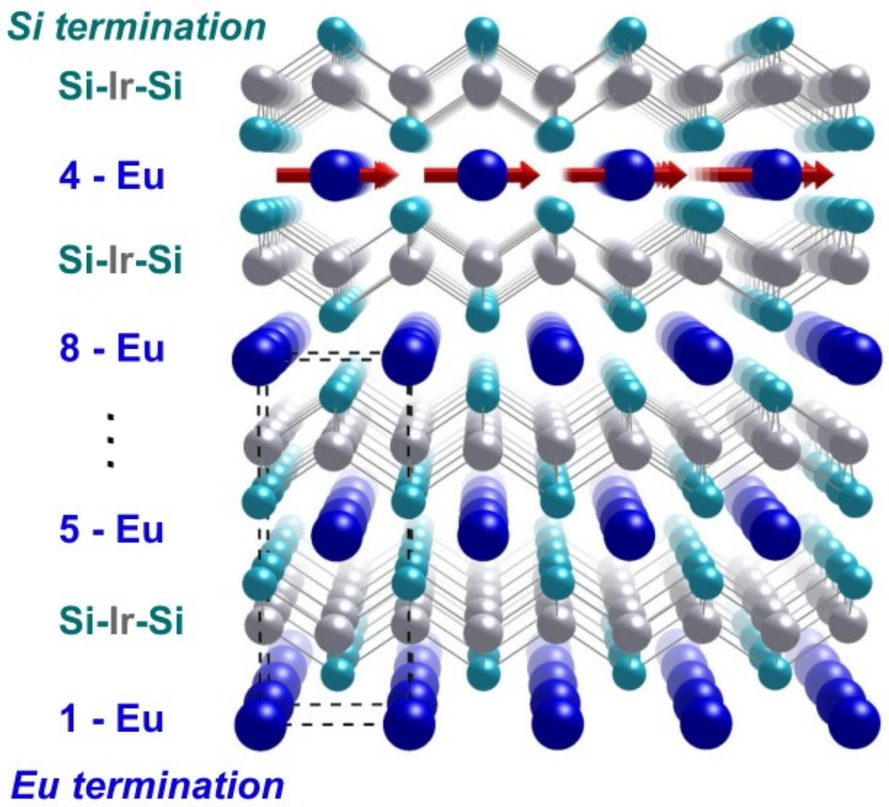

ARPES on Si termination:

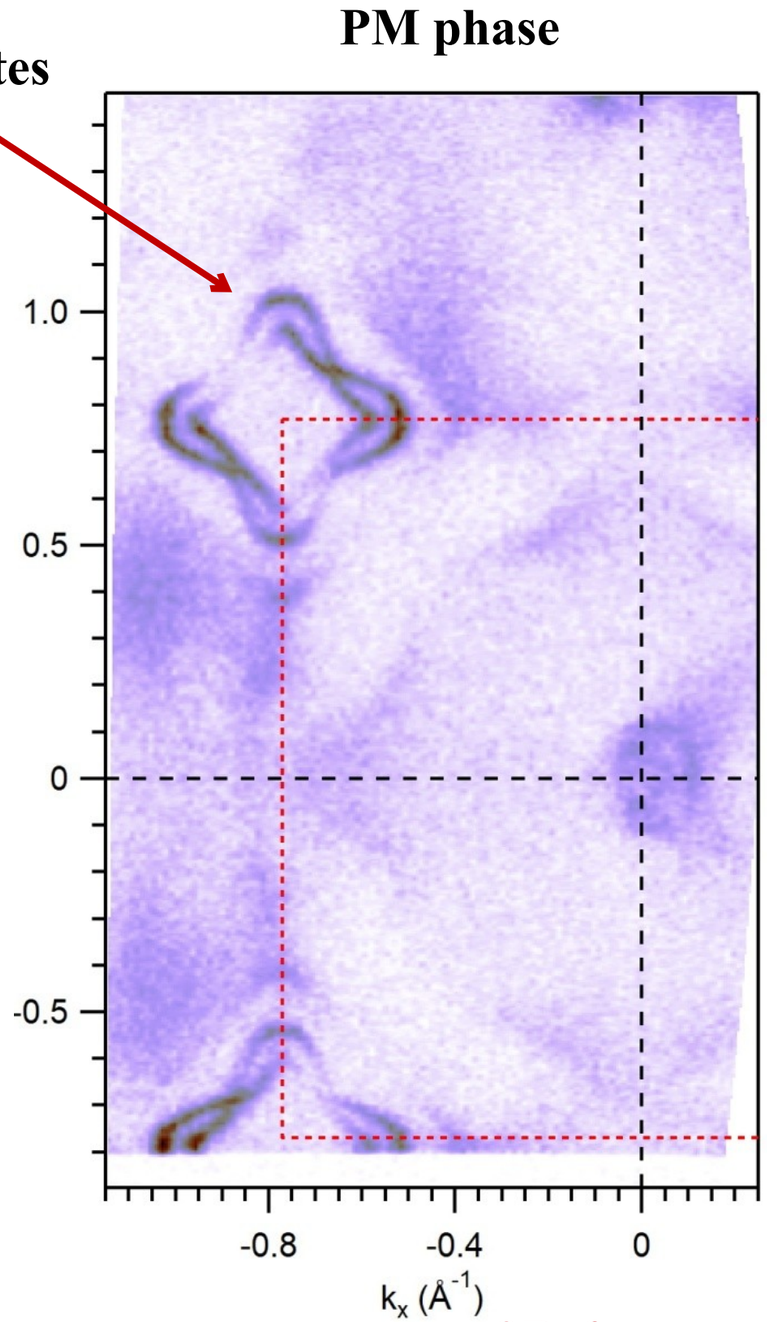

$E(k_x,k_y)$ =const

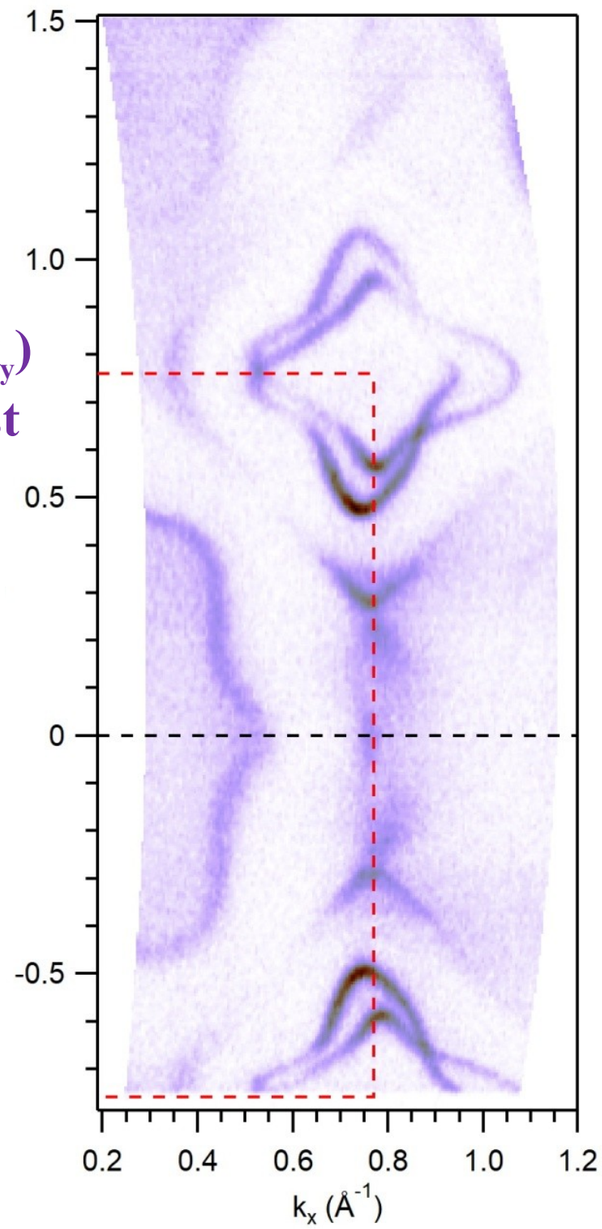

2D ferromagnetism below the Si surface

$EuIr_2Si_2$: SOI competing with exchange

SO-splitting

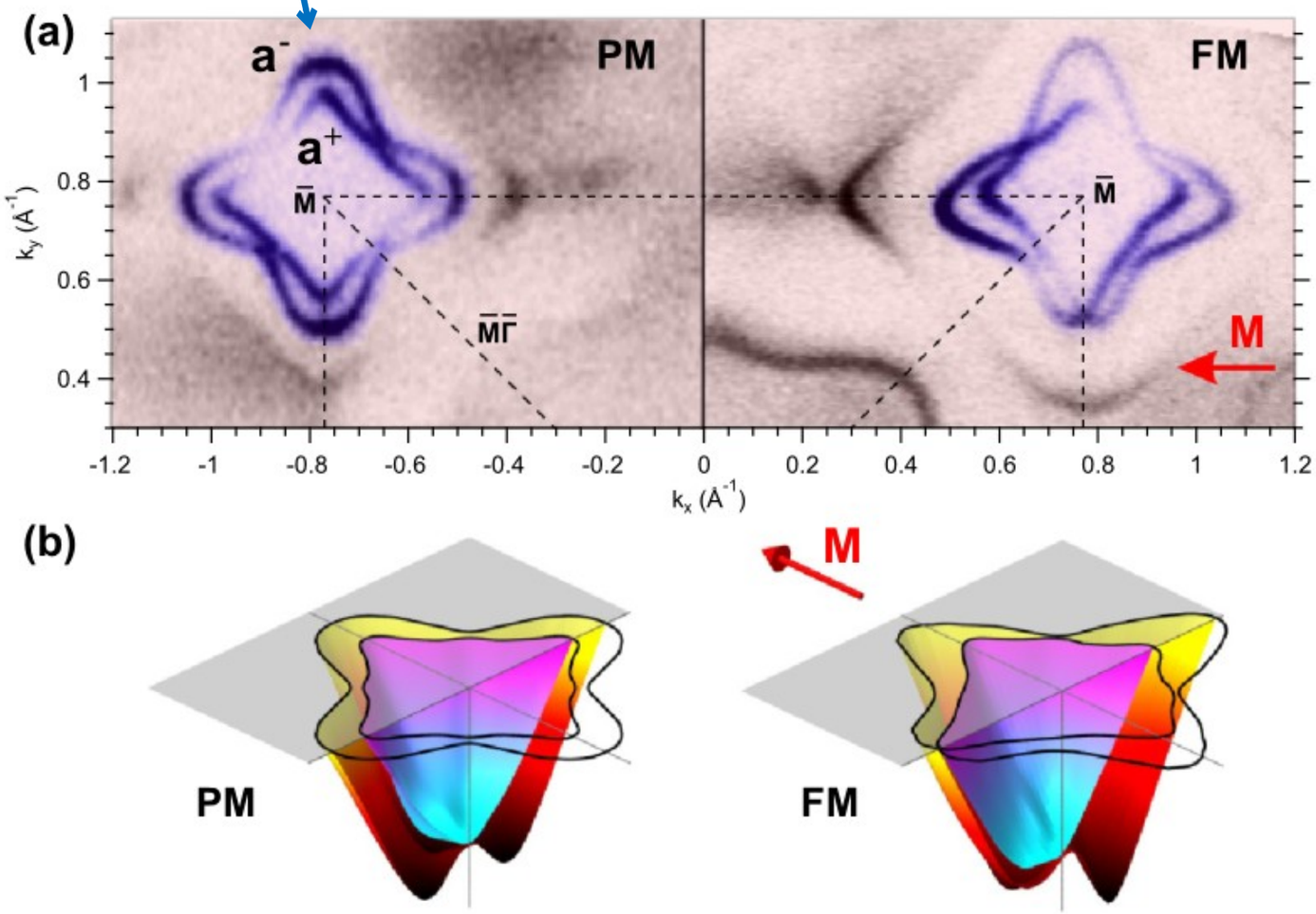

When the SO field **B** *is parallel or antiparallel to the exchange field* **J** *the energy splitting of the band gets smaller or larger*

Measured band splitting gives us:

One-electron Hamiltonian: $\hat{H} = \frac{\hat{\mathbf{p}}^2}{2m} + V + \frac{\hbar}{4m^2c^2}(\nabla V \times \hat{\mathbf{p}}) \cdot \hat{\boldsymbol{\sigma}} + J_{\mathrm{ex}}\mathbf{M} \cdot \hat{\boldsymbol{\sigma}}$

SOI *Exchange*

$$\hat{H}(\mathbf{k}) = U(\mathbf{k}) \cdot \sigma_0 + \mathbf{B}(\mathbf{k}) \cdot \hat{\boldsymbol{\sigma}} - \mathbf{J} \cdot \hat{\boldsymbol{\sigma}}$$

SOI *Exchange*

Single-band model:

$$E^{\pm}(\mathbf{k}) = U(\mathbf{k}) \pm |\mathbf{B}(\mathbf{k}) - \mathbf{J}|$$

Band splitting: $\Delta(\mathbf{k}) = E^{+}(\mathbf{k}) - E^{-}(\mathbf{k})$

$$\mathbf{B} \cdot \mathbf{J} = \frac{\Delta^2(-\mathbf{k}) - \Delta^2(\mathbf{k})}{16}$$

Magnetization direction (in-plane component of J)
Spin structure (B)
Strength of SO and exchange interactions

D. Usachov et al., PRB 101, 245140 (2020)

$EuIr_2Si_2$: SOI competing with exchange

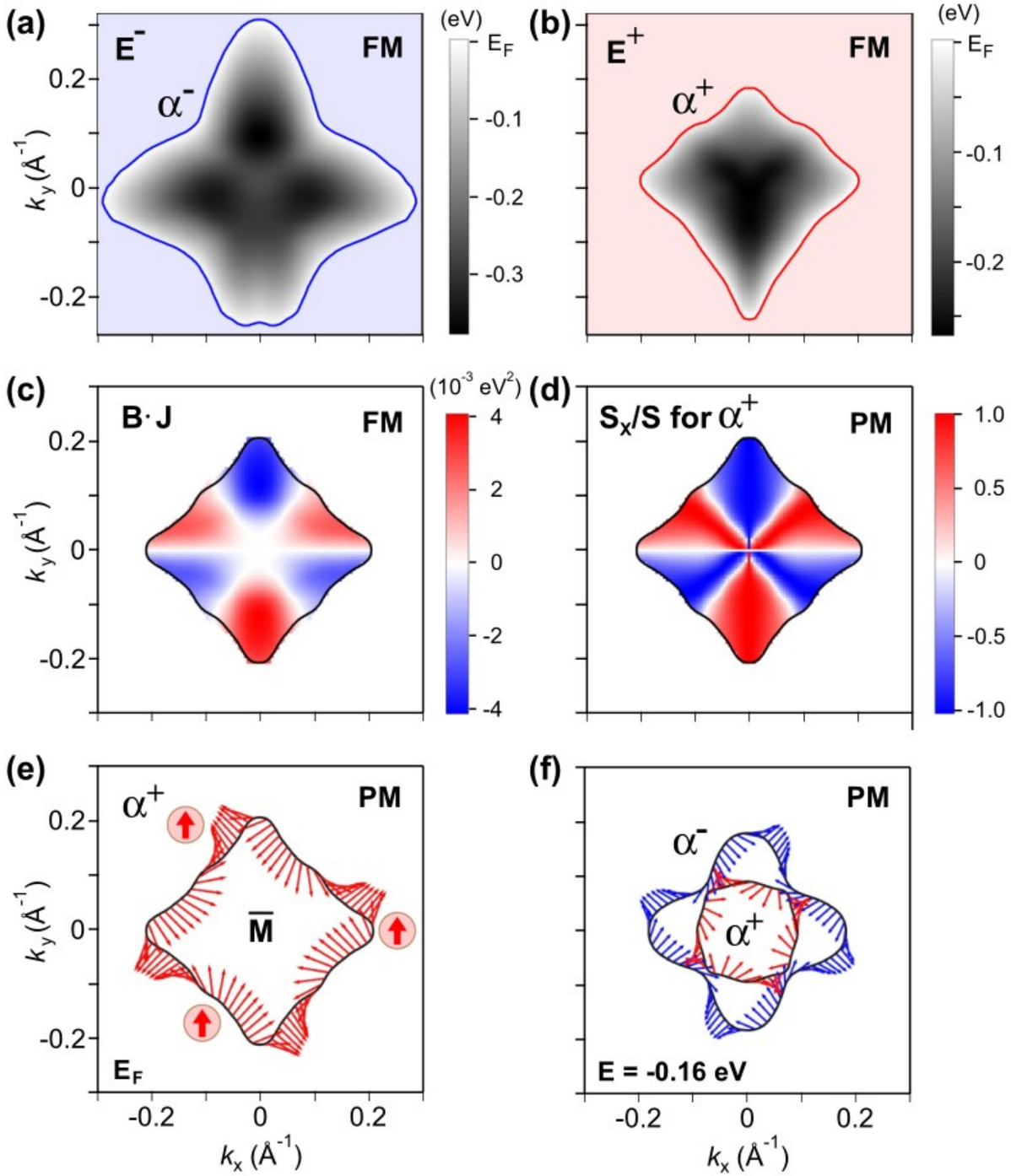

Band splitting from ARPES:

$$\Delta(\mathbf{k}) \equiv E^{+}(\mathbf{k}) - E^{-}(\mathbf{k})$$

$$\mathbf{B} \cdot \mathbf{J}$$

$$\mathbf{J} \parallel x$$

$$\frac{\mathbf{S}^{\pm}_{\mathrm{PM}}(\mathbf{k})}{S^{\pm}_{\mathrm{PM}}(\mathbf{k})} = \pm \frac{\mathbf{B}(\mathbf{k})}{B(\mathbf{k})}$$

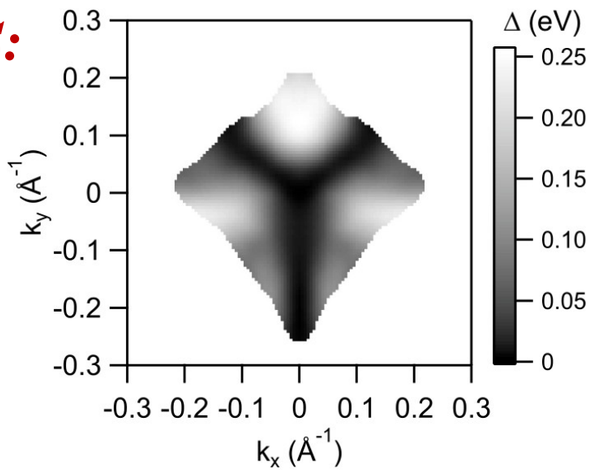

We can obtain spin structure even without spin-ARPES

Spin structure shows a cubic Rashba effect

D. Usachov et al., PRB 101, 245140 (2020), PRL 124, 237202 (2020)

$EuIr_2Si_2$: What can we learn from the 4f states?

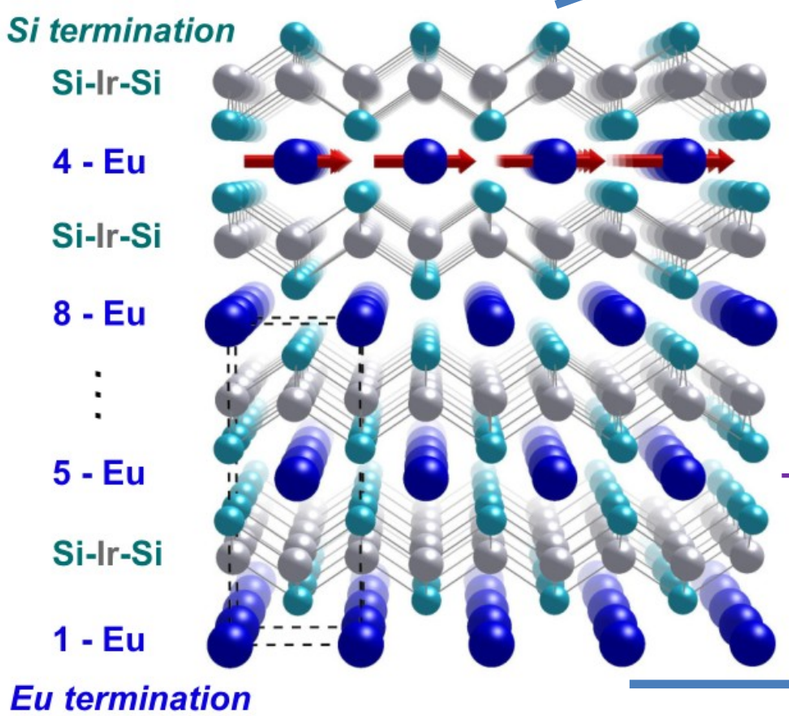

Noninteger valency of Eu:

ground state = a|4f $^6v^n$⟩ + b|4f $^7v^{n-1}$⟩

nonmagnetic magnetic

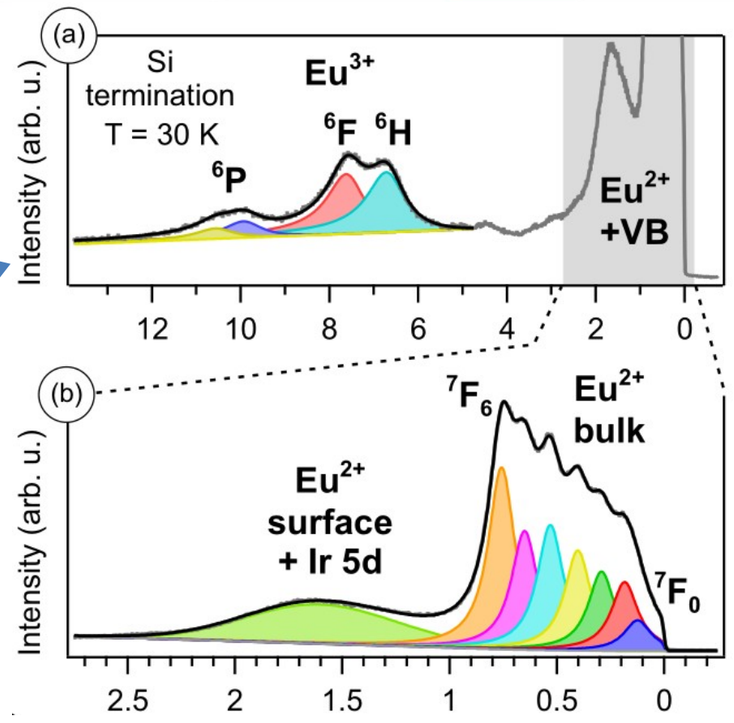

Strong Eu^{2+} signal: 4th layer is mostly divalent (that's why it is magnetic)

Circular dichroism in photoemission

(signal depends on the angle between the spin of photon and electrons)

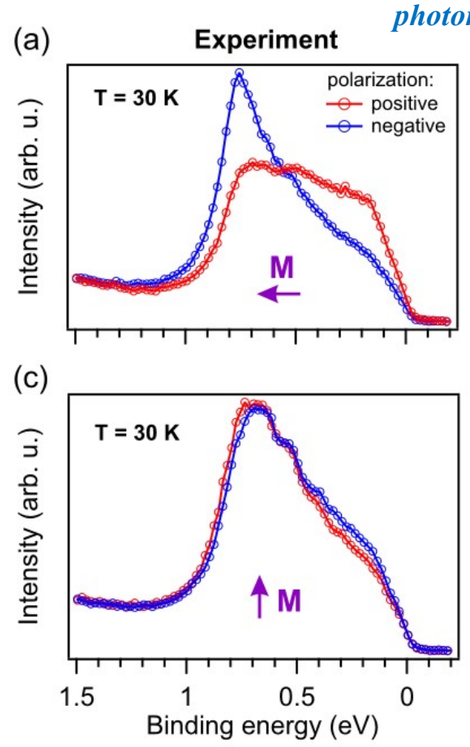

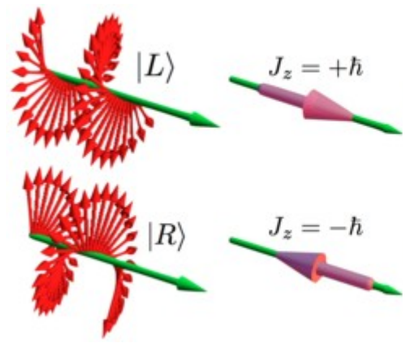

Easy magnetization axis is [100]

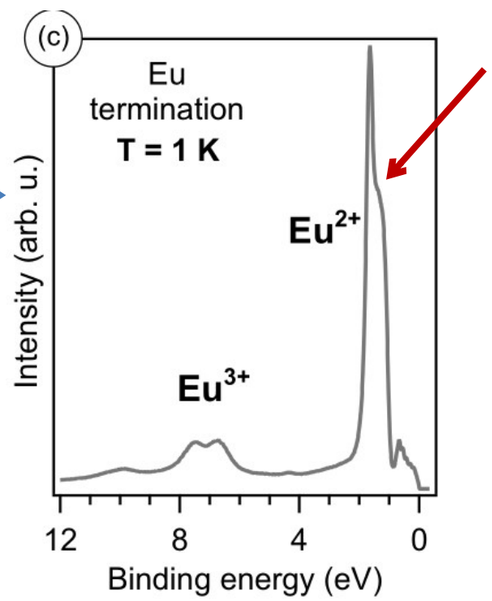

Strong Eu^{2+} signal: 1st layer is divalent (can be magnetically ordered)

Shape of 4f multiplet depends on the magnetic state and moment direction

Eu-terminated surface becomes FM-ordered below 10 K

T-dependence

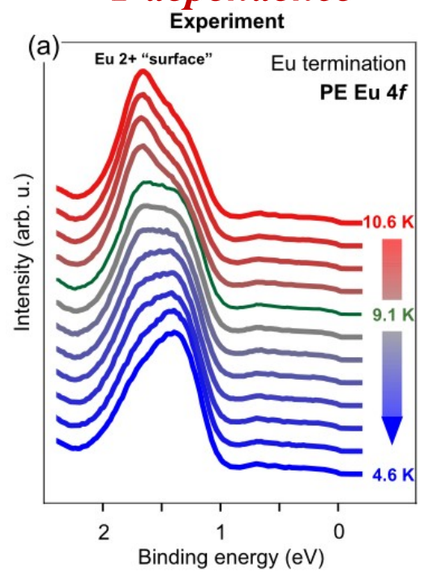

D. Usachov et al., PRB 102, 205102 (2020)

$EuIr_2Si_2$: 4f XPS and photoelectron diffraction (PED)

PED gives the answer from which layers the Eu^{2+} and Eu^{3+} signals come

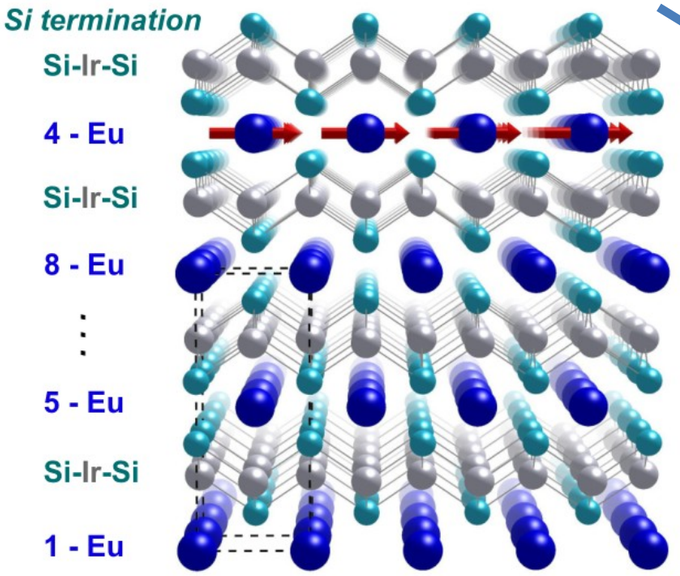

Eu 4f PED

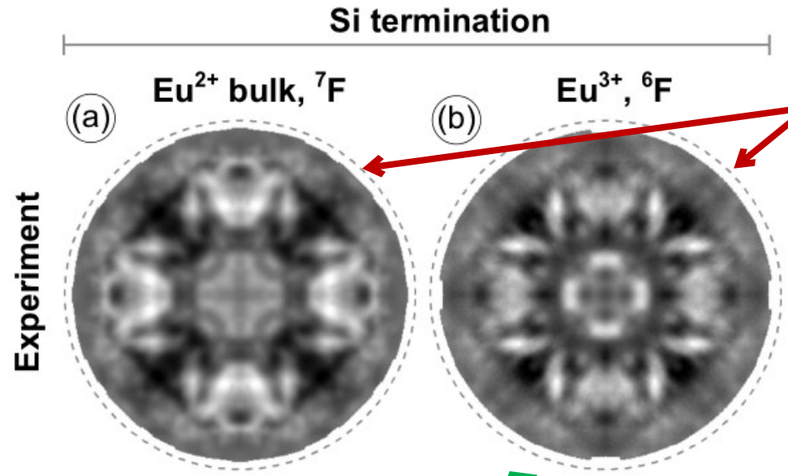

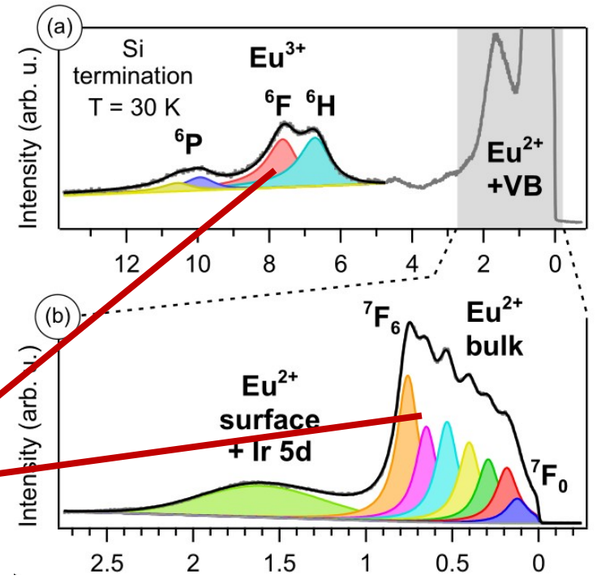

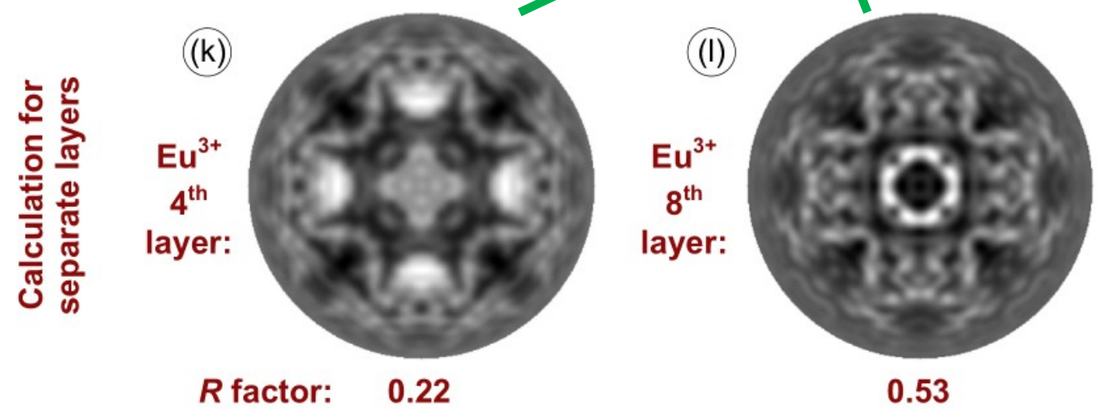

4th layer valency is 2.1 - FM
8th layer valency is 2.4 – PM
(bulk valency is 2.8)

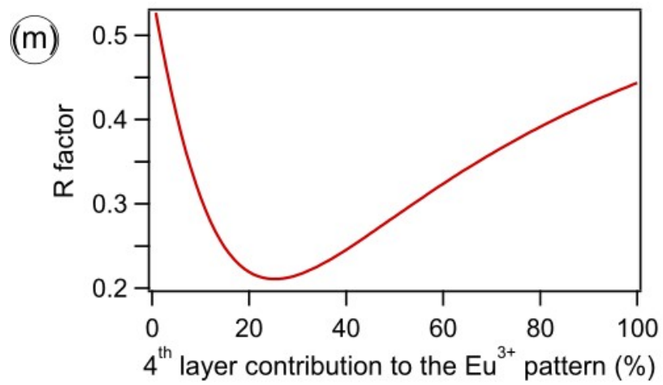

D. Usachov et al., PRB 102, 205102 (2020)

Conclusions from Part 2

- Surface electronic and magnetic properties of RE compounds may drastically differ from the bulk properties

- In $EuIr_2Si_2$ 2D ferromagnetism is present in a single Eu layer on Si termination (T_C=48 K) and on Eu termination (T_C=10 K).

- Spin structure of surface states, which experience both SO and magnetic exchange interactions, can be determined indirectly from the asymmetry of band dispersions

- ***In $TbRh_2Si_2$ the 4f moments on Tb termination are orthogonal to the moments in the bulk due to different CEF.***
- ***4f ARPES can be used to trace T-dependent canting of moments***

- Using 4f PED, we determined the valency of individual Eu layers

The 4f photoemission spectra give information about

- ***orientation of magnetic moments of RE layers,***
- ***valency of RE ions,***
- ***CEF splitting,***
- ***structure of the surface.***

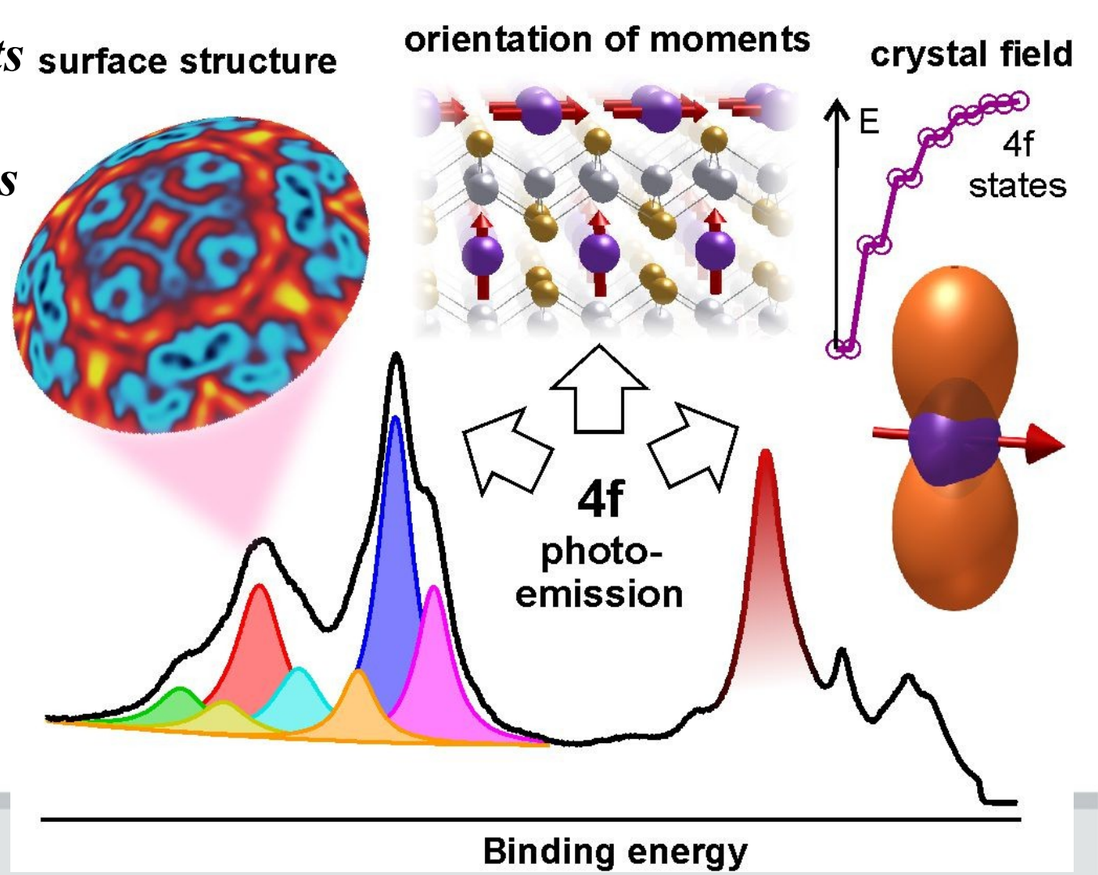

Part 3

Magnetic proximity effects in the interfaces of graphene and MoS_2 with cobalt

Inducing spin-orbit coupling (SOC) in graphene

✓ **Spin Hall effect (SHE)**

J. Balakrishnan et al., Nat. Phys. 9, 284 (2013)

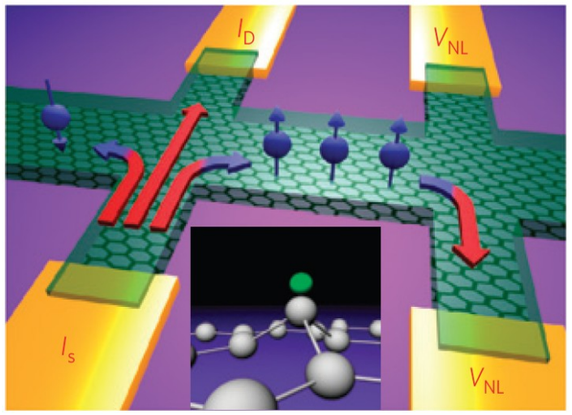

Increase of SOC by hydrogen adsorption

✓ **Quantum spin Hall effect(QSHE)**

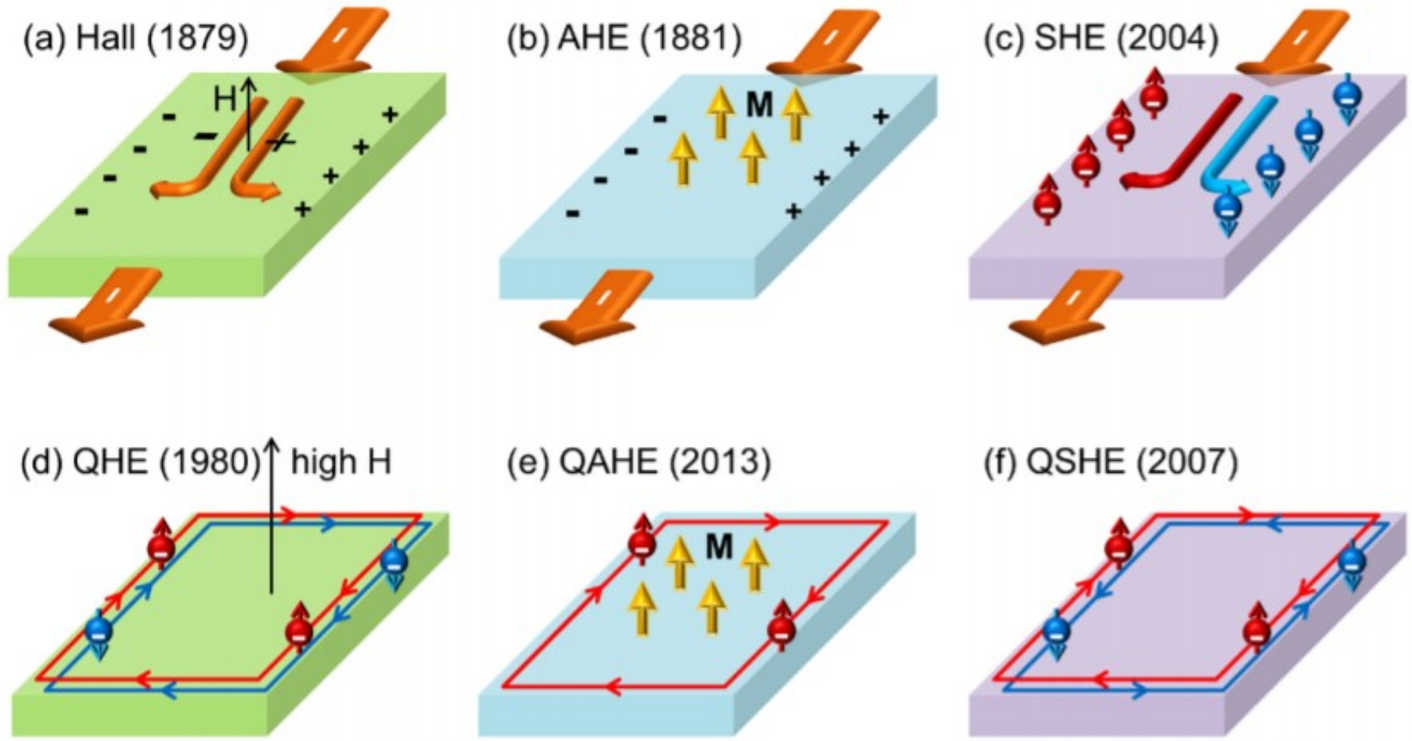

C.-Z. Chang and M. Li, J. Phys.: Cond. Matt. 28, 123002 (2016)

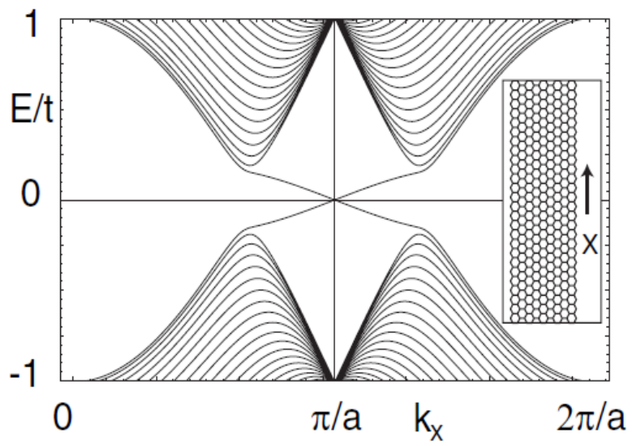

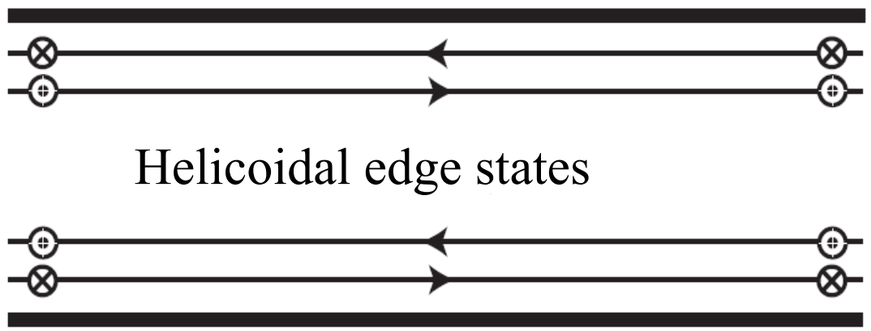

C. L. Kane and E. J. Mele, PRL 95, 226801 (2005) – model with SOC in graphene

Graphene with strong SOC becomes a topological insulator

With additional source of magnetism we may expect QAHE

Can we induce strong SOC and magnetism in graphene?

Graphene on metal surfaces

Proximity effect in graphene on magnetic substrate may induce magnetism in graphene

Good matching of lattice parameters:
graphene: 2.46 Å
Co(0001): 2.507 Å

STM-derived topography of graphene on metals:

Co(0001) or Ni (111)
< 2% mismatch

Rh (111), 9% mismatch

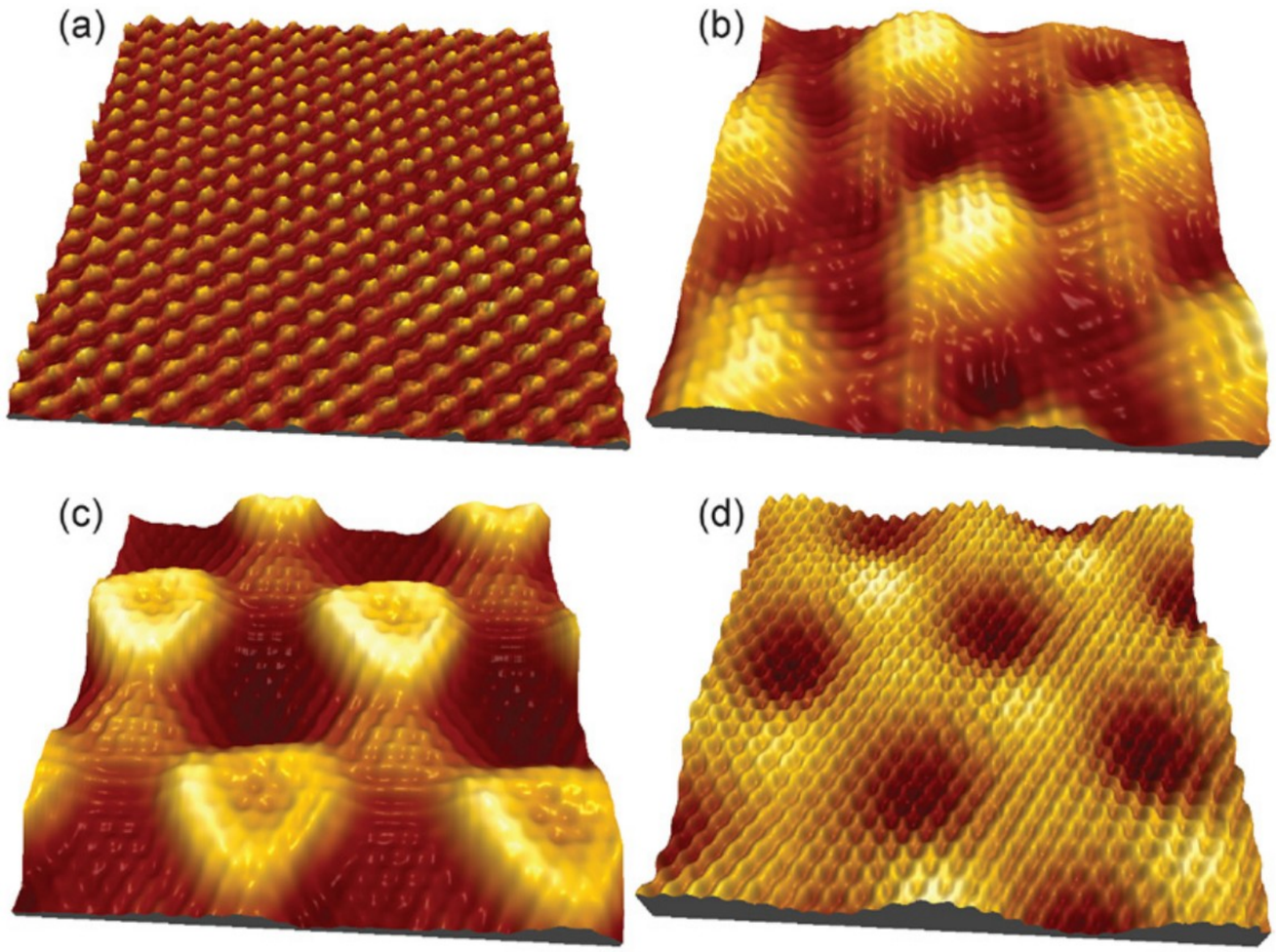

Ru (0001), 10%

Ir (111) , 10%

Yu. Dedkov, J. Phys.: Condens. Matter (2015)

graphene/Co interface: DFT

DFT-derived bands at different graphene-Co distances

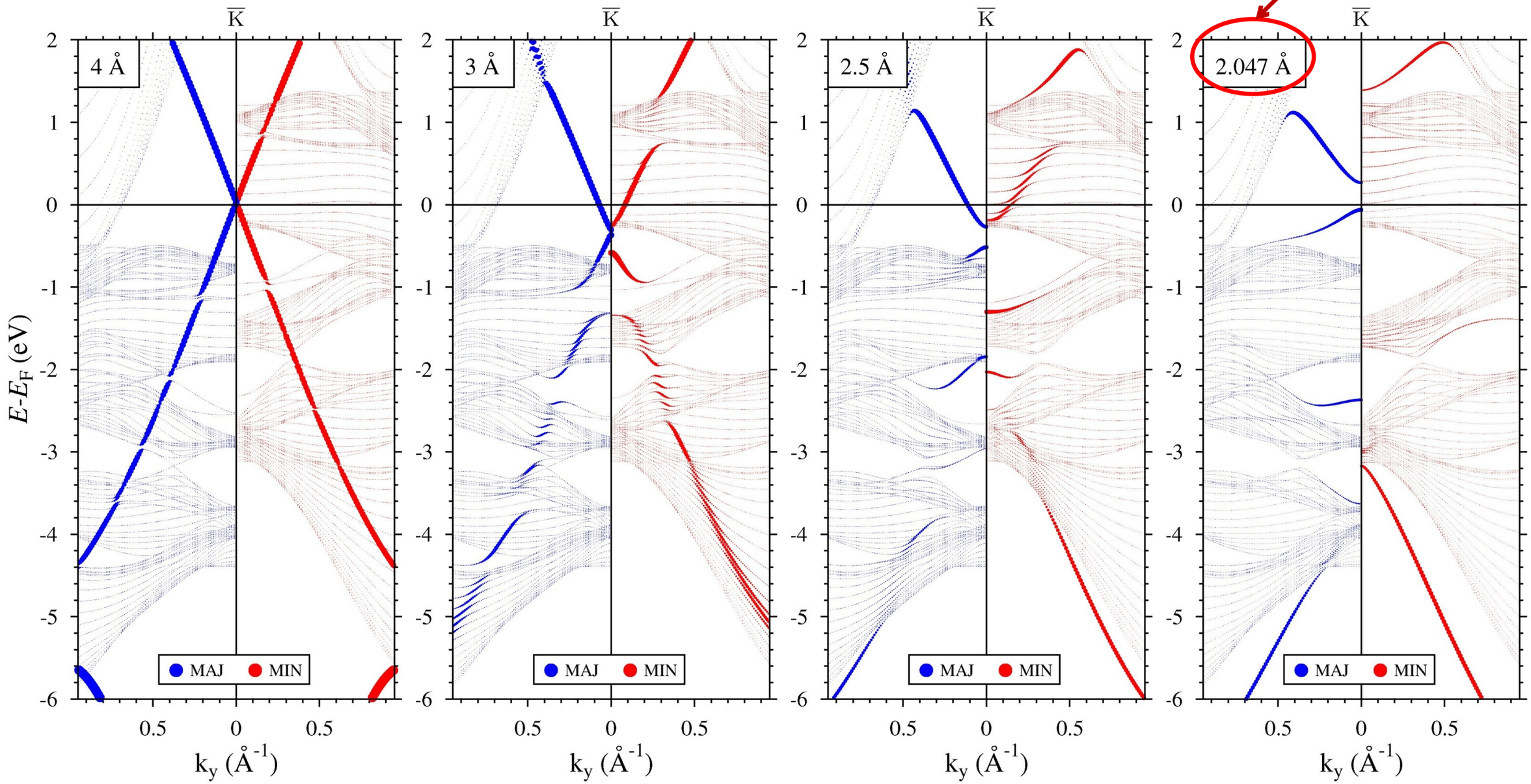

Dirac cone is mostly destroyed by hybridization with 3d states of Co

D. Usachov et al., Nano Lett. 2015

graphene/Co interface: (spin-)ARPES

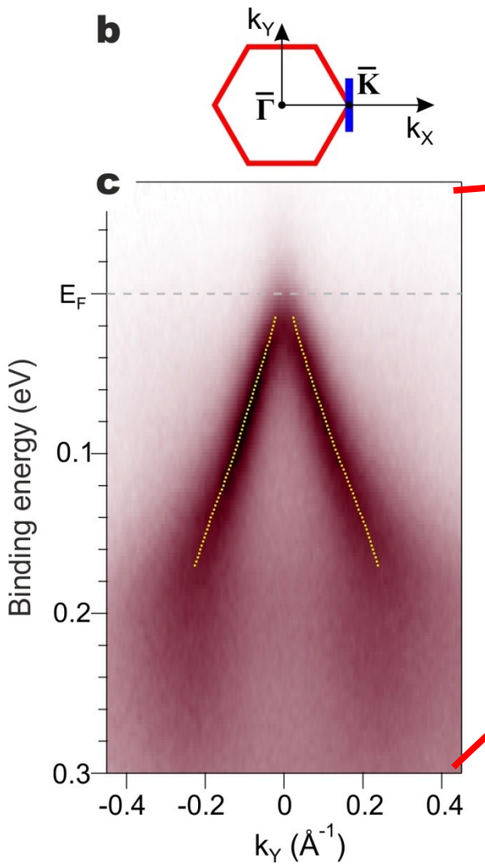

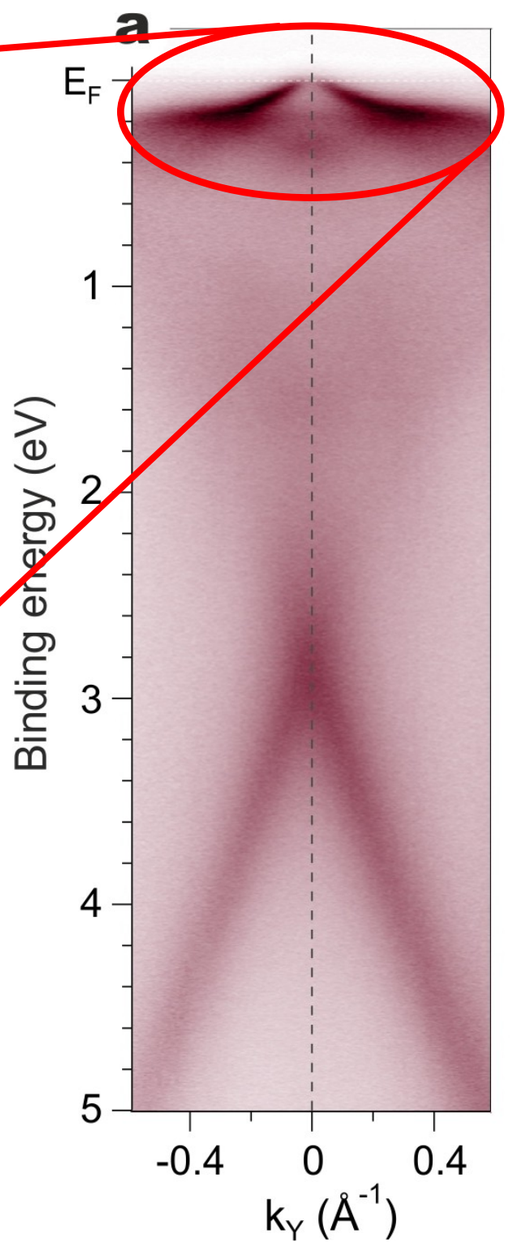

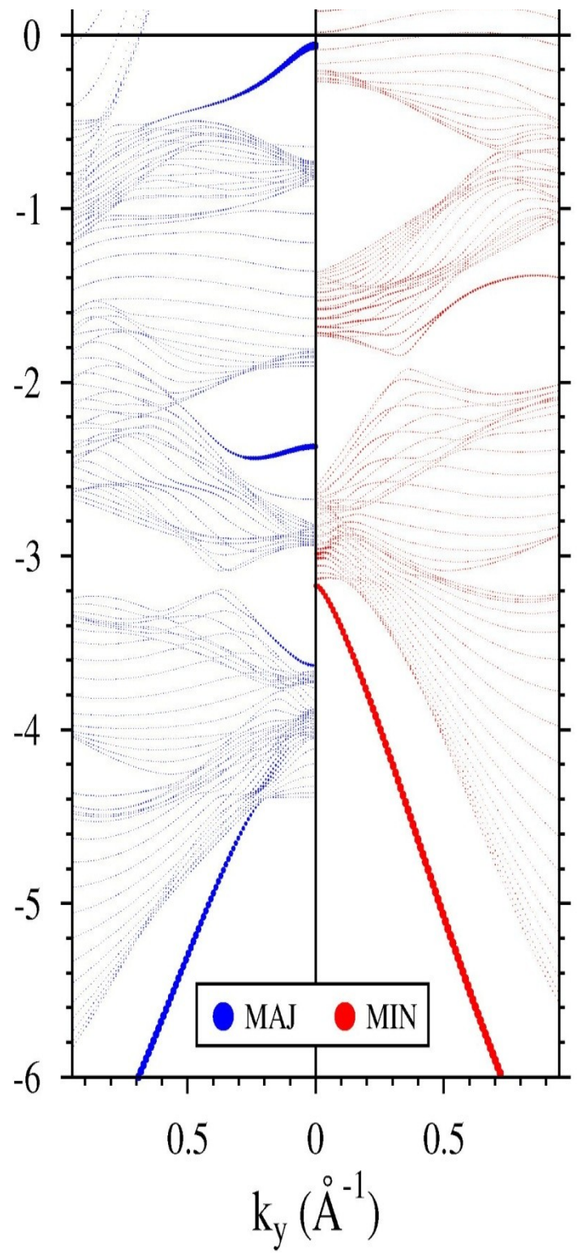

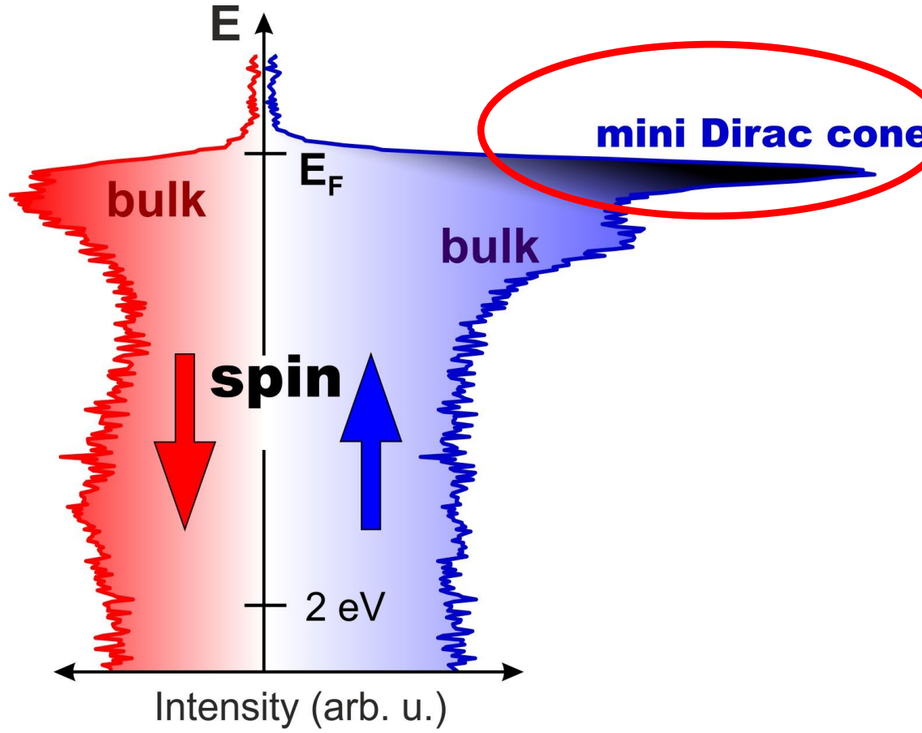

spin-ARPES

Spin-polarized hybrid graphene-Co states at the Fermi level

This is nice, but this is not graphene.
This is a compound of carbon and Co.

D. Usachov et al., Nano Lett. 2015

Graphene/Au/Co(0001) system

graphene/Co

graphene/Au/Co(0001)

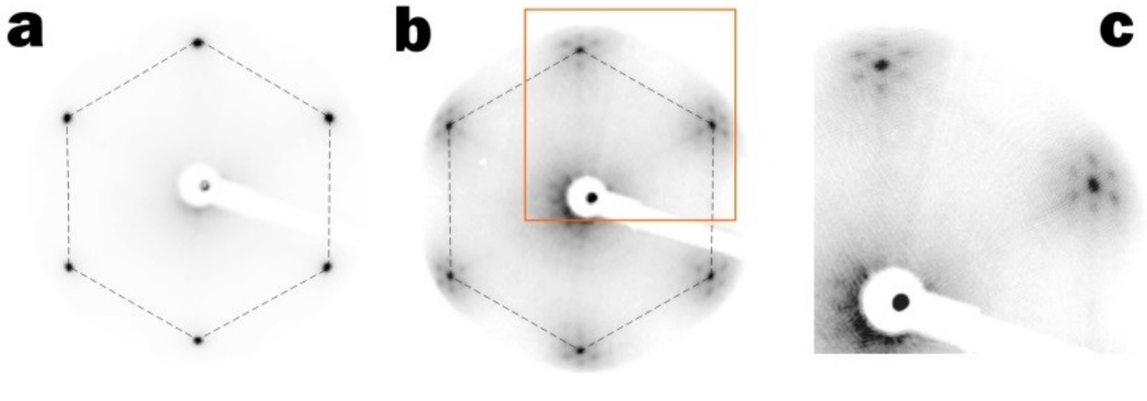

Low-energy electron diffraction (LEED)

ARPES

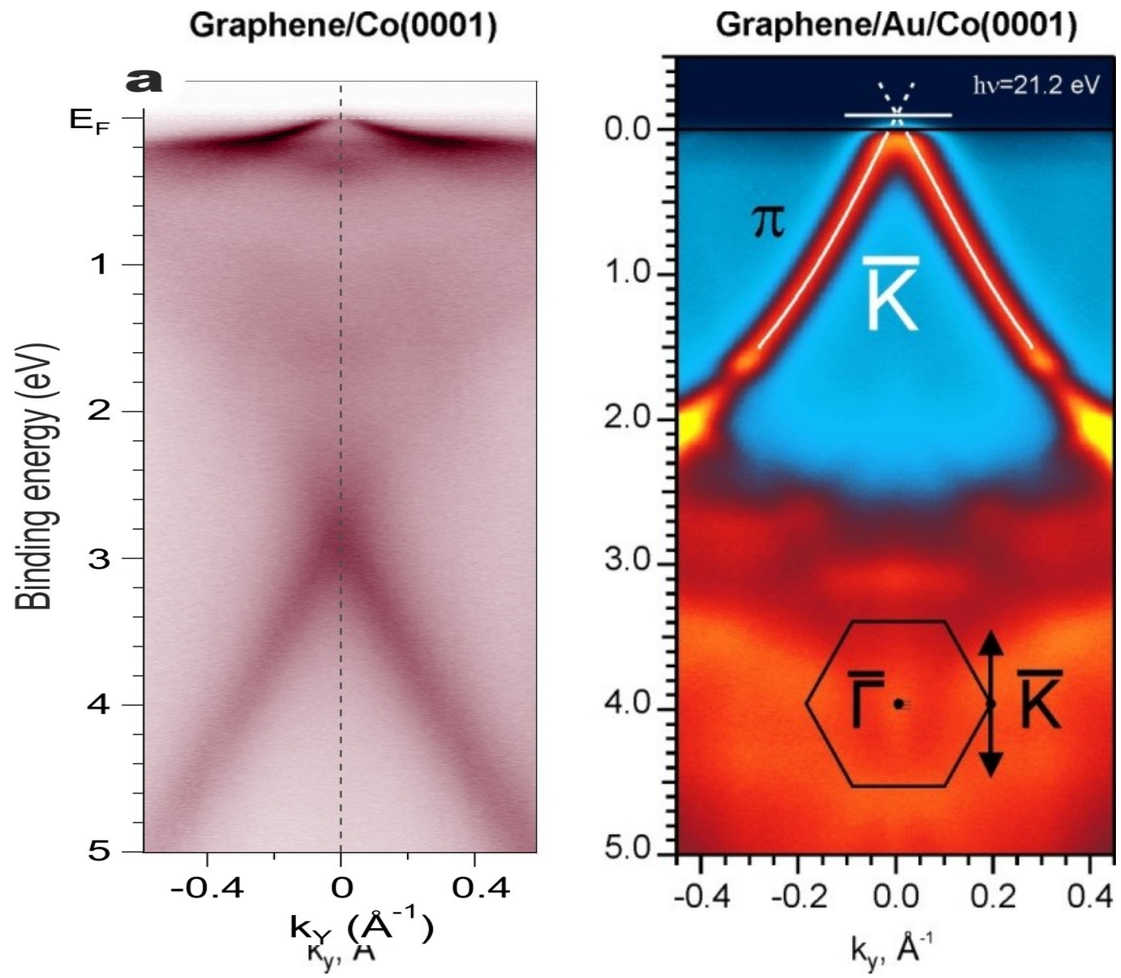

- **Intercalation decouples graphene from Co**
- **Au may induce spin-orbit coupling**
- **Co may induce magnetism in graphene**

A.G. Rybkin et al., Nano Lett. 18, 3, 1564–1574 (2018)

STM from graphene/Au/Co(0001)

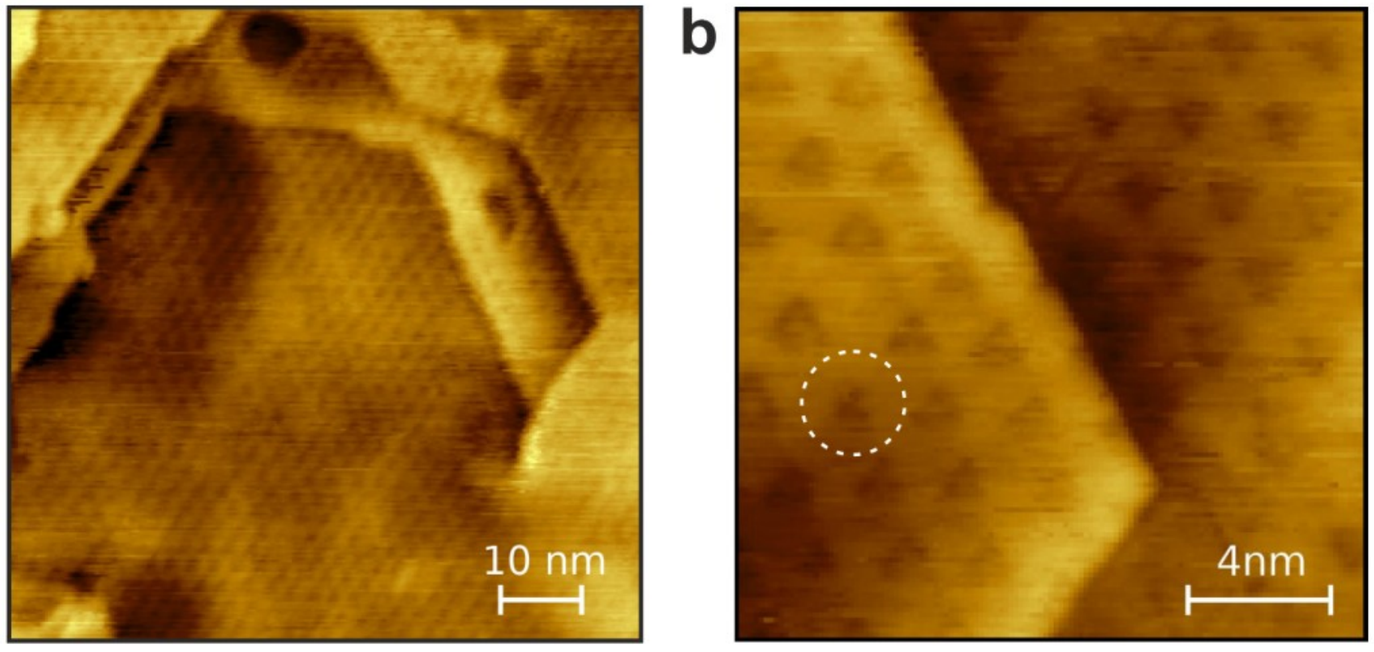

(9x9) periodic superlattice of dislocation loops below graphene

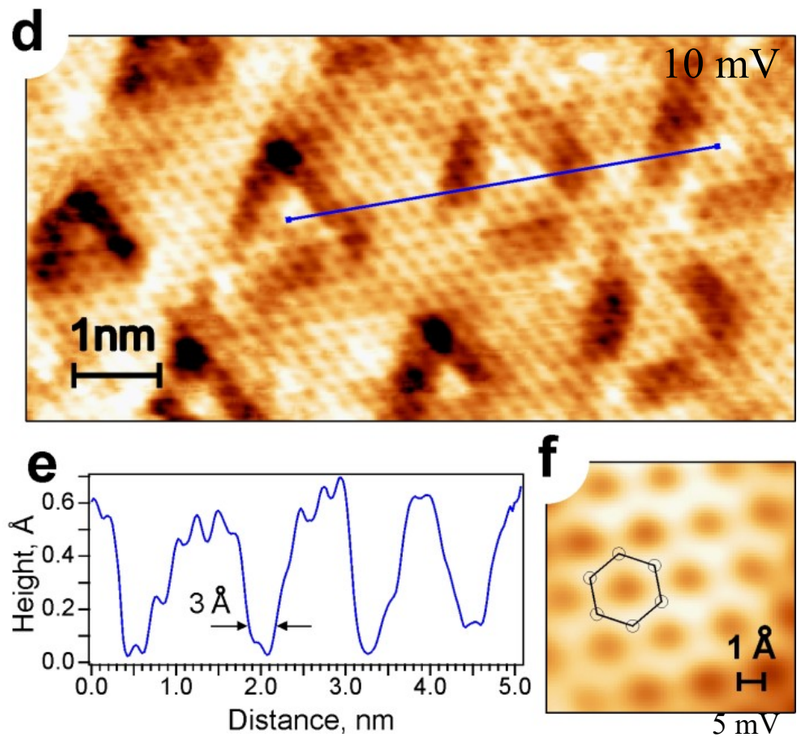

Dislocation loops in Au/Ni(111):

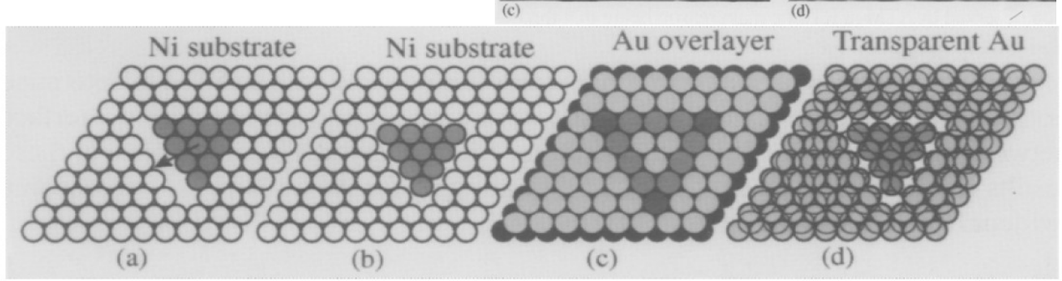

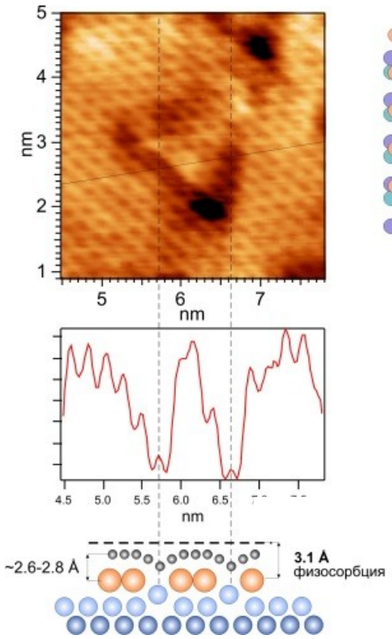

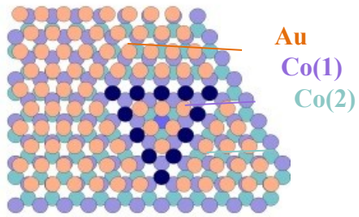

Dislocations are formed due to 10% lattice mismatch between Au and Co (or Ni)

A.G. Rybkin, Nano Lett. 18, 3, 1564 (2018)

F. Besenbacher, Growth and Properties of Ultrathin Epitaxial Layers, Elsevier Science, ch. 6, 207 (1997)

graphene/Au/Co interface: spin-ARPES

ARPES

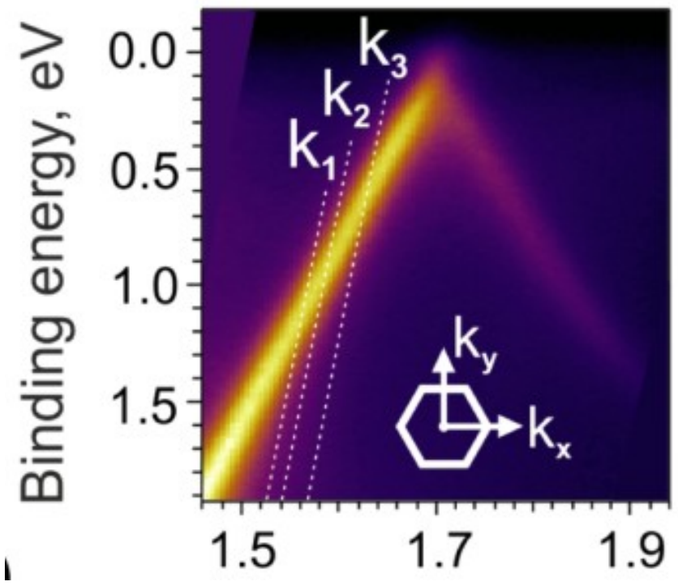

spin-ARPES

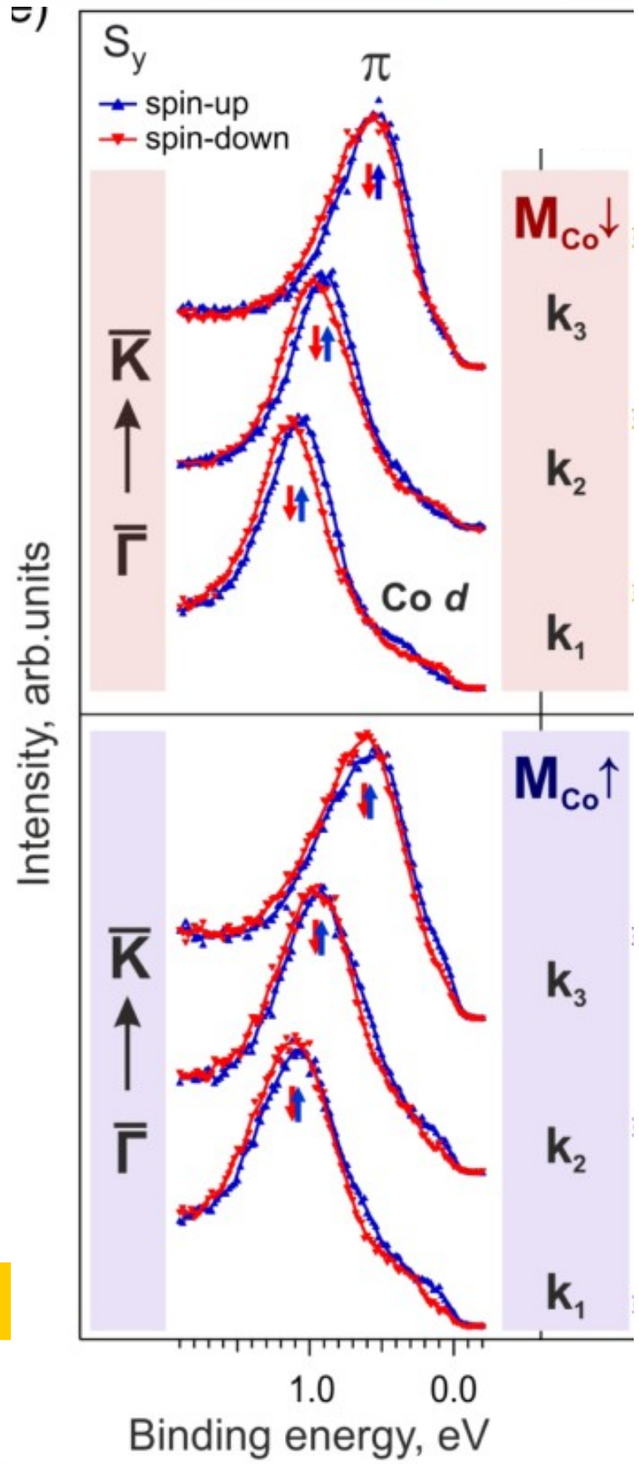

80 meV splitting

40 meV splitting

Spin splitting depends on magnetization direction

SOC + exchange

A. Rybkin, D. Usachov et al., PRL 2022

graphene/Au/Co interface: DFT

DFT

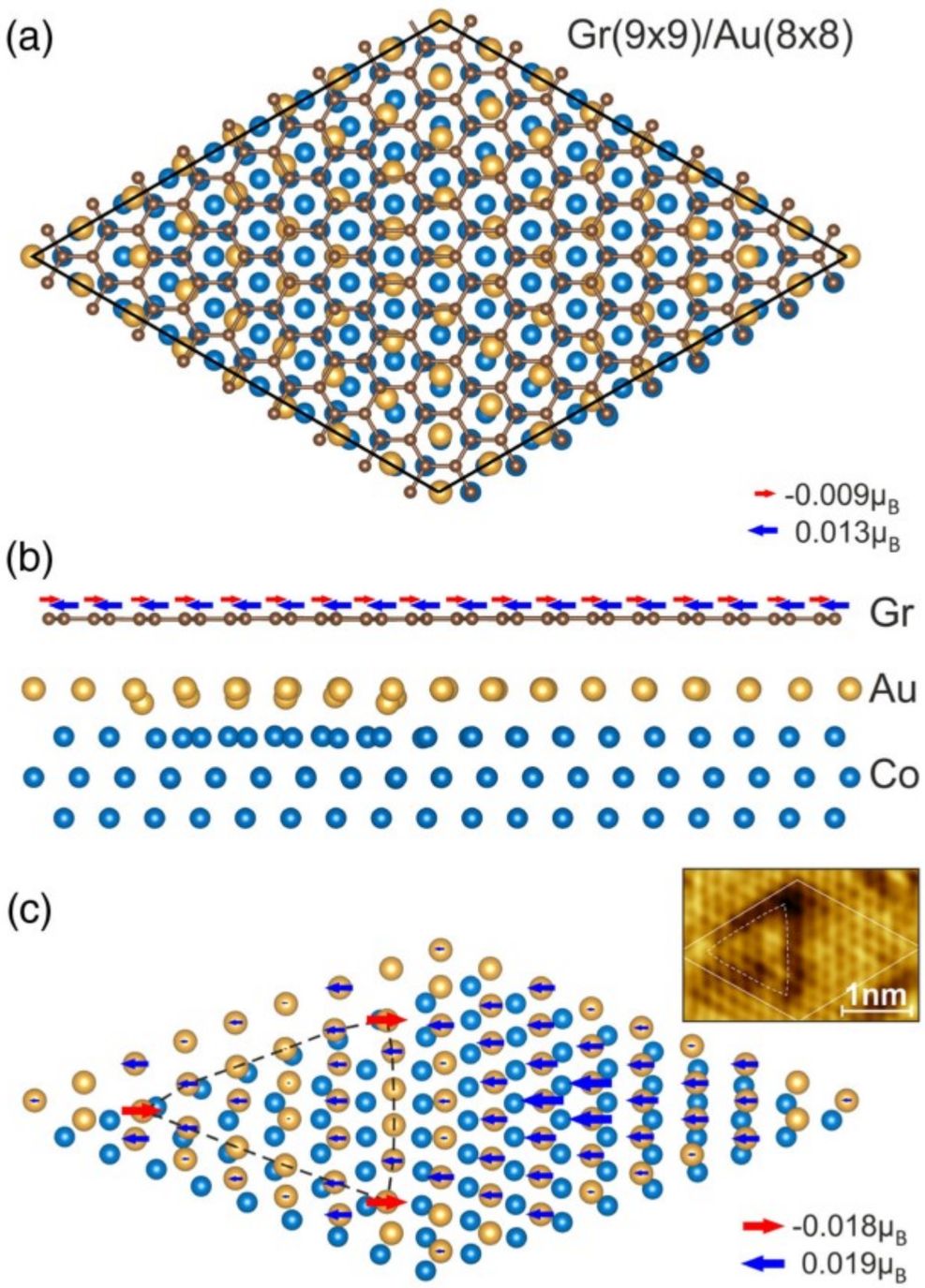

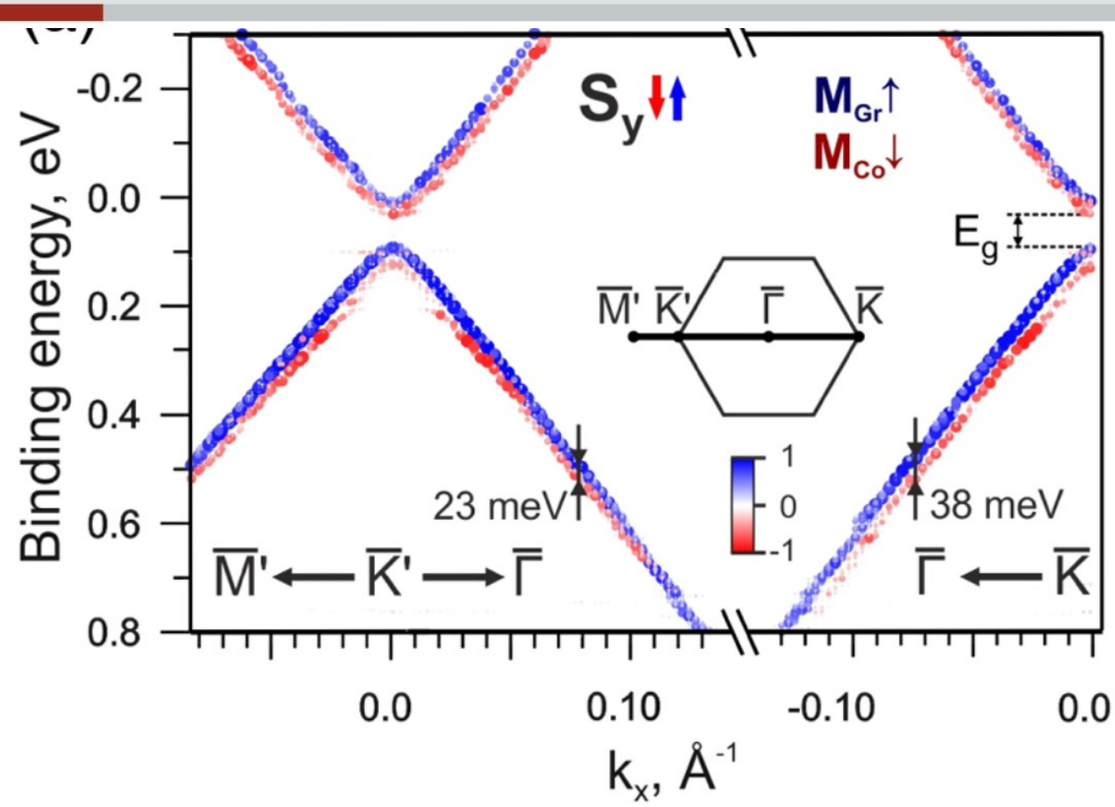

- **Graphene becomes ferrimagnetic**
- **DFT qualitatively correctly predicts asymmetric spin splitting as the result of both exchange and SO splitting**
- **The gap has magnetic origin (it closes when no magnetism)**
- **Graphene is not magnetized without dislocations loops**
- **Au induces SOC, but in experiment it is much stronger (60 meV) than in DFT (8 meV)**
- **This is a first step towards observation of QAHE in graphene**

A. Rybkin, D. Usachov et al., PRL 2022

Magnetic proximity effects in MoS_2/graphene/cobalt

MoS_2 monolayer in magnetic field: A DFT calculation

Electronic structure in transversal magnetic field (along Z)

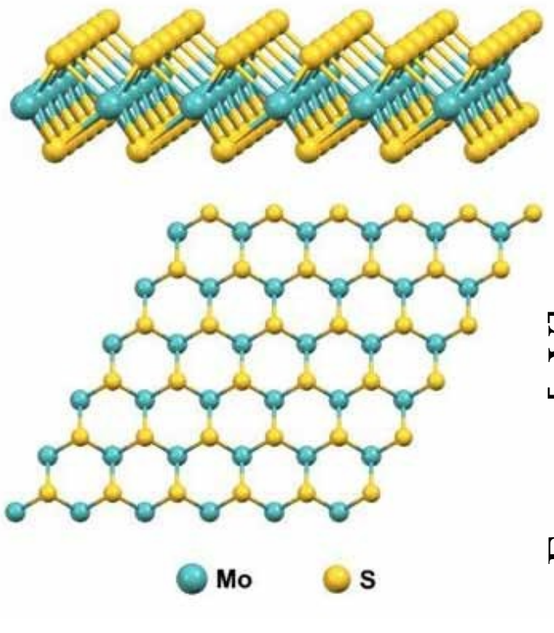

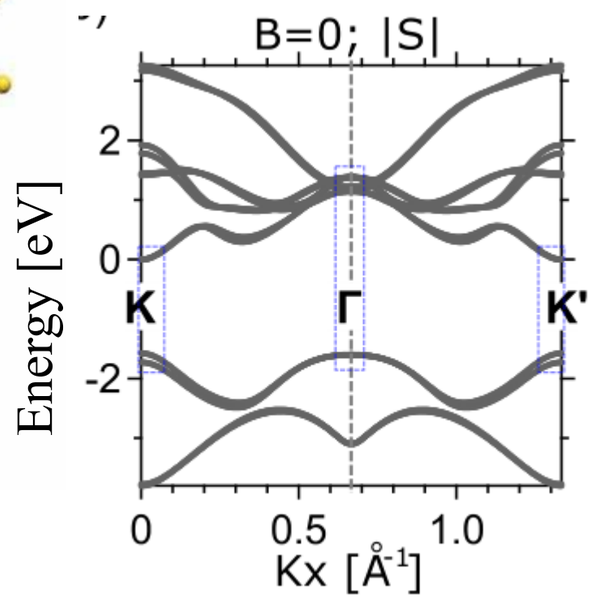

No field

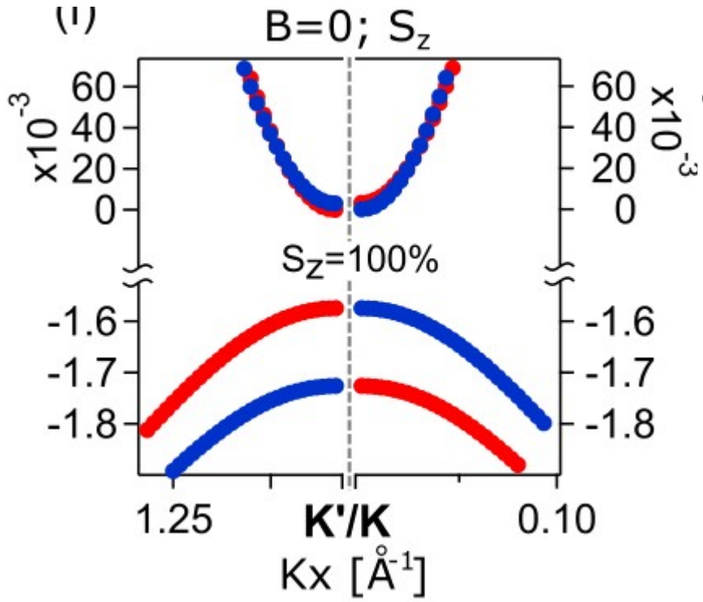

Field of 100 T

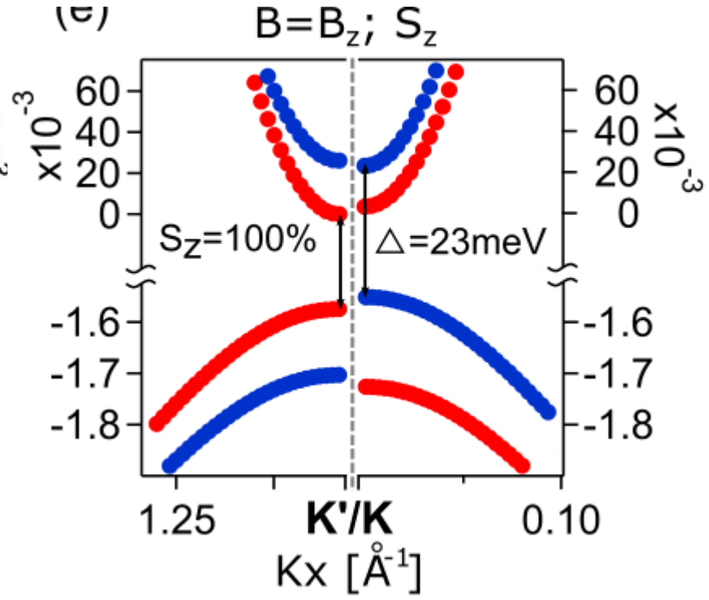

Gaps for spin-up and spin-down bands are different.

Optical generation of spin-polarized charge carriers

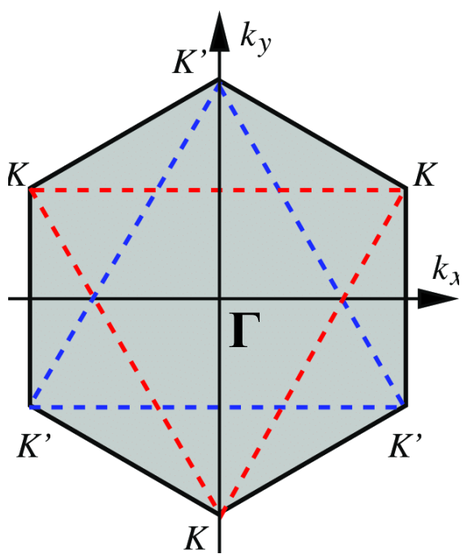

Brillouin zone

Can we replace strong magnetic field with a proximity to magnetic substrate?

V. Voroshnin, D. Usachov et al., ACS Nano 2022

Magnetic proximity in MoS_2/graphene/Co system

ARPES

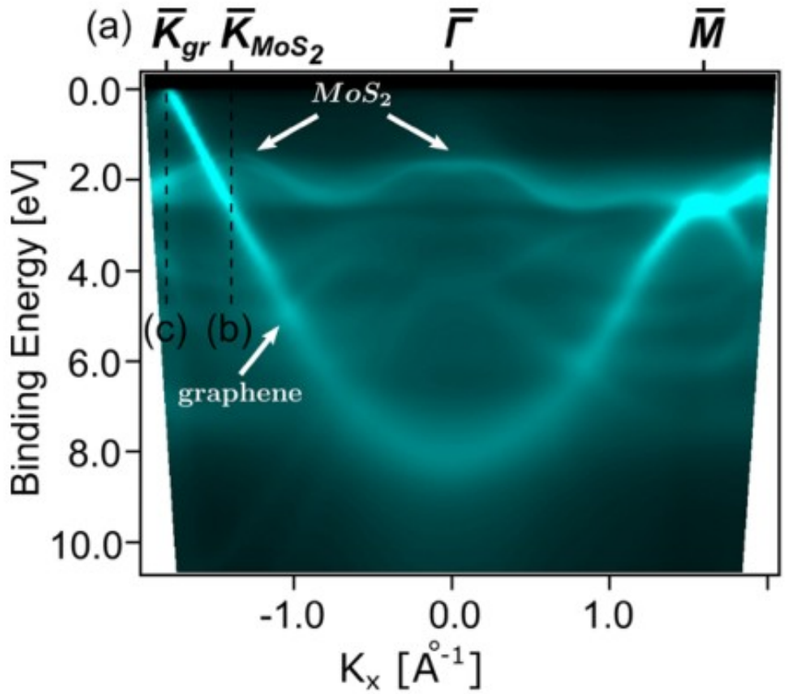

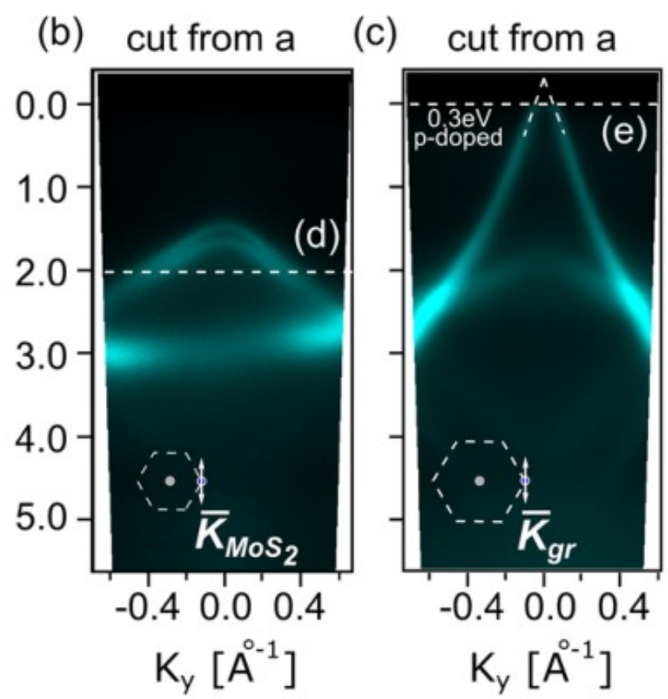

Model structure

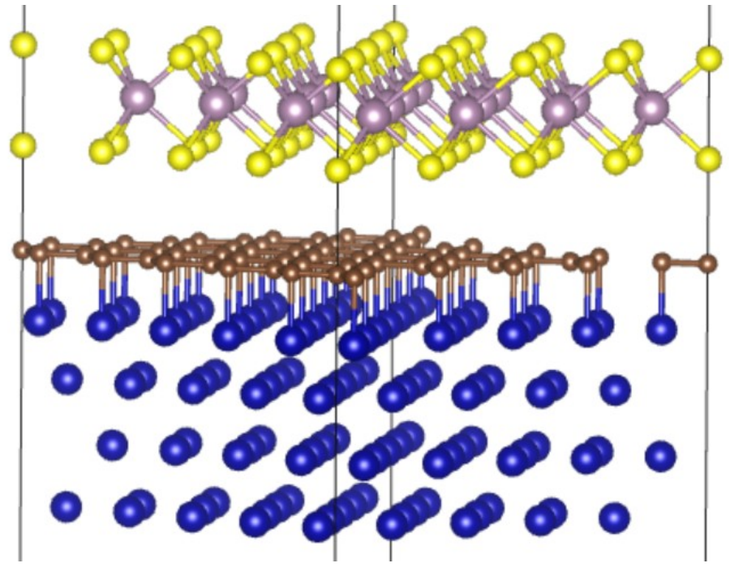

Co magnetization is in-plane

DFT

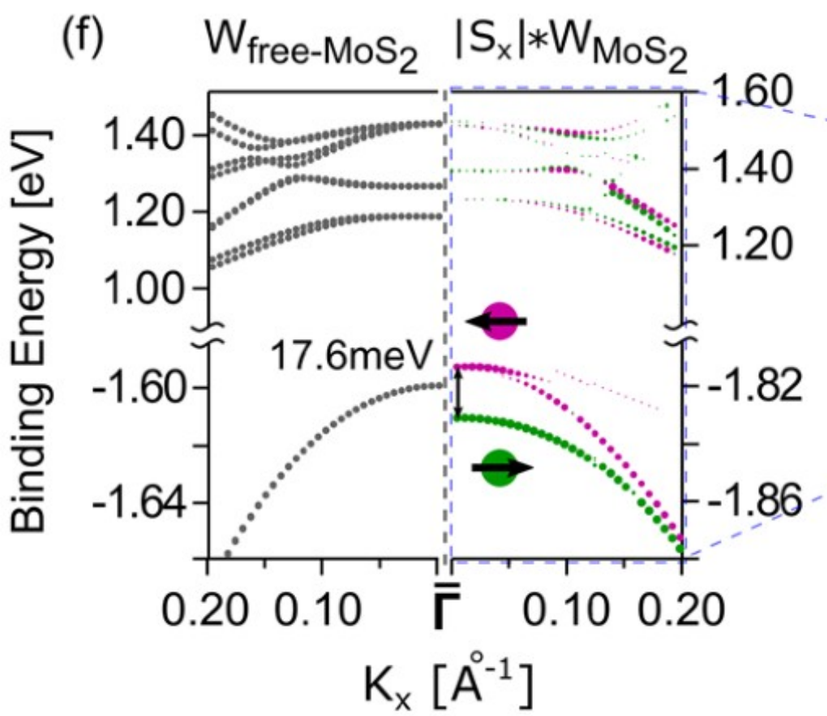

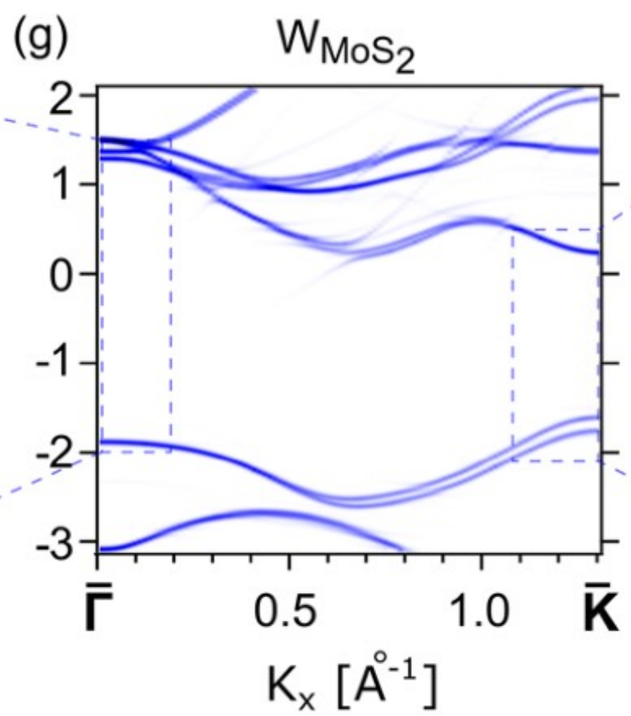

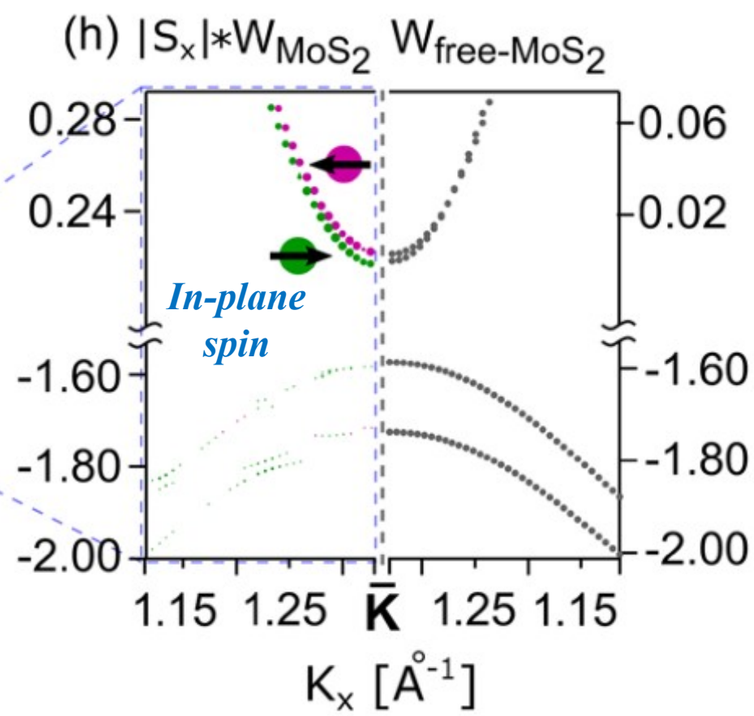

V. Voroshnin, D. Usachov et al., ACS Nano 2022

Magnetic proximity in MoS_2/graphene/Co system

spin-ARPES

Confirms spin splitting in Γ

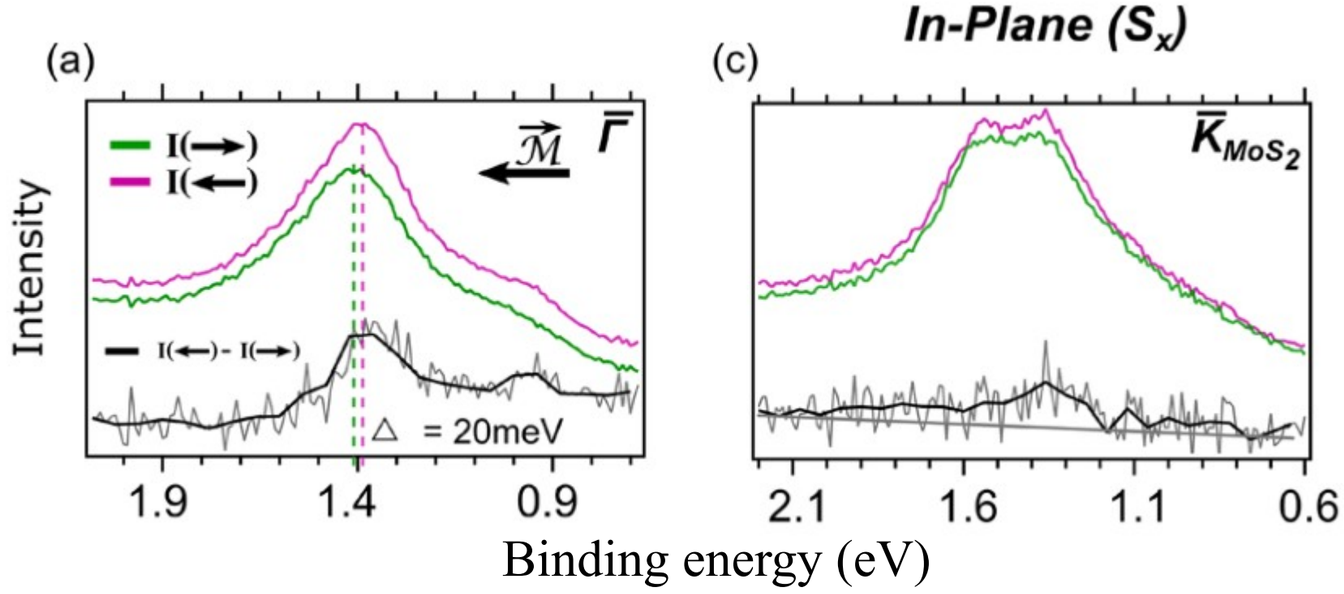

Confirms small spin polarization in K

DFT

Table 1. DFT-Simulated Splitting of the MoS_2 States in the $\bar{\Gamma}$ Point for the Set of Different Systems[a]

system	splitting (meV) FPLO	WIEN2k	OpenMX	Co to MoS_2 distance (Å)
MoS_2/graphene/Co	17.6	14	15	5.44
MoS_2/vacuum/Co		0.2	4	5.44
MoS_2/*h*-BN/Co			14	5.44
MoS_2/graphene bilayer/Co			0.5	8.79
MoS_2/Co			67	3.31
MoS_2/Cu/Co			66	5.44

[a]The splitting characterizes the strength of the magnetic proximity effect.

Spin-ARPES data confirm magnetic proximity effect in MoS_2 equivalent to the field of 100T

Probably the larger Cu radius relative to C and the higher number of valence electrons are responsible for the increased proximity effect

V. Voroshnin, D. Usachov et al., ACS Nano 2022

Conclusions from Part 3

- Ferrimagnetism in combination with Rashba effect can be induced in graphene under the following conditions:

- ***proximity with ferromagnetic Co,***
- ***proximity with Au monolayer, which has strong spin-orbit coupling,***
- ***dislocation loops, which break the symmetry.***

- This is a step towards observation of Quantum Anomalous Hall Effect in graphene

- A magnetic proximity effect is demonstrated for MoS_2 grown on top of the graphene/cobalt system.
- This effect is equivalent to the action of the magnetic field of about 100 T.
Potentially, it allows control over optical transitions in MoS_2 via Co magnetization.

- These examples demonstrate the broad capabilities of photoemission for the analysis of the electronic and spin structure of materials and their magnetic properties at the surface and in the bulk.

Thank you for your attention!